

MODELING AND DESIGN OF EXPLOSION-RESISTANT STEEL STUD WALL SYSTEMS

A Thesis Presented to the Faculty of the Graduate School of the
University of Missouri – Columbia

In Partial Fulfillment of the Requirements for the Degree

Master of Science

In

Civil and Environmental Engineering

By

JORDAN WHEELER LANE

Dr. Hani Salim, Thesis Supervisor

MAY 2003

The undersigned, appointed by the Dean of the Graduate School, have examined the thesis entitled

MODELING AND DESIGN OF EXPLOSION-RESISTANT STEEL STUD
WALL SYSTEMS

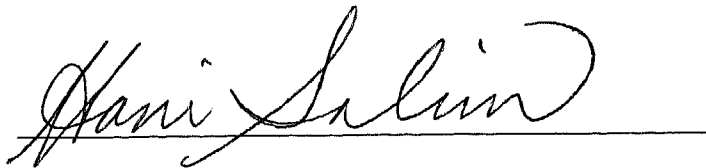
Presented by Jordan W. Lane

a candidate for the degree of Master of Science in Civil and Environmental Engineering

and hereby certify that in their opinion it is worthy of acceptance.







Y96002

ACKNOWLEDGEMENTS

I first would like to thank my advisor, Dr. Hani Salim, Assistant Professor of Civil and Environmental Engineering at the University of Missouri-Columbia for his invaluable guidance and encouragement throughout this project. He has been a great example to me both in and out of the class room.

I would also like to thank Robert Dinan, of the Air Force Research Laboratory, and Dr. Beverly DiPaolo of the U.S. Army Engineer Research and Development Center for their guidance in this investigation. Additionally, much gratitude is given to all the members of the Corps who have provided input. Without the funding and guidance by the Army Corps of Engineers, this research would have been impossible.

I would like to thank my fellow students, Dan Oesch, Josh Sebolt, John Bechtold, Silas Fitzmaurice, Steven Adams and Yancy Woodard, and others whose efforts were to my advantage. Their hard work in the office and lab has given me much needed assistance. I would also like to thank all the members of the University of Missouri who have provided assistance. Dr. Sam Kiger, Dr. Roger Laboube, and many others added valuable leadership and direction to this project. Also, C.H. Cassil and Richard Oberto provided immeasurable amounts of applicable knowledge and expertise to testing procedures, which is very much appreciated.

Finally, I would like to thank my friends and family for their support throughout this experience. I am sincerely grateful for the encouragement they have given to me. Most of all, I would like to thank God for the gifts and talents He has given to me which have enabled me to be here.

MODELING AND DESIGN OF EXPLOSION-RESISTANT STEEL STUD WALL SYSTEMS

Jordan Lane

Dr. Hani Salim, Thesis Supervisor

ABSTRACT

The need to protect structures, and the people inside these structures, has led to the Army Corps of Engineers developing blast design criteria for buildings. It is critical to know how a structure will behave under a given explosion and design wall systems to resist this type of load by developing adequate design criteria.

To predict the dynamic behavior of steel stud wall systems using dynamic modeling, a valid static resistance function for cold-formed steel studs must be developed. In conjunction with the U.S. Army Corps of Engineers, the University of Missouri-Columbia has been conducting experimental tests to define the entire static resistance function to failure for different wall systems.

The key to utilizing steel studs in a blast resistant wall system is by properly anchoring the steel studs to the structure to achieve cross-sectional failure of the stud in tension, as opposed to connection failure. Utilizing the steel stud strength and ductility allows for significant energy-absorbing capabilities important in blast resistance.

A modeling program has been developed to predict the dynamic response of cold-formed steel stud wall systems. Following details and discussion of testing procedures, experimental data for different steel stud wall systems is presented along with comparisons to the current modeling predictions.

TABLE OF CONTENTS

ACKNOWLEDGEMENTS	ii
ABSTRACT	iii
Chapter 1 Introduction	1
1.1 Literature review	2
1.2 Objective	4
1.3 Scope.....	5
Chapter 2 Modeling of Steel Stud Walls	7
2.1 Blast load	7
2.2 The Importance of Modeling	8
2.3 Dynamic Modeling	10
2.3.1 Single Degree of Freedom (SDOF) Model.....	12
2.3.2 Static Resistance Function	14
Chapter 3 Static Resistance Function	16
3.1 Previous Experience.....	16
3.2 Development of the Analytical Model.....	21
3.2.1 Linear Elastic Region.....	24
3.2.2 Softening Region	26
3.2.2 Tension Membrane Region.....	27
Chapter 4 Experimental Verification	37
4.1 Introduction.....	38
4.1.1 Experimental Setups	38
4.1.2 Design Concepts	40

4.1.3 Steel Stud Retrofit Connection	43
4.1.4 Proposed Anchorage Plate Design.....	44
4.2 Component Testing Via the Bending Tree	46
4.2.1 Experimental Evaluation Techniques	47
4.2.2 Maximum Moment Equivalency	51
4.3 Experimentation.....	54
4.3.1 Steel Hinge Connection	55
4.3.2 Steel Angle Connection	60
4.3.3 Experimental Results	63
4.3.3.1 Steel Hinge - Beam 0	65
4.3.3.2 Steel Hinge – Beam 20	67
4.3.3.3 Steel Hinge – Beam 21	69
4.3.3.4 Steel Hinge – Beam 25	71
4.3.3.5 Steel Angle – Beam 2	74
4.3.3.6 Steel Angle – Beam 18	77
4.3.3.7 Steel Angle – Beam 24	79
4.3.3.8 Steel Angle – Beam 33	81
4.3.4 Analytical Model Comparison.....	83
4.3.4.1 Modeling of the Steel Hinge Tests.....	84
4.3.4.2 Modeling of the Steel Angle Tests.....	90
4.4 Conclusions.....	94
Chapter 5 Design Procedures	96
5.1 General Design Steps.....	97

5.2 SSWAC.....	99
5.3 Dynamic Field Test.....	103
5.3.1 Experimental Setup.....	104
5.3.2 SSWAC Data Entry	107
5.3.3 Analytical Predictions.....	108
5.3.4 Experimental Results	111
5.3.5 Conclusions and Recommendations	113
Chapter 6 Conclusions and Recommendations.....	116
6.1 Conclusions.....	116
6.2 Recommendations and Future Studies.....	118
Appendix I – Typical Wall Test.....	121
Appendix II – Experimental Test Data.....	125
Appendix III – SSWAC.....	131
Appendix IV – Wall System Detail Summary.....	132
REFERENCES.....	138

LIST OF ILLUSTRATIONS

Figure 2.1: Beam Idealized as Spring-Mass System	11
Figure 2.2: Single Degree of Freedom Spring-Mass System	13
Figure 2.3: Free Body Diagram of Mass	13
Figure 2.4: Resistance Function.....	15
Figure 3.1: Test M1c, Steel Hinges used for Pinned Connection.....	18
Figure 3.2: Test M1c Post-Test Failure at Utility Hole	18
Figure 3.3: Test M1c, Pressure-Deflection Response.....	19
Figure 3.5: Typical Static Resistance Function for Steel Stud Members	22
Figure 3.6: Stud Under Uniform Applied Loading.....	30
Figure 3.7: Comparison of Shape Functions at Max Load	31
Figure 3.8: Parabolic Shape Function.....	31
Figure 4.1: Connection Failure (a) Crack Propagating (b) Bearing Failure	41
Figure 4.2: Load-Deflection Response of Clipped and Bent Flange Connection Test...	42
Figure 4.3: Non-Load Bearing Connection (a) Bottom Track (b) Slip Track	43
Figure 4.4: Stud-to-Floor Anchorage using a ½-in Thick Steel Angle Connection	45
Figure 4.5: Load Spacing of Mechanical Tree	49
Figure 4.6: Bracing System used in Testing	50
Figure 4.7: Load Applied to Steel Stud with Steel Angle Connection	52
Figure 4.8: 16-point Load Application with the Bending Tree	53
Figure 4.9: Steel Hinge Connecting Studs to Support System	55
Figure 4.10: Steel Hinge Details.....	56
Figure 4.11: Fully Constructed Steel Hinge Test Specimen.....	57

Figure 4.12: Fully Constructed Steel Hinge Test Specimen.....	58
Figure 4.13: Steel Hinge Specimen in Testing Apparatus.....	59
Figure 4.14: Steel Hinge Specimen with Nylon Straps Attached to Tree	59
Figure 4.15: Steel Angle Connecting Studs to Support System	61
Figure 4.16: Steel Angle Specimen with Nylon Straps Attached to Tree	62
Figure 4.17: Beam 0 (Steel Hinge Connection) – Proof of Concept	65
Figure 4.18: Beam 20 (Steel Hinge Connection) – Shiny Studs	68
Figure 4.19: Shiny Stud Failure (a) Initial Crack (b) Cross-sectional Failure.....	69
Figure 4.20: Beam 21 (Steel Hinge Connection).....	70
Figure 4.21: Beam 25 (Steel Hinge Connection) – No Utility Hole.....	72
Figure 4.22: Post Yield-Buckling Behavior at Utility Hole	73
Figure 4.23: Beam 2 (Steel Angle Connection).....	75
Figure 4.24: Beam 2 – Steel Angle Test (a) Deformed Shape (b) Connection Failure ..	76
Figure 4.25: Beam 18 (Steel Angle Connection).....	78
Figure 4.26: Beam 24 (Steel Angle) – Diamond Shape Utility Holes.....	79
Figure 4.27: Beam 24 Failure Crack at Utility Hole.....	80
Figure 4.28: Beam 33 (Steel Angle)	82
Figure 4.29: Analytical Model for Beam 0.....	84
Figure 4.30: Analytical Model for Beam 0 with an Increased Flat Portion.....	86
Figure 4.31: Analytical Model for Beam 20.....	87
Figure 4.32: Analytical Model for Beam 21 and Wall	88
Figure 4.33: Analytical Model for Beam 25 – No Utility Hole.....	89
Figure 4.34: Analytical Model for Beam 24 and Wall	91

Figure 4.35: Analytical Model for Beam 33.....	93
Figure 5.1: Data Entry Sheet for SSWAC.....	101
Figure 5.2: Response Sheet in SSWAC.....	102
Figure 5.3: Connection Detail at the Top of the Stud.....	105
Figure 5.4: Dynamic Field Test (a) Wall Construction (b) Pretest Exterior Photo	106
Figure 5.5: Parameters of the Blast Load for Dynamic Field Test.....	107
Figure 5.6: Dynamic Response for Brick Façade Wall from SSWAC.....	110
Figure 5.7: Dynamic Response for EIFS Façade Wall from SSWAC	110
Figure 5.8: Post-Test Exterior View of EIFS Façade and Brick Façade Walls.....	112
Figure 5.9: Measured and Predicted Center-Deflections.....	112
Figure A1.1: Typical Steel Stud Wall in the Vacuum Chamber	121
Figure A1.2: Typical Steel Stud Wall Test with Latex Membrane in Place	122
Figure A1.3: Failed Wall with Ruptured Steel Stud at Center Utility Hole.....	123
Figure A1.4: Typical Steel Stud Wall Static Resistance Function	124
Figure A2.1: Slope Comparison of Tension Membrane Region for Beam 0	125
Figure A2.2: Steel Hinge Pressure-Deflection Curve.....	126
Figure A2.3: Pure Tension Action verses Catenary Action.....	127
Figure A2.4: Mode Shape of Beams (a) Triangular Shape (b) Arch Shape	128
Figure A2.5: Beam 2 and Beam 18 Comparison.....	129
Figure A2.6: Analytical Model for Beam 18.....	130
Figure A3.1: SSWAC Showing Veneer Drop Down Menu	131
Figure A4.1: Suggested Connection Detail for New Construction	132
Figure A4.2: Suggested Connection Detail for Retrofit Construction.....	133

Figure A4.3: Steel Stud Wall-Angle Connections and Muntin Window Frame	1334
Figure A4.4: Interior Elevation View of Muntin Frame Window	135
Figure A4.5: Muntin Window Frame Detail	136
Figure A4.6: Muntin Window Frame Detail	137

LIST OF TABLES

Table 1: Cold-formed Steel Stud Section Properties	644
Table 2: Summary of Beams Tested with Material Properties.....	64

1 Introduction

A rise in terrorism in recent years has created a need to protect buildings and their occupants. The United States became a victim of terrorism on a large scale when a powerful car bomb exploded in the World Trade Center In New York City in 1993 (NRC 1995). This act of terror on the World Trade Center was followed by an even more deadly and devastating attack on the Alfred P. Murrah Federal Building in Oklahoma City in April 1995.

These two attacks as well as other acts of terror that followed have created a great concern for homeland safety. The course of action taken has been to examine existing blast hardening technologies and design principles that are used for militaristic purposes and to implement them into the civilian world (NRC 1995). However, because of an incomplete knowledge base, these technologies and principles must be expanded to be more applicable, accessible, and usable by the civilian engineering community (NRC 1995).

One way to protect people inside buildings is with the use of cold-formed steel stud walls, which are becoming one of the popular methods of blast protection. Recent improvements in manufacturing of the studs as well as construction technologies have led to an increase in popularity (Whitten 1999). Cold-formed steel is used in commercial

structures as well as residential buildings and is particularly popular in countries where resources are scarce. There is an endless variety of ways in which cold-formed steel sections can be fabricated. The need to improve and expand on existing design tools and methodologies has led to the Army Corps of Engineers developing blast design criteria for buildings. The US Army Corps of Engineers, Engineer Research and Development Center (ERDC) in Vicksburg, Mississippi, along with the National Center for Explosion Resistant Design (NCERD) at the University of Missouri-Columbia are currently working to develop design criteria for wall systems against blast loads.

The NCERD at the University of Missouri-Columbia has designed and constructed a static vacuum chamber (Brown 2003). The vacuum chamber has been used to create a uniform static load to test complete wall systems which provide experimental data to define the static resistance function. It is our goal at NCERD to not only improve on existing design tools, but also create new ones as well.

1.1 LITERATURE REVIEW

A general review of the literature has been performed to examine previous works related to modeling and design of steel stud wall systems. New construction ideas as well as retrofit designs for steel stud wall systems will be investigated in this thesis. A steel hinge connection as well as a steel angle connection will be the two main types of connections that will be tested. The steel hinge is a connection designed primarily for academic research, and is not used for construction purposes in the field. For a steel angle connection, the objective is to provide adequate strength during a blast event to

allow the steel stud to develop its full capacity before connection failure occurs or the anchor that attaches the connection to the structure fails (Shull 2002).

Previous research focused on the development of a general static resistance function that presented all regions of the function, which was based on stud capacity alone, and did not account for connection details (Roth 2002). However, since the majority of the previous testing was conducted using the static vacuum chamber, the region just after buckling could not be obtained because of the nature of the testing, being load-controlled. The behavior of the studs just after buckling in the vacuum chamber can not be recorded because of the type of loading. However, much progress was made through full-scale testing which created a foundation for subsequent testing and also gave an important understanding of stud wall system behaviors. It was also found that if a wall is to be intended to provide blast resistance, the engineer should design the wall-to-structure connections with adequate anchorage, such as a steel hinge or a steel angle, rather than a non-load bearing wall with a slip track connection (Muller 2002).

The static resistance function is crucial in predicting the behavior of a steel stud wall system under blast loading. Previous research at the University of Missouri focused on determining these resistance functions for steel stud wall systems under lateral uniform pressure and has provided a sense of direction for current research. In previous research at the University of Missouri, the viability of existing predictions were explored and compared to the static resistance functions found through experimentation (Muller 2002 and Roth 2002). Through this exploration, improvements were made to these approximate previous predictions. In past tests, construction detail was of main concern, but now since adequate research in this area has been conducted (Muller 2002), the focus

will be placed on predicting the static resistance of any wall system and using a single degree of freedom (SDOF) model along with numerical integration (Biggs 1964) to predict the dynamic response under blast loads. The predicted dynamic response can then be verified via live explosion field tests.

Because of a lack of good behavior prediction in previous research, empirical models were developed for the static resistance function (Muller 2002). However, with more testing and improved results, an analytical procedure for predictions has been developed and is described in this thesis.

1.2 OBJECTIVE

The objective of this research is to improve on the experimental work conducted by previous researchers and to develop an analytical model for predicting the static resistance of cold-formed steel stud walls under blast loads. The static resistance function can then be used in predicting the dynamic response of the steel stud wall systems. Advances made with this research will improve the engineering tools available for blast design. The main objective of the current research is to obtain data in the post-buckling regions of a wall system to predict the behavior and better understand the static resistance function in such regions. The best way to do this is through testing stud pairs using a mechanical loading tree. Testing components of the wall systems with a loading tree is cheap, easy and fast compared to testing complete steel stud wall systems in the vacuum chamber. With the use of a hydraulic actuator, deflection controlled testing can be done without the loading limits of the vacuum chamber (the vacuum chamber is limited by atmospheric pressure, 14.7-psi).

The stud behavior in the softening region after yield will be evaluated using a “good” working experimental bending tree setup. Tension membrane behavior will also be of main concern, since this region accounts for most of the energy-absorbing capabilities of a wall system.

1.3 SCOPE

This thesis summarizes concepts and procedures for the design of steel stud wall systems against blast resistance. The tests that are included in this thesis were performed at the University of Missouri-Columbia between the Fall of 2001 and Winter of 2003. This research is a collaborative effort between the ERDC and the University of Missouri-Columbia. The ERDC conducted full-scale and half-scale dynamic tests on various cold-formed steel stud designs using live explosions, while the University of Missouri-Columbia conducted static tests on various wall systems and wall system components. These static experiments were performed using a mechanical loading tree to test various components of the wall systems and were verified using the static vacuum chamber. The steel hinge connection test and the steel angle connection tests are two types of tests included in this thesis and are the focus of the current research.

The wall systems and components of the wall systems that have been tested up to date are similar in that they all utilize a cold-formed steel stud section. All studs tested were channel sections with stiffening lips on the flanges (Clark 2000). All studs were 6-in sections, which means they measure 6-in from outside flange to outside flange. The thickness of the channel was varied (0.043-in to 0.054-in), depending on the type of test

conducted. Two major manufacturers provided the studs: Dietrich Industries and Clark Steel Framing Systems.

In Chapter 2, the idea of dynamic modeling of wall systems is introduced as well as the importance of modeling. An SDOF model is defined and how it represents actual structures to simplify modeling procedures is shown. A general static resistance function is defined and how the stiffness of a system affects its ability to resist loads is introduced.

In Chapter 3, previous attempts to develop a static resistance function are presented, and an analytical model that defines the entire region of steel stud behavior is developed. Each region of behavior is defined and how these regions are calculated is shown. In Chapter 4, data from experimental testing that was conducted over the last two years is presented. The testing setup and the design concepts for testing are discussed, and then the results are evaluated. With the use of experimental data, the analytical model developed is verified.

The analytical static resistance model developed is used in Chapter 5 along with an SDOF model to predict the dynamic behavior of a steel stud wall system. The predicted behavior is compared with a component test, a full-scale vacuum chamber test, and a live explosion field test. Finally, conclusions and recommendations are presented in Chapter 6. The Appendix included at the end of the thesis provides supplementary information.

2 Modeling of Steel Stud Walls

When a blast occurs near a structure, a very high pressure is applied in a very short amount of time. The structural response under severe loadings of this nature is significantly different from much slower loadings, such as wind loading. If the structure is not able to elastically absorb all of the blast energy, then permanent deformations will occur, and could result in complete failure. It is important to understand the behavior of a system under such extreme loadings to design against them. This portion of the thesis focuses on the dynamic behavior and modeling of steel stud walls. A definition of “failure” will be given, and an SDOF model will be introduced as well as a static resistance function, both of which are necessary to predict the response of walls under blast loads.

2.1 BLAST LOAD

Dynamic modeling of a steel stud wall system is used to predict the response of the wall under a certain short-duration blast loading. Any blast load can be defined using two parameters, the pressure of the blast and the impulse. When a blast occurs, a violent release of energy occurs producing a high-intensity shock front that expands outward from the surface of the explosive. As this shock front, also called a blast wave, travels

away from the source, it loses strength and velocity, and increases in duration. As the blast wave expands in the air, the front impinges on any structure within its path, resulting in a pressure force being applied to the structure (TM5-1300).

The impulse of a blast can be defined as the area under the load-time curve. A pressure applied to a structure over a short period of time has a lower impulse than the same pressure applied over a long period of time. A highly impulsive loading consists of a relatively high pressure applied quickly, while a static loading consists of a pressure that slowly rises to its peak value applied over a long period of time. If the duration of a blast pressure applied to a structure is very short compared to the natural frequency of the structure, the load can be considered as pure impulse (Biggs 1964).

2.2 THE IMPORTANCE OF MODELING

The goal of this research in the area of blast design is primarily to protect people inside the buildings subjected to blast loading. When an explosion near a building occurs, the building can have catastrophic effects, destroying or causing major damage to the buildings structural framework, collapsing walls, shattering windows, and closing off fire- and life-safety systems (NRC 1995). High blast pressures or projectiles flying into a building as a result of shattered windows and failed walls can cause serious or fatal injury to the occupants.

To protect people inside buildings from blasts, it is critical to know how the structure will behave under a certain pressure and impulse. If a building is not able to absorb the amount of energy created by a blast, the walls of the building will fail and the structure may collapse. It is usually impractical to design a building against blasts so that

the structure remains undamaged. However, the objective of dynamic modeling is to minimize injury and death of the occupants. Modeling allows researchers to determine whether a building will survive a certain dynamic loading, and to predict the condition of the building afterward. So given the two parameters of pressure and impulse, the dynamic response of a structure can be determined using engineering methods.

In this thesis, wall failure is considered near collapse of the wall system. Typically in design, failure is any behavior beyond the elastic region of response, and if a steel beam buckles in a building under normal loads, it is considered to be failure. In the field of blast design, the plastic region, or post-buckling region, is a critical part of the behavior and is the region where a system absorbs a large amount of energy in resisting extreme loads. This concept of energy absorption is of great importance in structural design for dynamic loads since it accounts for a large portion of the energy-absorption capabilities of a wall system. Dynamic modeling of steel stud walls requires knowledge of the loading, the pressure and impulse, and accounts for both the elastic and inelastic region of response.

All structural dynamic systems contain a certain amount of damping and the effect can be significant if the load is oscillatory in nature. Structural damping during plastic response cannot be clearly defined or verified experimentally, and therefore its effects should not be considered in the plastic region of response (Kiger and Salim 1998). For the purposes of this thesis, damping will not be a factor in the wall systems that are modeled.

2.3 DYNAMIC MODELING

Dynamic modeling in this thesis is referred to as predicting the behavior of a steel stud wall system under a blast load. There are two primary methods for dynamic modeling: numerical procedures and rigorous solutions. Numerical analysis is the most general and straightforward approach and is based on physical phenomena (Biggs 1964). Numerical integration will be further discussed in Section 2.3.1. Rigorous solutions are closed form solutions that give the displacement as a function of time by solving the differential equations of motion. Dynamic models were analyzed using numerical analysis and will be discussed based on the methodology presented in Biggs (1964).

Real world structures can be idealized and represented by a combination of springs and masses. For example, a beam that is subjected to a uniform pressure, such as a dynamic load, can be represented by a simple spring-mass system, shown in Figure 2.1. In order for modeling to be accurate, the idealized system must represent the actual structure. Therefore, it is important to select the proper system parameters, these being the spring constant k_e and the mass M_e . The spring constant k_e is simply the resistance of the system and can be found from the properties of the beam, since it is the ratio of force to deflection. For complicated systems, the force-displacement relation can not be defined by a single k_e , and thus the static resistance function is normally utilized and will be described in Section 2.3.2.

To define an equivalent one-degree system, like the one shown in Figure 2.1, it is necessary to evaluate certain parameters, these being M_e , k_e , and F_e . The equivalent system is chosen so that the deflection, y , of the concentrated mass is the same as that for some significant point on the structure, such as the mid-span of a beam. The constants of

the equivalent system are evaluated on the basis of an assumed deformed shape of the actual structure resulting from the static application of the dynamic loads. It is convenient to introduce certain transformation factors to convert the real system into the equivalent system. The total load, mass and resistance of the real structure are then multiplied by the corresponding transformation factors to obtain the parameters for the equivalent one-degree system. Details of this procedure can be found in Chapter 5 of Biggs (1964).

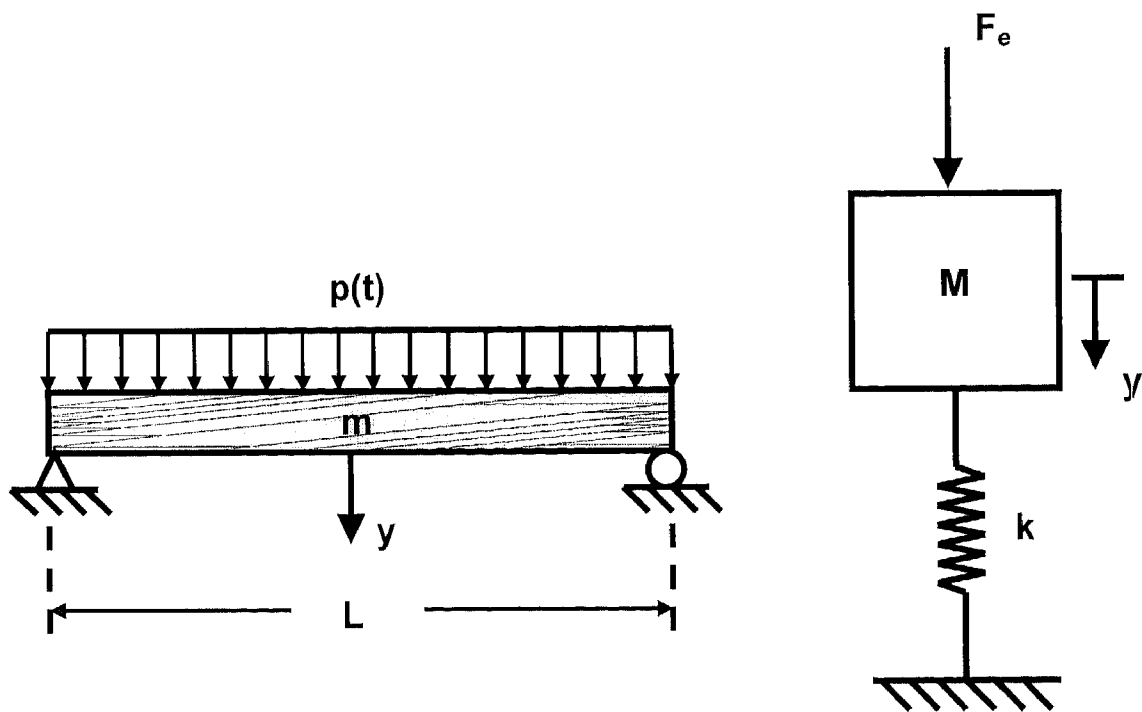


Figure 2.1: Beam Idealized as Spring-Mass System

2.3.1 Single Degree of Freedom (SDOF) Model

When a blast is exerted on a structure, there are many uncertainties regarding how the structure can react. In general, when a load is applied to a structure, it will travel in the path of least resistance. When an explosion takes place, pressures are placed on the outside of a building structure, often resulting in permanent deflections which push the walls toward the inside of a building. When modeling, this inward movement of a wall system is simplified in order to more easily predict the behavior of a system.

This simplified system is commonly referred to as an SDOF model. As discussed in Biggs (1964), with this model only one type of motion is possible; or in other words, the motion of the system at any instant can be defined by a single coordinate system. For example, if the system shown in Figure 2.1 is assumed to be an SDOF system, the mass could only move in a vertical direction. Restraints can be put in place to show that movement from side to side is restricted, shown in Figure 2.2.

The first step in dynamic modeling is to isolate the mass as a free body diagram (Figure 2.3), and then write an equation of motion by applying the concept of dynamic equilibrium (Equation 2.1). For Figure 2.3, the equation of motion is:

$$M\ddot{y} + R - F(t) = 0 \quad (2.1)$$

where:

$M\ddot{y}$ = force of inertia

R = resistance of the spring force; during elastic response, $R = ky$

$F(t)$ = applied external force

y = displacement

\ddot{y} = acceleration

This differential equation can be solved to determine the variation of displacement with time, once the specific parameters are defined.

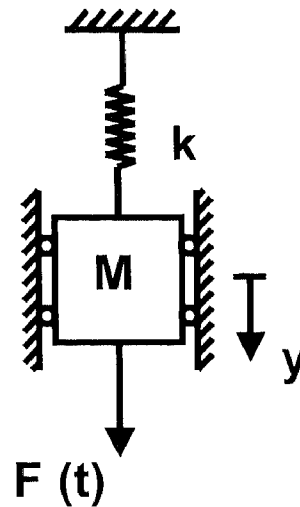


Figure 2.2: Single Degree of Freedom Spring-Mass System

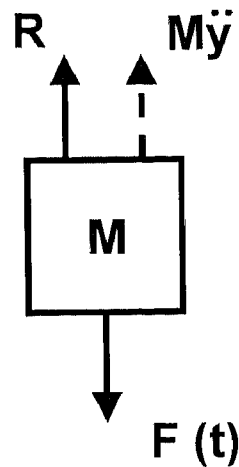


Figure 2.3: Free Body Diagram of Mass

Once the system is represented as an SDOF model and the loading function and initial conditions are defined, the numerical integration can then be performed. This is a procedure by which the differential equation of motion, Equation 2.1, is solved step by step, starting at time zero, when the displacement and velocity are known. Once the time step is defined, the displacement can be extrapolated from one time step to the next. A specific design example will be performed using this procedure of numerical integration in Section 5.3. In predicting dynamic behavior, not only must the system be modeled correctly, but the static resistance of the structure, R , must be known.

2.3.2 Static Resistance Function

When modeling an ideal system, an SDOF model is developed, dynamic equilibrium is applied, and then an equation of motion can be determined. Before one can perform numerical integration, the loading function must be known as well as the initial conditions, which include the mass and the resistance of the system. The resistance of a system is the internal force that tends to restore the system to its unloaded static position (Biggs 1964). As mentioned previously, the resistance of a linear elastic system is modeled using the spring constant k , which is the ratio of force to deflection. In a linear system, the spring constant is represented by a single number. In a more practical system, where the resistance of a system varies with deflection, the resistance function can be represented as a bilinear or tri-linear function.

Consider the resistance function of Figure 2.4. As the displacement increases from zero, the resistance also increases linearly with a slope of k_e , the spring constant, until the elastic limit displacement y_{el} is reached. As the displacement continues to increase, the resistance remains constant at R_m , which is the plastic resistance, and has a

slope of $k_2 = 0$. The resistance then increases at a slope of k_3 during the tension membrane region of behavior. The displacement will continue at this resistance of k_3 until the structure reaches its ductility limit and failure of the system occurs. If a maximum displacement occurs before the ductility limit is reached, the system is said to rebound, and will continue to rebound at a slope assumed to be the same as the slope in the elastic region of response.

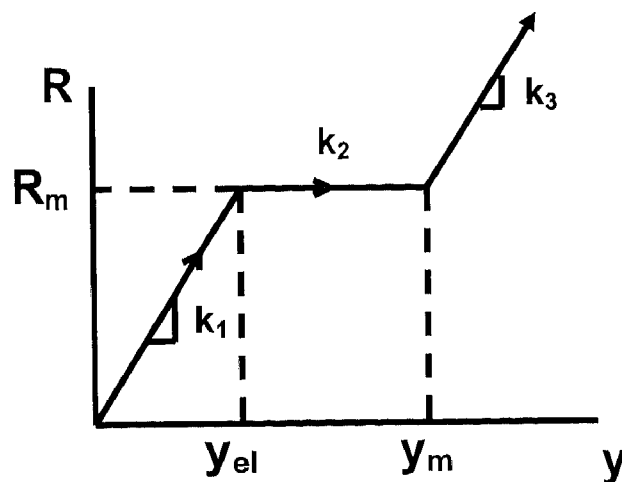


Figure 2.4: Resistance Function

So in predicting the dynamic behavior of steel stud walls using an SDOF model, a resistance function must be defined. As discussed in Chapter 1, the ERDC, the University of Missouri-Rolla, and the University of Missouri-Columbia have collaborated in conducting experimental tests and using this data to define the static resistance functions of different wall systems. A valid static resistance function must be developed to predict cold-formed steel stud wall behavior under blast loads and to improve design methods. This static resistance function is developed in Chapter 3.

3 Static Resistance Function

The static resistance function of a structure is simply the load versus deflection response under static loads. For the purposes of this thesis, a load caused from a blast or explosion is considered to be a dynamic load, while a load applied in a slow and steady fashion is considered to be a static load. Young and Budynas (2002) describes a static load as one being applied so gradually that at any instant, equilibrium is essentially maintained. For example, a wind load is considered static loading, while a pressure wave exerted from a blast is considered dynamic loading, even though both loads are in motion.

The static resistance function has been defined and the need for a valid static resistance function for cold-formed steel studs has been stated. In this chapter, experience of previous researches will be introduced, including experimental tests and data. Also, a valid analytical model will be developed and discussed in detail.

3.1 PREVIOUS EXPERIENCE

The goal of previous research in defining a static resistance function was to conduct wall tests that fully develop the capacity of the cold-formed steel stud sections to form a base resistance function that presented every region of the resistance function (Roth 2002).

The tests conducted to achieve this goal provide a good starting point for a general resistance function and a design code.

One test that will be considered is a steel stud wall with a steel hinge connection, referred to as Test M1. Muller (2002) provides construction and testing detail for this wall along with the comprehensive experimental results. For the purposes of this thesis, this test and the experimental data will briefly be discussed in relation to the static resistance function.

The goal of Test M1 was to produce the static resistance function for a single stud wall system that incorporated all failure modes and all regions of the function until ultimate failure of the stud cross-section. Three different M1 tests were conducted (Test M1a, Test M1b, and Test M1c) because of premature failure in the first two experiments. For each one of these tests, steel hinges were designed and fabricated for the wall system so that each stud would behave as a true pin-pin beam, Figure 3.1.

Test M1c gave the desired failure results, a cross-sectional failure of an interior stud at the utility hole, Figure 3.2, therefore utilizing the stud capacity. All studs yielded near the mid-height, and the pressure versus deflection behavior is presented in Figure 3.3. Stud behavior after yielding of the steel is characterized by localized plastic deformation at mid-height while the majority of the wall still behaves elastically. Park and Gamble (1980) demonstrated that reinforced concrete slabs subjected to uniform load exhibit tensile membrane behavior similar to the behavior seen with this wall after yield.

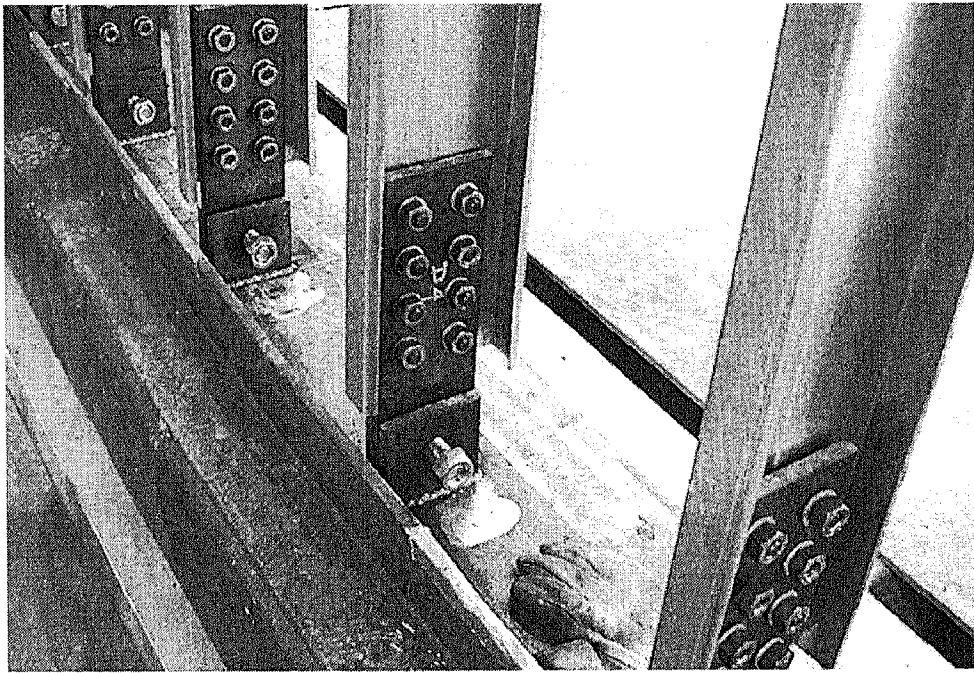


Figure 3.1: Test M1c, Steel Hinges used for Pinned Connection

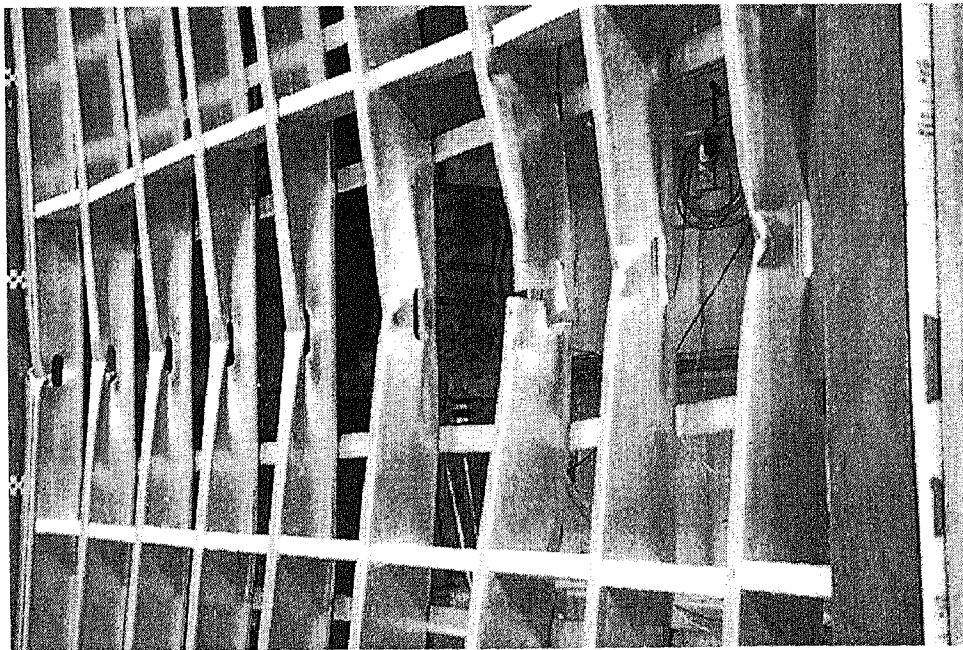


Figure 3.2: Test M1c Post-Test Failure at Utility Hole

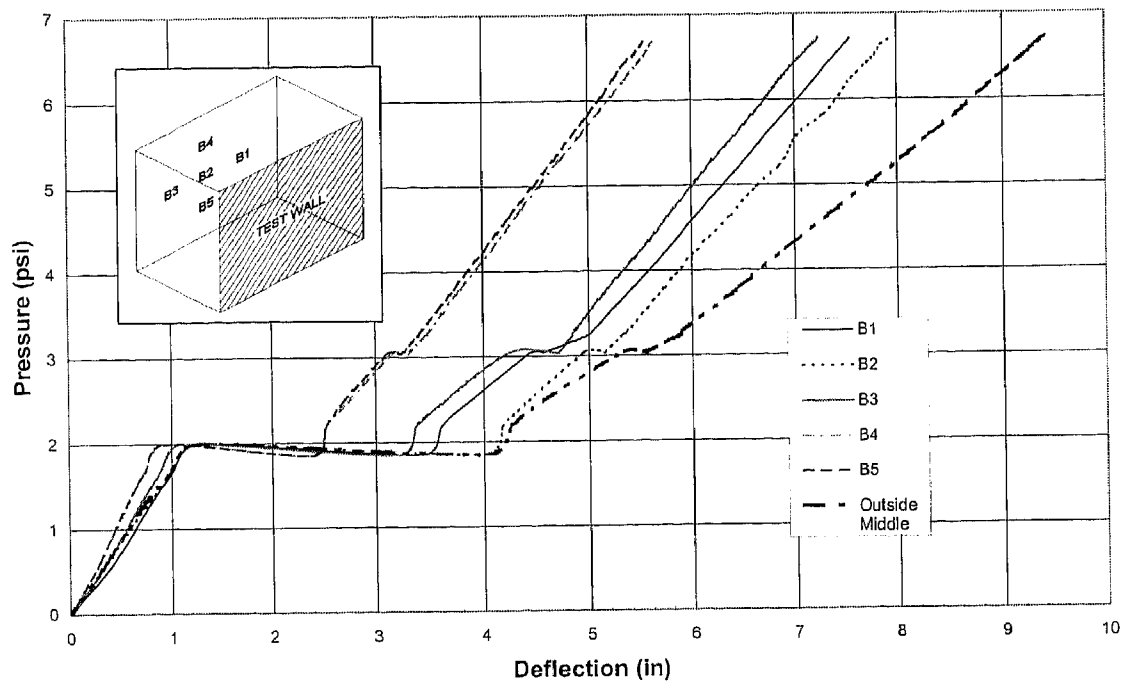


Figure 3.3: Test M1c, Pressure-Deflection Response (Roth 2002)

From this test as well as other tests conducted, a general static resistance function was obtained. From this general resistance function, Figure 3.4, general observations and conservative assumptions can be made. An empirical/analytical model was developed by assuming the elastic capacity portion and the plastic capacity portion as straight lines and assuming a softening behavior. The linear elastic portion of the model is predicted from classic beam theory, while the linear inelastic portion is determined using experimental data from the pressure – deflection response of Test M1c, as well as data from other tests. Since no experimental data was available for the softening region due to the nature of the loading with the vacuum chamber, a softening region had to be assumed. The nature of the loading with the vacuum chamber and solutions to this problem will be presented in

Chapter 4. The empirical model, as well as the other tests performed and used for modeling, are discussed in further detail by Roth (2002).

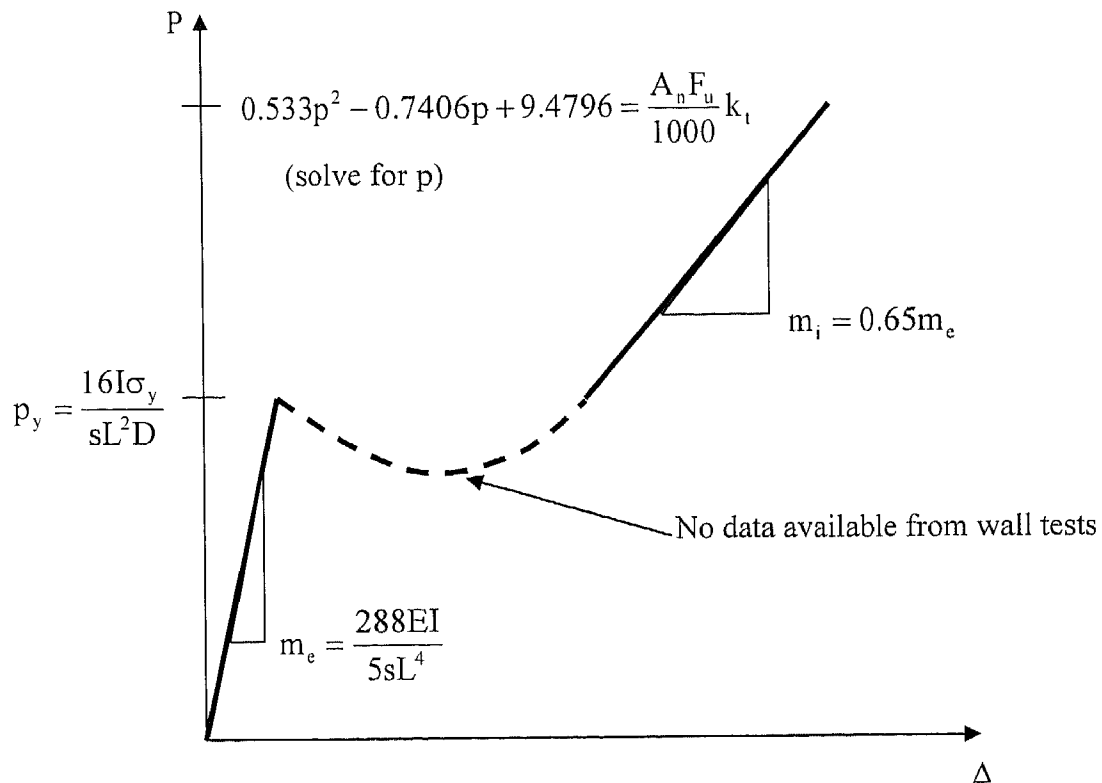


Figure 3.4: General Static Resistance Function (Roth 2002)

Additional experiments were performed by previous researchers for other steel stud wall systems, and these results have been implemented into design in the field. However, since the empirical/analytical model shown above, and that presented by Muller (2002), are based on a limited number of tests, and since the model developed has to be a general model that can be applied to nearly any type of stud wall, a more useful and more precise analytical model is needed. The model shown here provides great insight for the modeling of steel stud wall systems, and its importance is not to be

overlooked. However, analytical predictions that can be applied to specific wall system designs are needed. Because of the nature of experimental data, results can not be applied directly to design in the field, and therefore an analytical model based on stud size and material properties is desirable and can be of great importance in design.

3.2 DEVELOPMENT OF THE ANALYTICAL MODEL

An analytical static resistance function based on stud size and material properties has been developed and verified using a combination of many tests. These tests include field tests using live explosives, vacuum chamber tests of wall systems, and component tests of the wall systems using a bending tree. Although the analytical model provided in this thesis is of great value and believed to be useful in design, a broader range of stud sizes and material properties should be incorporated into the predictions for this model. Up to this point, an adequate number of tests have been performed and used in developing a good working analytical model, but improvements to make this model more comprehensive for design are encouraged and will be discussed in Chapter 6.

The static resistance function for steel stud members is based on both theory and experimental data. The model is a function of pressure and deflection. The elastic portion of the model is well known and easily predicted using classic beam theory (Yu 2000) while the inelastic portion of the model is based on equilibrium along with an adequate amount of experimental data. The elastic and inelastic region is joined together with a horizontal line in the post-buckling region. An upper and lower limit for the resistance function in the tension membrane region was developed to account for two different types of stud behavior, Figure 3.5.

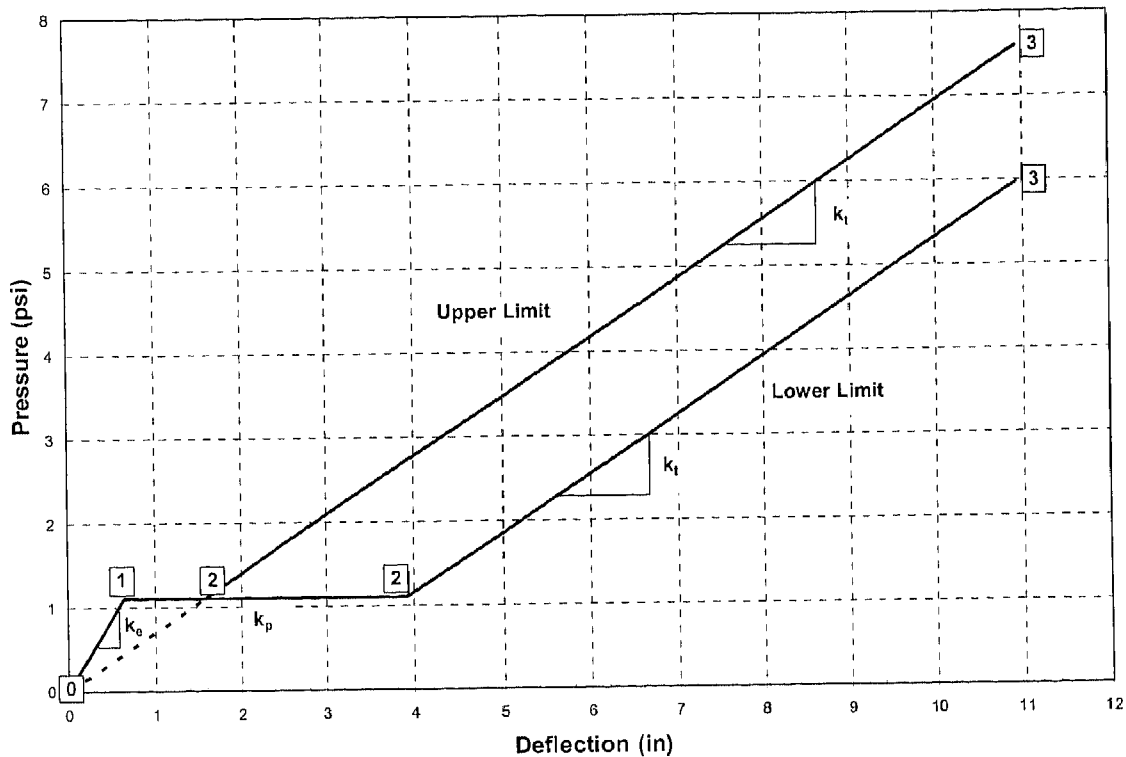


Figure 3.5: Typical Static Resistance Function for Steel Stud Members

Figure 3.5 is a typical static resistance function for steel stud members that is primarily based on theory, but also incorporates some experimental observations into its definition. The static resistance function is defined by a number of points, 0, 1, 2, and 3, and by the slopes between each of the points, k_e , k_p , and k_t . The points and slopes are as follows:

Points: 0 – the origin (0,0)

1 – the mid-span deflection at yield-buckling and the pressure at yield-buckling

2 – tension membrane resistance begins to control behavior

3 – stud rupture due to excessive elongation

Slopes: k_e – slope of elastic response

k_p – slope during plastic softening which is assumed flat

k_t – slope of tension membrane region

The static resistance function in Figure 3.5 can be divided into three regions, the linear elastic region (between points 0 and 1), the post-buckling softening region (between points 1 and 2), and the tension membrane region (between points 2 and 3). The resistance of a steel stud, as seen in Figure 3.5, depends on its region of behavior. Before the yield-buckling, point 1, the wall system resistance comes primarily from the bending capacity of the studs, and after buckling, the wall resistance is achieved through tension membrane resistance of the studs, from point 2 to 3. From experimental testing, two major observations were made and implemented into properly defining the static resistance function. First, the softening region, between points 1 and 2, was observed when the stud forms a hinge. When this takes place with a steel stud, the section acts like a hinge and is commonly referred to as a plastic hinge and can be compared to an ordinary hinge with a constant amount of friction (Smith and Sidebottom 1965). The amount of softening that takes place varies from test to test and is not well-defined.

Also, an upper limit and a lower limit have been defined for the function to account for the different amounts of softening that occurs. So as it is seen, a combination of theory and experimental observation are used in the development of the static resistance function. It is important to note that defining a valid static resistance function for the design of steel stud members can not be obtained by theory alone, or by experimental data alone. Due to many of the behavioral uncertainties of steel studs, both theory and testing are important in the predictions.

3.2.1 Linear Elastic Region

To define the points of the static resistance function, both pressure and deflection must be computed at each transition. The region between points 0 and 1 is the linear elastic region. Point 0 is simply the origin. Point 1 is when the material no longer behaves linearly and permanent deformation starts to take place. This point is commonly referred to as “yield-buckling” and is important in determining stud behavior. The elastic strength of the cold-formed steel stud sections can directly be correlated to the yield point (Yu 2000). The center deflection of a beam with an applied uniform load can be computed as follows:

$$\delta = \frac{5wL^4}{384EI}$$

where:

δ = center deflection

w = uniform load per unit length

L = length of beam

E = Young’s modulus

I = moment of inertia of section

For a steel stud wall system under lateral uniform pressure:

$$w = pS \tag{3.1}$$

where:

p = pressure per unit area

S = spacing of steel studs in the wall

Therefore, the center deflection at yield for a typical steel stud member in a wall system is:

$$\delta_y = \left(\frac{5SL^4}{384EI_{eff}} \right) p_y \quad (3.2)$$

where:

p_y = pressure at yield

L = length of steel stud

I_{eff} = effective strong axis moment of inertia for the steel stud (Yu 2000)

The pressure at yield is computed from the yield stress based on flexure, and the maximum moment of a simply supported beam with a uniformly applied load. The yield stress produced due to the moment is:

$$\sigma_y = \frac{Mc}{I}$$

where:

M = the resultant internal moment

c = the perpendicular distance from the neural axis to the extreme fiber of the section

For a typical steel stud member, the yield stress becomes:

$$\sigma_y = \frac{M_y \left(\frac{h}{2} \right)}{I_{eff}} \quad (3.3)$$

where:

M_y = the moment at yield

h = the depth of steel stud section

The maximum moment at yield of a simply supported beam is:

$$M_y = \frac{wL^2}{8}$$

and with the substitution of Equation 3.1, the yield moment becomes:

$$M_y = \frac{p_y SL^2}{8} \quad (3.4)$$

Substituting Equation 3.4 into Equation 3.3 and solving for p_y results in the pressure at yield for a typical steel stud section:

$$p_y = \frac{8\sigma_y I_{eff}}{SL^2 \left(\frac{h}{2}\right)} \quad (3.5)$$

The slope of the elastic region is the pressure at yield divided by the deflection at yield:

$$k_e = \frac{p_y}{\delta_y}$$

and substituting for the deflection at yield from Equation 3.2, the slope becomes:

$$k_e = \frac{384EI_{eff}}{5SL^4} \quad (3.6)$$

3.2.2 Softening Region

The “softening” region is the flat portion of the static resistance function, and is due to the formation of a hinge. Any structure will have a curved transition phase even when only one plastic hinge is necessary to develop the full plastic strength of the structure (Biggs 1964). The characteristics of this transition period depend on how many hinges are formed during softening. However, the amount of deflection that occurs during the softening region is not well-defined. From experiments, it is observed that in some instances the studs experience a “well-defined” softening region after yield-buckling and

before going into the tension membrane region. When this type of behavior occurs, the studs will typically deflect three inches for 10-ft span beams before tensile capacity is developed. In other instances, the studs go into tension membrane right after yield-buckling is achieved, and typically deflect one inch before tensile capacity is developed. The combination of both types of response has even been observed in testing and will be presented later in this thesis.

The different responses are believed to depend on the mode shape the beam experiences as it approaches buckling, which might be controlled by the load application. Therefore, the analytical model developed accounts for both behaviors by incorporating an “upper limit” response and a “lower limit” response. The upper limit response represents studs with little softening before tension membrane dominates, while the lower limit response represents studs with more softening. Studs that form a well-defined three-hinge mechanism tend to soften more and are characterized by the lower limit response. This type of response as well as the upper limit response will be discussed in more detail in Chapter 4. The slope during plastic softening is assumed flat and therefore:

$$k_p = 0 \tag{3.7}$$

3.2.2 Tension Membrane Region

The plastic region of behavior for a steel stud is the region after softening occurs and the stud begins to develop more resistance, which is the region between points 2 and 3, Figure 3.5. This type of response is important to achieve since this is the region where the majority of energy is absorbed in a system. If the structural members in a system fail due to insufficient material properties, a bad connection failure, etc., its purpose to absorb

energy is not achieved because of a reduction of capacity. In dynamic analysis, a stud's ability to absorb energy is critical in surviving a blast load. Therefore, adequate predictions in the plastic, tension membrane region are needed for design.

To properly predict the static resistance function in the tension membrane region, defining an upper and lower limit is necessary. Two types of behaviors have been observed in the lab and will be defined in this section. The first type of behavior is characterized by the upper limit response and is referred to as catenary action. In this type of behavior, tension membrane dominates soon after yield-buckling. A limited amount of softening takes place because of the mode shape of the beam. When a beam experiences catenary action, there is no definite formation of a plastic hinge and the beam takes on an arch shape. In this type of behavior, the beam experiences a combination of tensile stress as well as bending stress.

The second type of behavior is characterized by the lower limit response and is referred to as pure tension action. It must be noted that the beam is not experiencing pure tension, but tensile stress is dominating compared to the amount of bending stress present. In this type of behavior, a definite plastic hinge is formed, which results in a more noticeable softening region. When the beam forms the plastic hinge, it is commonly known as a three-hinge mechanism, and a significant amount of softening occurs, Figure 3.5. Both types of behavior have been observed in testing and will be presented in Chapter 4, Section 4.3.3.

Regardless of the type of stud behavior, whether it is catenary action or pure tension action, the slopes are consistent with each other. The only difference in the two types of behavior is at what instance tension membrane dominates. The slope of the

response is known and the point at which it begins is predicted. The slope of the tension membrane region can be determined from equilibrium and geometry of a stud under uniform applied loading.

It is important to determine the point in the static resistance function at which failure is reached, p_u . This is a crucial point since it directly affects the amount of energy the system will absorb. Figure 3.6 shows a stud under uniform applied loading, the forces that are present, and a general deformed shape. When tension membrane is dominant, the tension in a stud is equal to the stress in the stud at yield multiplied by the effective area of the stud ($T = \sigma_y A_e$). For the forces in the y direction and assuming a positive direction up, equilibrium is as follows:

$$2T \sin \theta = wL$$

and substituting for T and assuming a small angle theta yields:

$$2\sigma_y A_e \theta = wL \tag{3.8}$$

Now applying Equation 3.1 and solving for the pressure at ultimate, p_u , Equation 3.8

becomes:

$$p_u = \frac{2\sigma_y A_e}{SL} \theta \tag{3.9}$$

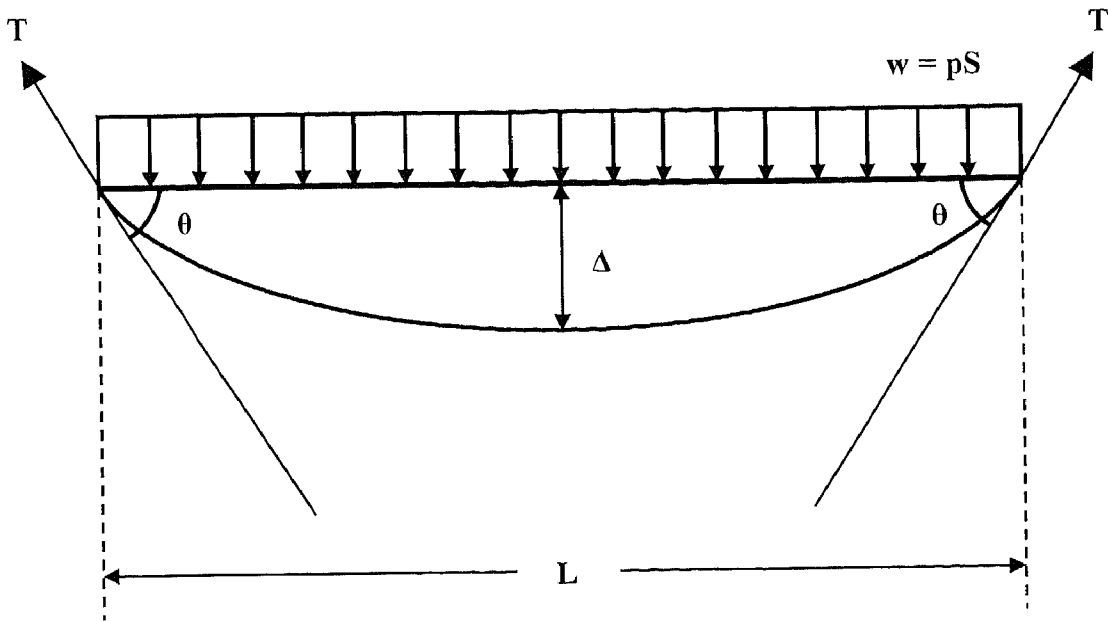


Figure 3.6: Stud Under Uniform Applied Loading

To determine the pressure at ultimate for a steel stud in a wall system, it can be seen from Equation 3.9 that a relationship between θ and the deformed shape of the stud needs to be established. To establish this relationship, a deformed shape has to be assumed and a relationship between θ and Δ , Figure 3.6, has to be obtained. From a number of tests performed on steel studs, it has been observed that a stud most closely follows the shape of a parabola. In the early stages of research, a deformed shape was assumed using a linear deformed shape (Roth 2002). But the calculations performed from the linear shape function did not compare well with experimental data.

To assume a deformed shape, the deflection was measured along the length of a typical beam that was tested. It was determined from the measurements of the deformed shape, that the stud closely follows the path of a parabola, Figure 3.7.

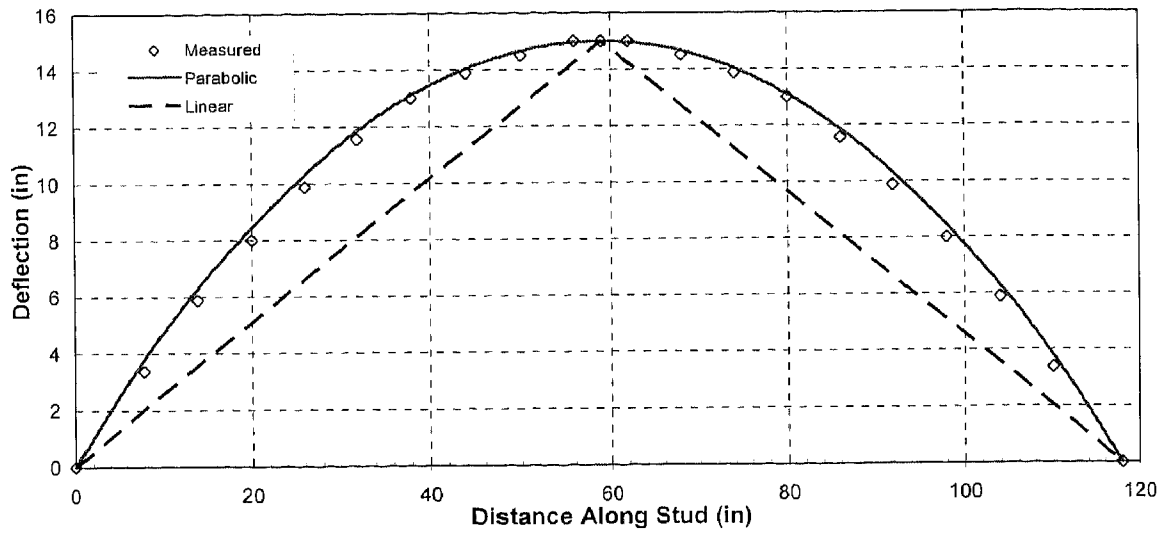


Figure 3.7: Comparison of Shape Functions at Max Load

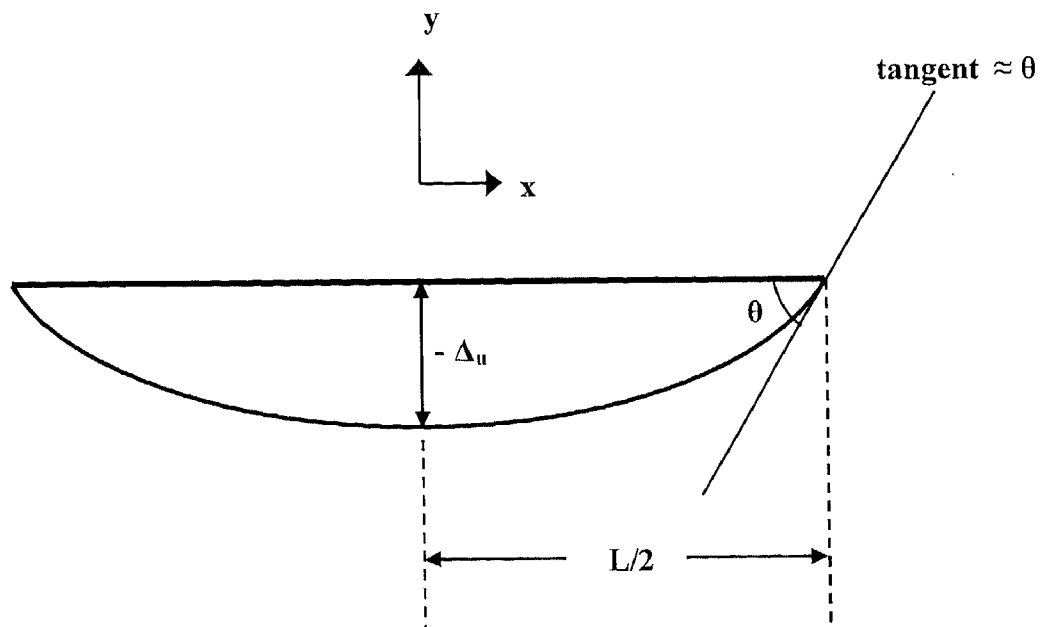


Figure 3.8: Parabolic Shape Function

Assuming a parabolic shape function, a relationship between θ and Δ_u can now be established to determine the ultimate pressure, Figure 3.8. An approximate equation for a parabola is used, Equation 3.10, and the following boundary conditions are applied to the parabolic shape function.

$$y = ax^2 + bx + c \quad (3.10)$$

Boundary conditions:

$$\text{At } x = 0: \quad y = -\Delta_u$$

$$y' = 0$$

$$\text{At } x = \frac{L}{2}: \quad y = 0$$

$$y' = \theta$$

Solving for a, b, and c results:

$$a = \frac{4}{L^2} \Delta_u$$

$$b = 0$$

$$c = -\Delta_u$$

and

$$y(x) = \left(\frac{4}{L^2} \Delta_u \right) x^2 + \Delta_u \quad (3.11)$$

Hence, the following relationship is obtained at $x = \frac{L}{2}$:

$$\theta = y' \left(x = \frac{L}{2} \right) = \frac{4}{L} \Delta_u \quad (3.12)$$

Substituting Equation 3.12 into Equation 3.9, the pressure now becomes:

$$p_u = \left(\frac{8\sigma_y A_e}{SL^2} \right) \Delta_u \quad (3.13a)$$

or in general:

$$p = \left(\frac{8\sigma_y A_e}{SL^2} \right) \Delta \quad (3.13b)$$

To determine the ultimate deflection, failure is assumed to be localized over a reduced cross-sectional area of a stud. This is valid in determining the deformed length since it is known that plastic strain is almost invariably localized. The letter xi, ξ , will be used to represent the localized cross-sectional area of a stud. From definition, ultimate strain is the change in length divided by the original length, or:

$$\Delta_\ell = \varepsilon_u \ell \quad (3.14)$$

where:

Δ_ℓ = change in length of the localized cross-sectional area

ε_u = strain at failure, ductility

ℓ = length of the localized cross-sectional area

Keeping Equation 3.14 in general terms, the length of the localized cross-sectional area is calculated as follows:

$$\ell = \xi L \quad (3.15)$$

where:

ξ = percent of the total length, L, that is assumed to be the length of the

localized cross-sectional area of a stud

L = total length of a stud

Substituting Equation 3.15 into Equation 3.14, the general form for Δ_f now becomes:

$$\Delta_f = \varepsilon_u \xi L \quad (3.16)$$

The deformed length, L' , of the stud is equal to the original length of the stud plus the change in length over the localized cross-sectional area, and is as follows:

$$L' = L + \Delta_f \quad (3.17)$$

Substituting Equation 3.16 into Equation 3.17 and only considering half of the stud length, Equation 3.17 now becomes:

$$\frac{L'}{2} = \frac{L}{2} + \left[2\varepsilon_u \xi \left(\frac{L}{2} \right) \right] \quad (3.18)$$

Equation 3.18 gives a deformed length based on a certain amount of ductility of a stud. Relating ductility to ultimate deflection is very important in predicting an accurate static resistance function. This is true because of the variability of material properties in the manufacturing of cold-formed steel studs. Ductility in steel studs can range anywhere from five percent elongation to fifty percent elongation, which significantly effects ultimate deflection.

To relate the ductility to the ultimate deflection, the definition of an arc length is used, which gives a relationship between the ultimate deflection and deformed length of a stud. The definition is as follows:

$$S = \int_a^b \sqrt{1 + [y'(x)]^2} dx \quad (3.19)$$

where:

$$S = \frac{L'}{2}$$

L' = deformed length of stud

Taking the first derivative of Equation 3.11 yields:

$$y'(x) = \frac{8\Delta_u}{L^2} x$$

Substituting this relationship into Equation 3.19 and applying the appropriate integration limits gives:

$$\frac{L'}{2} = \int_0^{L/2} \sqrt{1 + \left(\frac{8\Delta_u}{L^2} x\right)^2} dx \quad (3.20)$$

let: $a = 1$ and $c = \frac{8^2 \Delta_u^2}{L^4}$, Equation 3.20 becomes:

$$\frac{L'}{2} = \int_0^{L/2} \sqrt{a + cx^2} dx \quad (3.21)$$

Integrating with the use of an appropriate integration table, Equation 3.21 now becomes:

$$\frac{L'}{2} = \frac{2cx\sqrt{a+cx^2}}{4c} + \frac{4c}{8c} \left[\frac{1}{\sqrt{c}} \sinh^{-1} \left(\frac{2cx}{\sqrt{4c}} \right) \right]_0^{L/2} \quad (3.22)$$

Substituting the values of a and c into Equation 3.22 gives a relationship between the deformed length of the stud and the ultimate deflection at failure:

$$\frac{L'}{2} = \frac{2 \left(\frac{8^2 \Delta_u^2}{L^4} \right) \frac{L}{2} \sqrt{1 + \left(\frac{8^2 \Delta_u^2}{L^4} \right) \left(\frac{L}{2} \right)^2}}{4 \left(\frac{8^2 \Delta_u^2}{L^4} \right)} + \frac{1}{2} \left[\frac{1}{\sqrt{\frac{8^2 \Delta_u^2}{L^4}}} \sinh^{-1} \left(\frac{2 \left(\frac{8^2 \Delta_u^2}{L^4} \right) \frac{L}{2}}{\sqrt{4 \left(\frac{8^2 \Delta_u^2}{L^4} \right)}} \right) \right] \quad (3.23)$$

Equation 3.23 and Equation 3.18 can now be used to find the ultimate deflection.

With the use of these two equations, the deformed length is both a function of ductility (Equation 3.18) and ultimate deflection (Equation 3.23). The two equations can be set

equal to each other and solved numerically to determine Δ_u , which represents the ultimate beam deflection, based on a given value for ξ .

The value of ξ is directly affected by the ductility of the stud material. So now, the ultimate deflection can be determined for any stud if the ductility is known, and a value of ξ is selected. Once again, ξ represents the percent of the total length L that is assumed to be the localized cross-sectional area of a stud where most of the yielding occurs, and will be discussed more in Chapter 4, Section 4.3.4. Since the ultimate deflection is known, the pressure at ultimate can be determined from Equation 3.13.

Finally, the slope of the tension membrane region can be derived from Equation 3.13b for any value of p and Δ :

$$k_t = \frac{p}{\Delta} = \left(\frac{8\sigma_y A_e}{SL^2} \right) \quad (3.24)$$

Now the static resistance function can properly be predicted in the tension membrane region of behavior, for both the upper limit response and lower limit response. Each point on the resistance function has been defined as well as the slope in each of the regions. Again, properly defining the function throughout all regions of stud behavior is crucial for dynamic modeling a wall system. Now that the analytical static resistance function has been developed and is a function of stud size and material properties, the experimental data will be presented for further verification.

4 Experimental Verification

Now that the analytical static resistance function has been defined for each region of behavior, experimental data will be presented for verification. Once the analytical model has been verified experimentally, it can be implemented into design procedures.

In previous research at the University of Missouri-Columbia, the majority of the tests were conducted using a static vacuum chamber designed and constructed by Brown (2003). Since testing complete wall systems in the vacuum chamber is so time consuming, only a limited number of walls were tested. Because of this limitation, a general static resistance function was developed using a limited amount of data. Testing complete wall systems using the vacuum chamber present a number of other problems as well, and therefore testing wall system components via a “loading tree” is essential in current research.

Component testing is much faster and cheaper than testing complete wall systems. With the ability to test the designs of more steel studs and the connection detail, an analytical static resistance model based on both theory and test data was more accurately developed. After developing the model, it can now be verified using a number of experimental tests. Component testing of the wall systems, such as one stud or a stud

pair, allows for an analytical resistance model to be verified through testing, rather than testing to develop a resistance model.

In this chapter, an overview of previous testing will be presented, including different experimental setups as well as different design concepts. The need for component testing of wall systems and the development of a good working experimental setup for component testing will be described and discussed. And finally, experimental verification of the analytical model through a number of different tests will be given.

4.1 INTRODUCTION

Laboratory and field experiments have recently been conducted to understand the blast capacity of steel stud wall systems and to verify the design of the anchorage of steel studs into the structure (Dinan et al. 2003, Shull 2002). In blast design, it does not suffice to have strength alone, rather, a wall system must be able to deform plastically to absorb energy. Steel studs used for construction have the desired combination of strength and ductility for blast resistance.

Proper anchorage of the steel studs, which allows for development of the tensile membrane capacity of the steel stud wall, is crucial in resisting a dynamic load after the yielding of steel. The tensile membrane capacity enables a wall system to absorb much of the energy that is exerted during a blast.

4.1.1 Experimental Setups

As previously mentioned, testing complete wall systems via the static vacuum chamber has been the primary focus of past steel stud research at NCERD, as discussed by Muller (2002). The static vacuum chamber is essentially a box with one open face where a steel

stud wall system can be built and tested. With the wall system in place, a latex membrane is placed over the open face of the box to seal the chamber and create a vacuum.

The vacuum is created inside the chamber by a vacuum pump, and in turn applies an atmospheric pressure to the outside of the wall. The atmospheric pressure creates a uniform lateral pressure on the wall system. The pressure exerted on the wall system as well as the displacements and strains the steel studs undergo can all be recorded using National Instruments' Labview® data acquisition system.

Flexural testing using three-point and four-point bending creates a faster and more efficient way of obtaining experimental data. The results from the four-point bending tests were comparable to AISI predictions, however, certain problems did exist. For example, failure mode and out-of-plane rotation in the linear elastic phase of the stud did not represent behavior of a wall system (Muller 2002). Three-point bending tests were also performed, however, failure resulted from web crippling and did not offer much insight on connection behavior. Three and four-point bending tests results can be used for comparison in the elastic region of behavior, but they are not suitable for exploring inelastic region of behavior.

Limitations in the vacuum chamber as well as the limitation of three and four-point bending tests have increased the need for a more beneficial method of testing. This need led to the development of the "bending tree." The bending tree can be used to gain insight in the elastic region of behavior, inelastic region of behavior, and failure at high loads. The experimental setup of the bending tree and its capabilities will be discussed in more detail in Section 4.2.

4.1.2 Design Concepts

The original concept for anchoring steel studs into the floor and ceiling slab of a structure is referred to as a clipped and bent flange connection (DOS 2001). This concept involved cutting of a steel stud approximately 6 inches from the end of a stud and bending the web at a 90-degree angle to form bent leg. A hole was then punched in the center of the leg to anchor the stud at the top and bottom to the structural system. This method of construction allows for quick and easy construction in the field. This method was used successfully in a dynamic field experiment, EWRP-2, and described by Wesevich (2001).

However, this type of connection detail does not significantly increase the tension capacity of the stud from that of the conventional two-screw method, discussed later in this section. Connection failure with this type of configuration usually happens before significant tension membrane is achieved. Studs typically fail at the connections from a crack initiating at the anchor hole and propagating outward. The crack at the anchor hole results in the hole becoming oversized and the bent flange pulling out over the anchor in complete connection failure, Figure 4.1.

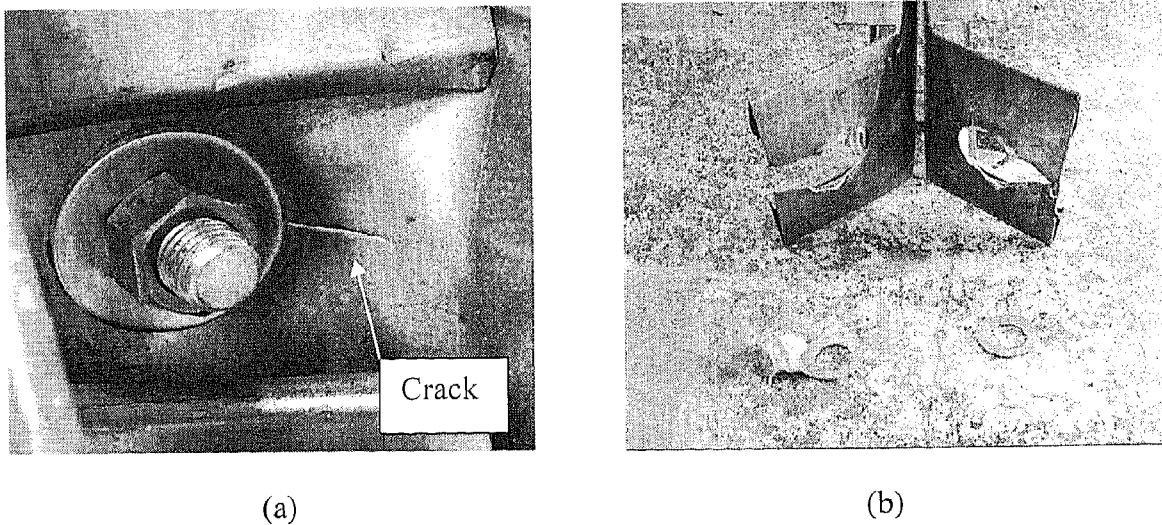


Figure 4.1: Connection Failure (a) Crack Propagating (b) Bearing Failure

As just mentioned, with this type of connection failure, the stud does not experience significant tension membrane action. It can be observed from the load-deflection response, Figure 4.2, that a limited amount of inelastic response is achieved, which is not desirable for blast resistance. The clipped flange test seen below only experienced about 50% more load than it did at yield-buckling load. This test experienced higher loads than any of the other clipped flange tests conducted. In other tests, connection failure happened after softening and before the load reached the initial buckling load. This method of connection does not greatly increase the connection capacity from that of the conventional two-screw method, because of the bearing failure described.

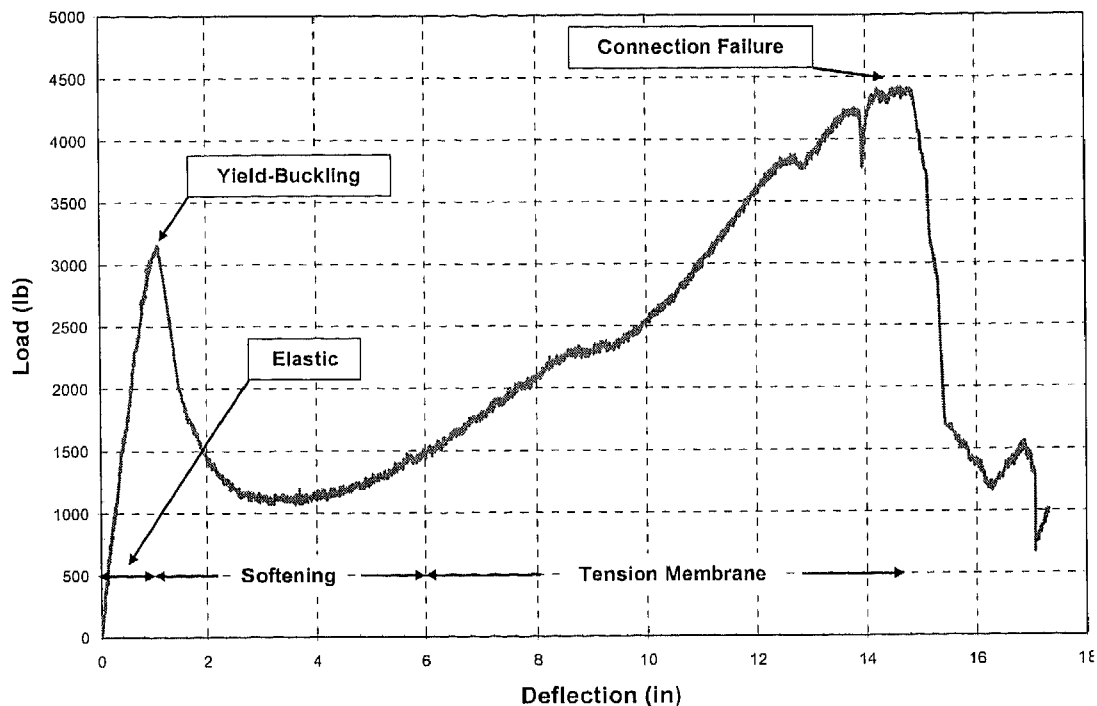


Figure 4.2: Load-Deflection Response of Clipped and Bent Flange Connection Test

Another concept for anchoring steel studs into the floor and ceiling slab of a structure in conventional design is referred to as a non-load bearing wall system (Muller 2002). These non-load bearing walls are typical of military construction in accordance with the TI-809 (1998), army stud wall standards. The term non-load bearing implies that vertical loads to the surrounding structure are not transferred to the steel stud wall system. This is accomplished through the use of a slip-track connection at one end of the wall system, Figure 4.3. The other connection is a pinned connection achieved by screwing the stud directly into the track using two, or sometimes four, self-tapping screws. It has been determined through experimental testing that these screw connections are insufficient in developing the full tension membrane capacity of the steel studs.

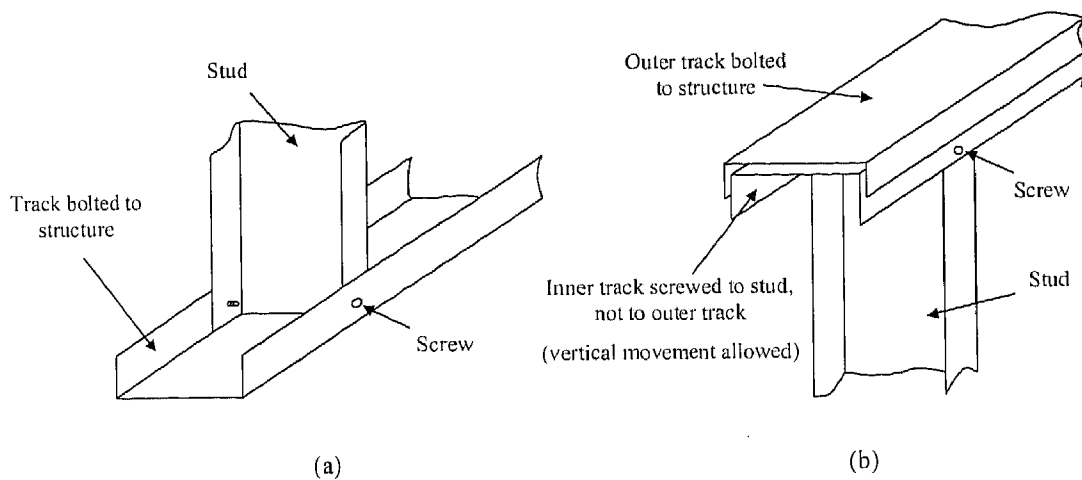


Figure 4.3: Non-Load Bearing Connection (a) Bottom Track (b) Slip Track (Muller 2002)

The key to utilizing steel studs in a blast resistant wall system is designing for stud failure from yielding of the steel stud cross-section in tension, and eventually failing due to the strain elongation limits at the yielded cross-section (Dinan et al. 2003). Connection failure in testing, like that of the clipped and bent flanges and the non-load bearing wall systems, is not a desirable type of failure when designing against blasts. Utilizing the stud strength as well as its ductility allows for significant energy-absorption during plastic elongation of the steel stud. This ductile behavior also reduces reaction forces where the stud connects to the floor and ceiling slab. The idea of minimizing the line loads at the floor and ceiling by utilizing the full region of stud behavior is important in design and will be discussed in further detail in Section 5.1. To utilize the full region of stud behavior, an adequate stud to structure connection is needed.

4.1.3 Steel Stud Retrofit Connection

To utilize both the strength and ductility of a stud, the connection capacity must exceed the tensile yield capacity of the stud. This can be done with the use of a steel angle to

connect the steel stud to the structure. The approach to designing the required anchorage requires proper bolt spacing for angle to stud connection, and proper anchorage base plate thickness to connect the angle to the structure (Shull 2002). The basic connection geometry development and verification was obtained using AISI design specifications and from a series of tensile and bending tests, described in detail by Shull (2002).

The concept chosen for development utilizes a steel angle that is slightly narrower than the width of the steel stud web. The vertical leg of the angle connection attaches to the web of the stud using six bolts and the horizontal leg of the connection attaches to an anchor bolt in the floor and ceiling slab through a pass hole in the angle. The four basic failure modes the angle connection was designed to prevent are the following:

1. Shearing failure of the six connecting bolts
2. Block shear failure of the steel stud material in the bolt pattern
3. Bearing tear out of the stud material directly below the bolt holes
4. Cross-sectional tension failure of the steel angle

4.1.4 Proposed Anchorage Plate Design

From obtaining a basic geometry connection design from AISI and from Load Factor Resistant Design Code (LRFD) design equations and from verifying this connection design through the use of tensile and bending tests, an adequate steel angle connection design was achieved. This angle, which allows for desirable stud performance, consists of ½” steel angle, with the vertical leg attaching to the steel stud using six bolts, and the horizontal leg anchored to either the floor or ceiling slab using an anchor bolt. The critical factor controlling the thickness of the steel angle material is bearing failure of the anchor. Pullover of the anchor bolt that is used to attach the steel angle to the floor or

ceiling slab had to be prevented, resulting in a conservative angle thickness. Details of the angle connection are shown in Figure 4.4 and are discussed in more detail by Shull (2002).

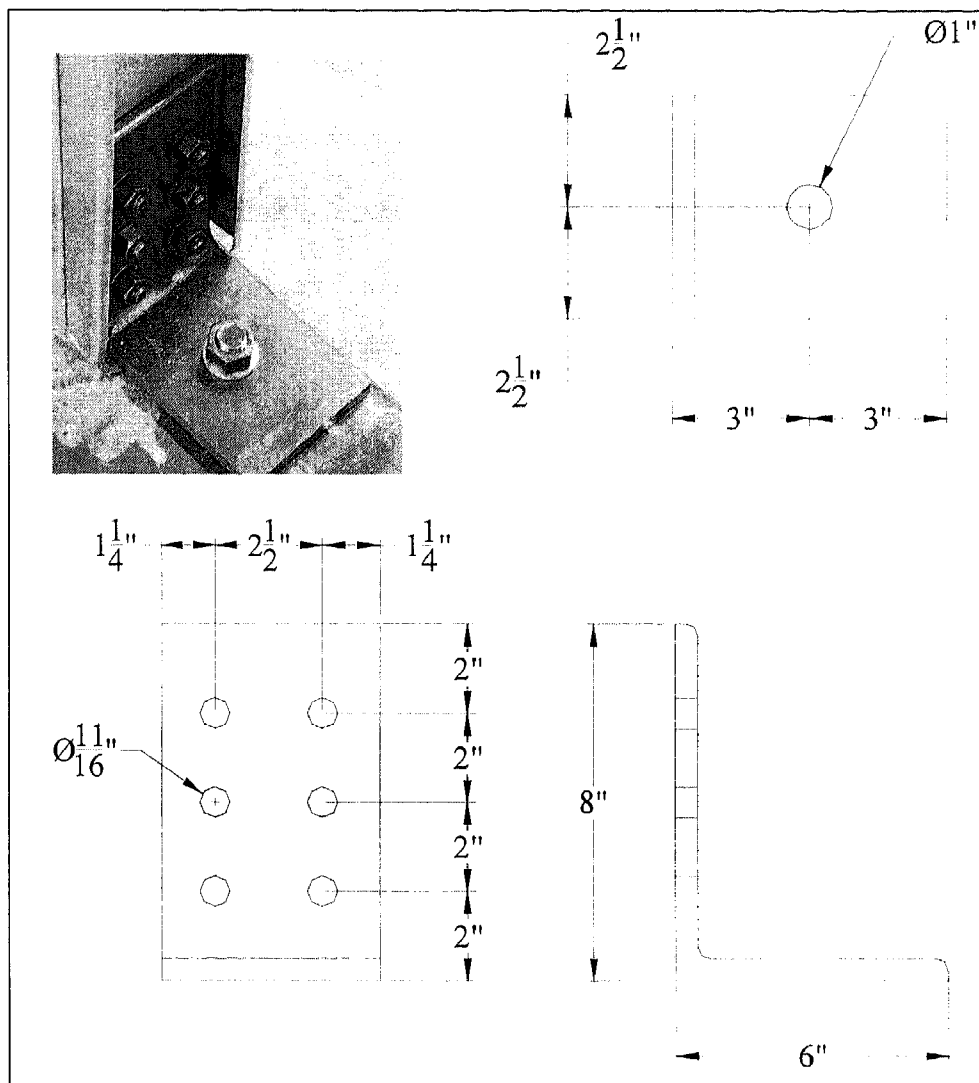


Figure 4.4: Stud-to-Floor Anchorage using a 1/2-in Thick Steel Angle Connection

The connection details have been developed and tested and the analytical static resistance function has been predicted, the next step is to determine the load-deflection response of a transversely loaded steel stud wall system, which can be used in dynamic modeling. The determination of a load-deflection response can be obtained by using an experimental test setup described in Section 4.1.1. As previously stated, the majority of the wall systems tested at the University of Missouri has been conducted using a static vacuum chamber. (See Appendix I, Figures A1.1 – A1.4, for a typical steel stud wall system test) However, due to limitations of the vacuum chamber and high costs, an alternative way of tested is needed.

4.2 COMPONENT TESTING VIA THE BENDING TREE

The problem with testing full-scale walls in a vacuum chamber is that each test is quite expensive to conduct and requires many hours of labor. Each time a wall is tested, there are design changes that need to be made to the wall. Some changes are very significant, while other changes are very small, such as adding an extra screw to a steel stud. Testing with the vacuum chamber is very beneficial in defining a static resistance function for steel stud wall systems, but this type of testing is costly. Limitations in the vacuum chamber have also created a need for a different type of testing. Pressure created in the chamber can only exert a certain amount of load on a steel stud wall, which is restricted by atmospheric pressure.

Flexural testing of the wall components creates a much more efficient means of acquiring needed data. Information from component testing can then be verified by

available wall testing results. One way to test at the component level is by using a “loading tree” with a number of point loads that simulate a uniform load.

A wall test using the vacuum chamber requires many days of construction and high material expenses while testing with the bending tree is much easier to perform. Many different component tests can be conducted in one day, with material expenses being only about 1/10 of the full-scale material cost. A system called the mechanical testing and simulation, or the MTS, is used during testing and is capable of applying much higher loads than atmospheric pressure.

The idea of a loading tree or whiffle tree has been around for many years. People have been using them for experimental testing for over a hundred years. They can be as simple as a few beams connected together like the one described in this thesis, or as complicated as three dimensional trees for testing thin shelled structures consisting of hundreds of individual beams and plates used at Universities throughout the world. The one used in this experiment is relatively simple consisting of four beams on the lowest tear.

4.2.1 Experimental Evaluation Techniques

The system used on the component level is capable of performing deflection controlled testing while the vacuum chamber can only perform load-controlled testing. When performing an experiment with load-controlled testing, the load applied to the wall is increasing at a constant rate, which is not ideal during the yielding of steel. However, with deflection controlled testing, the load depends on the beam’s resistance. During the yielding of steel, the load drops and the deflection remains at a constant rate, which gives a more accurate pressure-deflection curve through enhanced data acquisition.

The test setup consists of a structural steel loading frame where a 110 kip actuator is attached and connected to the MTS control module, shown in Figure 4.5a. The loading tree utilizes mechanical distribution of the load applied to simulate approximate uniform load along eight loading points. In the setup, the load is applied by the actuator and disperses throughout a mechanical system of beams with pinned connections. The mechanical beams then transfer the distributed load to the beam specimen through eight point loads. The loading points are spaced over a span of 120-in, which makes the spacing in between each load 15-in, and the spacing between the end loads and the support 7.5-in, shown in Figure 4.5b.

Heavy duty 1-ply web sling nylon straps with twisted eyes are used in testing to avoid stress concentrations in the steel beam. In a previous test, steel rods were used to apply the load to the beam which caused local crippling from concentrated stress. These nylon straps act softly and disperse the point loads throughout the length of the beam. As the beam deforms, the bending tree follows the shape of the beam, while keeping the fraction of the total load at each loading point constant.

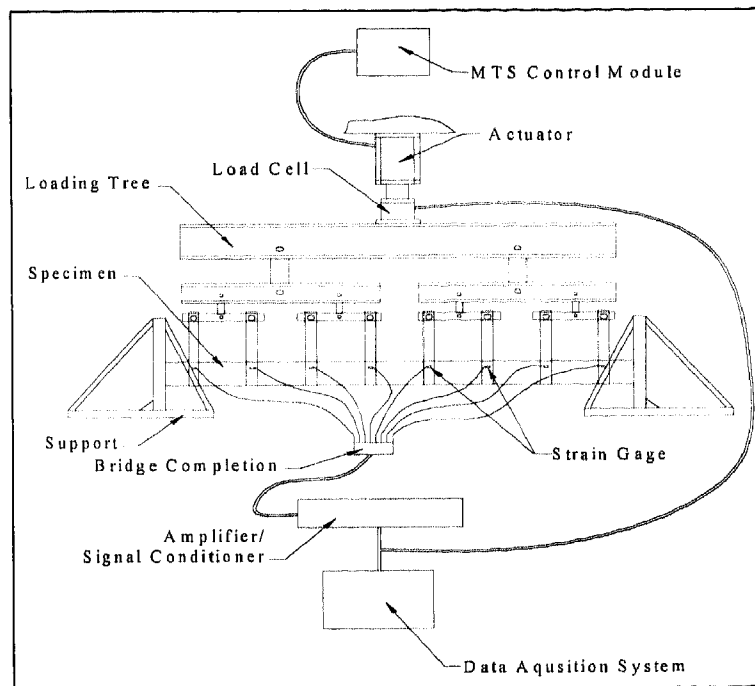


Figure 4.5a: Component Testing Setup

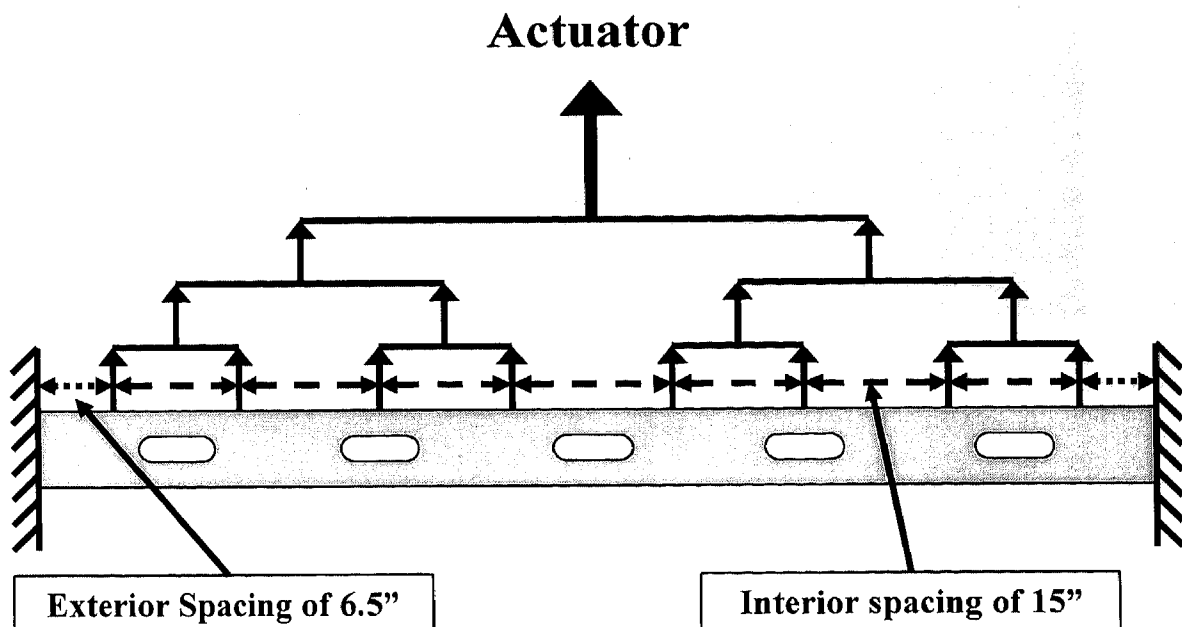


Figure 4.5b: Load Spacing of Mechanical Tree

The setup also includes a system for bracing the beam to prevent lateral torsional buckling. The bracing system used in these tests includes four vertical T-beams that are adjustable to account for different size beams. The braces use a sliding system to move next to the beam tightly to prevent the beam from traveling in the path of least resistance, Figure 4.6.

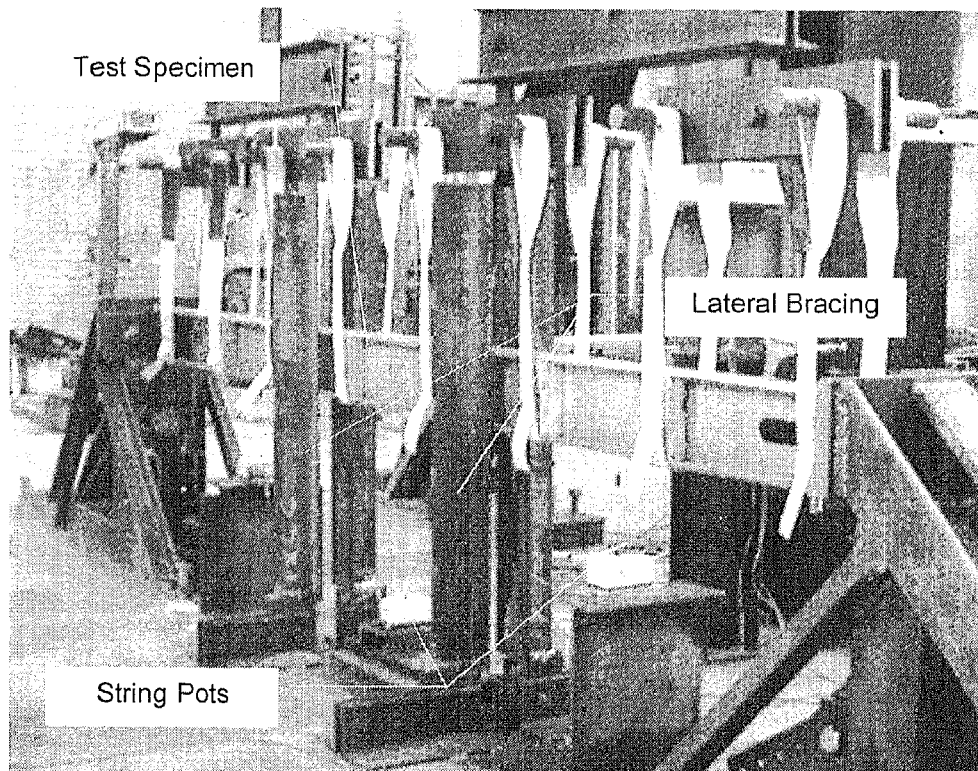


Figure 4.6: Bracing System used in Testing

Three string potentiometers are used during testing to record the deflection at quarter points along the beam. The load applied to the beam and deflection of the beam are both recorded using a data acquisition system. The supports used in the testing were built to be used for various types of connections.

To prove the validity of testing steel studs using the bending tree, the results must be compared to that of the complete wall systems tested up to this point. When testing using the vacuum chamber, a uniform pressure is applied to the wall and recorded with time. The amount of deflection that the beam experiences can then be correlated to the amount of pressure that is applied to the wall in pounds per square inch (psi). When testing using the bending tree, a load is applied to the beam by the actuator which disperses through the mechanical tree and into the nylon straps which transfer the load along the beam at eight points in a uniform fashion. The amount of deflection the beam experiences depends on the amount of load that is applied in pounds (lbs). Therefore, to compare the results obtained from each test, the load applied in the component bending test needs to be related to the pressure applied in the vacuum chamber wall test.

4.2.2 Maximum Moment Equivalency

One method for relating the load applied by the bending tree P , and the pressure exerted on the wall p , is by using the maximum moment equivalency concept. This is a good method to use since it is equilibrium based, as compared to the maximum deflection equivalency, which is true only for the elastic behavioral region. Using the maximum moment equivalency, the moment is calculated by summing the forces applied around the mid-point of the steel stud. The forces acting upon the stud can be seen in Figure 4.7.

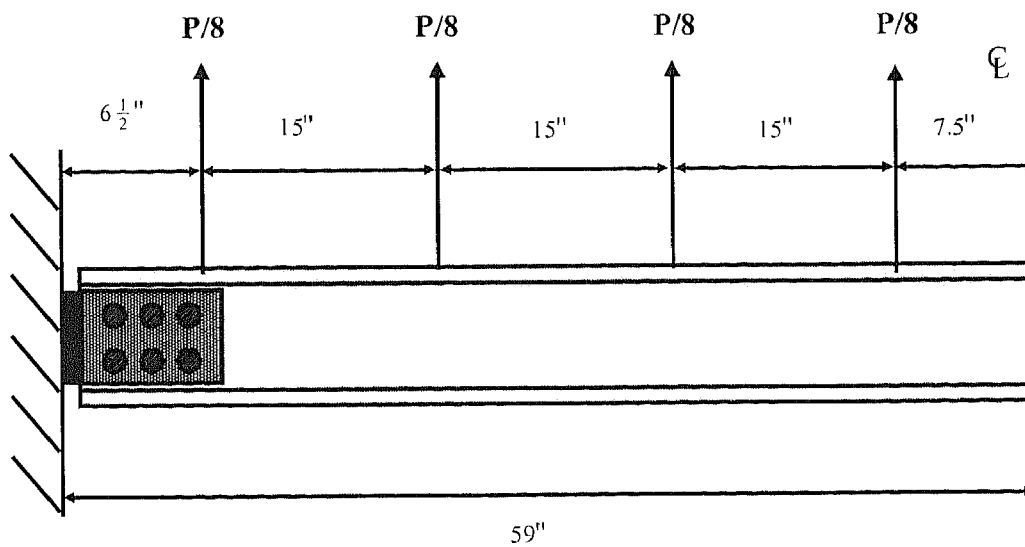


Figure 4.7: Load Applied to Steel Stud with Steel Angle Connection

Summing the moment about the center-line of the beam, the moment applied is as follows:

$$M = \frac{P}{2}[59.5] - \frac{P}{8}[7.5 + 22.5 + 37.5 + 52.5]$$

$$M = 14.75P \quad (4.1)$$

Assuming uniform loading over the length of the beam, the moment applied to the beam is:

$$M = \frac{wL^2}{8} \quad (4.2)$$

Since the spacing of the steel studs in the wall systems tested are 16-in apart, it can be said that $w = 16p$. Substituting the moment calculated from the bending tree, Equation 4.1, and substituting the load equivalent from the spacing of the full scale wall into Equation 4.2, the moment equation becomes:

$$14.75P = \frac{16pL^2}{8}$$

Substituting in the span length of 118-in and solving gives the relation needed between the equivalent pressure, p (psi), and the total load applied by the actuator, P (lbs).

$$p = \frac{P}{1888} \quad (4.3)$$

The maximum moment equivalency will be the primary method of comparing component tests with the bending tree to the wall system tests with the vacuum chamber.

Changes continue to take place with the bending tree to improve the experimental testing setup. One improvement to the bending tree is a change in the spacing of the load application from eight point loads to sixteen point loads, Figure 4.8. It is believed that the change in spacing creates a more uniform load applied to the beam, comparing better to the uniform pressure applied to a wall system using the vacuum chamber.

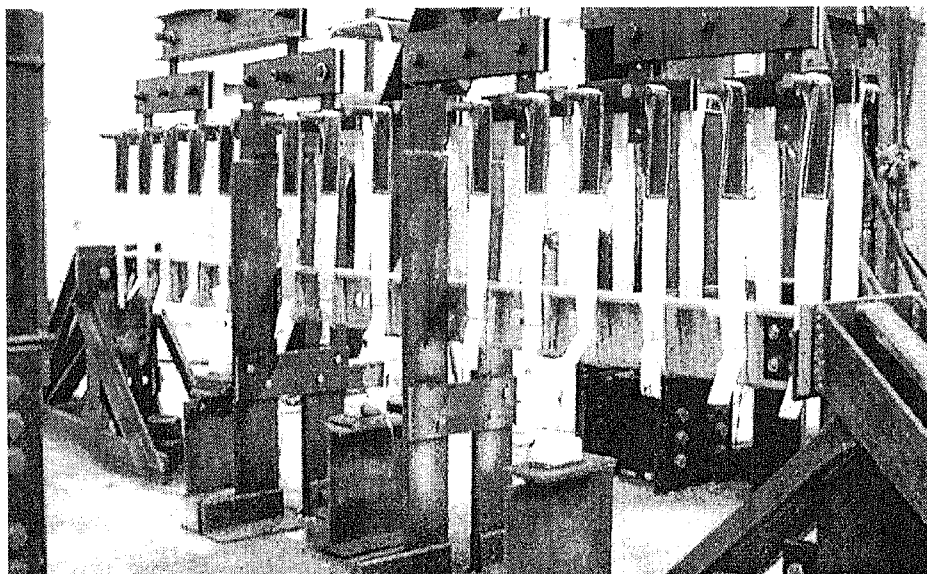


Figure 4.8: 16-point Load Application with the Bending Tree

A good experimental testing setup has been developed to test steel stud component beams via the bending tree. An accurate method of relating load applied to a steel stud in the bending tree and pressure applied to a wall system in the vacuum chamber has been discussed. A proper connection has been developed to attach the steel studs into a structural system. In the next section, experimental data for tests conducted will be presented to verify the analytical model developed in Section 3.2.

4.3 EXPERIMENTATION

As mentioned previously, the key to utilizing steel studs in blast resistance is to design for stud failure, as opposed to connection failure. To utilize both strength and ductility, connection capacity must exceed stud capacity. Due to the limitations and complications that connection detail adds to a steel stud wall system, a steel hinge connection was conceived to create a “true” pin-pin connection and designed in such a manner to eliminate connection failure. The steel hinge connection tests are not considered for field implementation, but rather for academic purposes.

The steel hinge connection test provides a good way of analyzing the behavior of steel studs in the bending tree and comparing to that of a wall system. It also allows research to focus on utilizing stud strength and ductility through cross-sectional failure. In this section, experimental data will be presented for both steel hinge tests as well as steel angle tests. First, the connection details of each test connection will be discussed.

4.3.1 Steel Hinge Connection

For the hinge connection, steel hinges attach the cold-formed steel studs to the support system, which are designed to allow free rotation. The hinges were designed by Shull (2002), and their details are given in Figures 4.9 and 4.10.

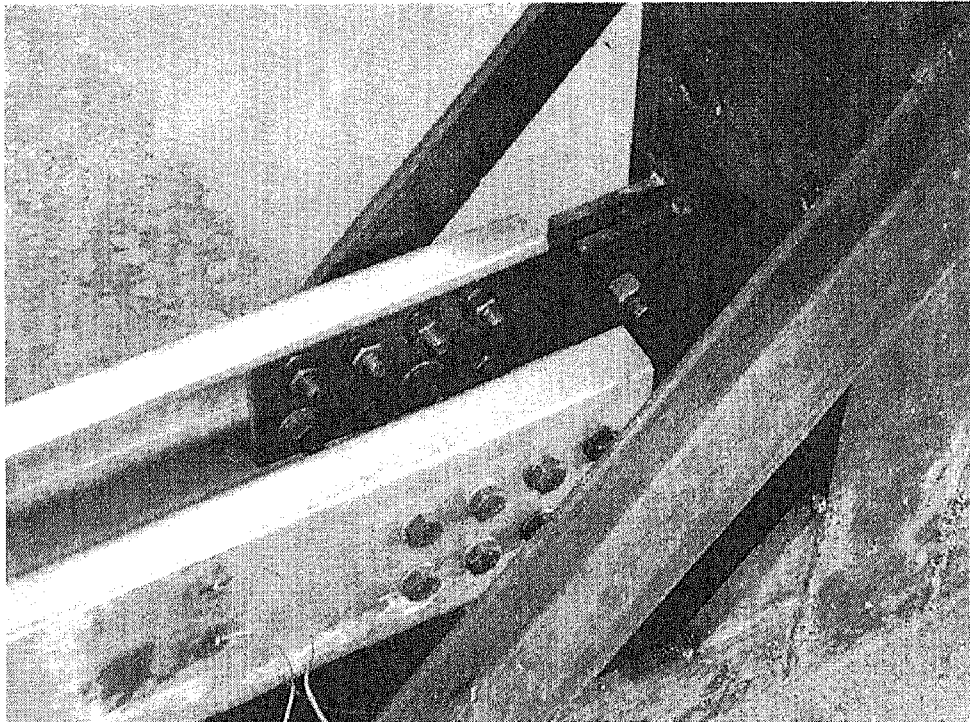


Figure 4.9: Steel Hinge Connecting Studs to Support System

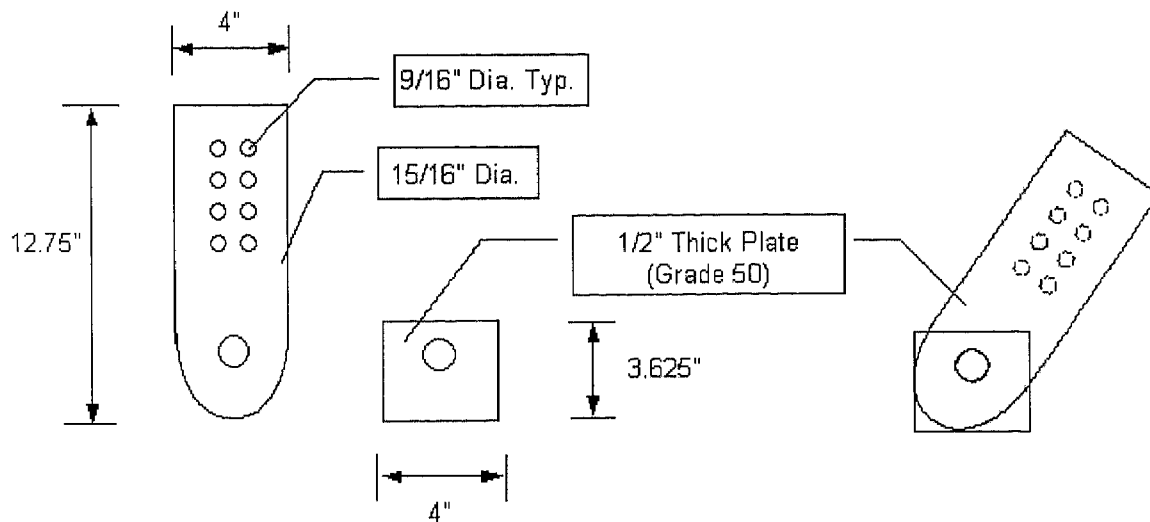


Figure 4.10: Steel Hinge Details

The goal of testing in the bending tree is to imitate one stud or stud pair in the same manner it is tested in a wall system with the vacuum chamber. When steel hinge connection tests are performed using the vacuum chamber, steel sheathing is placed on the outside of the studs to create a surface for the latex membrane. Steel strapping and wood blocking is used to prevent torsional buckling of the studs after the studs yield. Therefore, steel sheathing, straps, and wood blocks are implemented into bending tests to keep testing consistent.

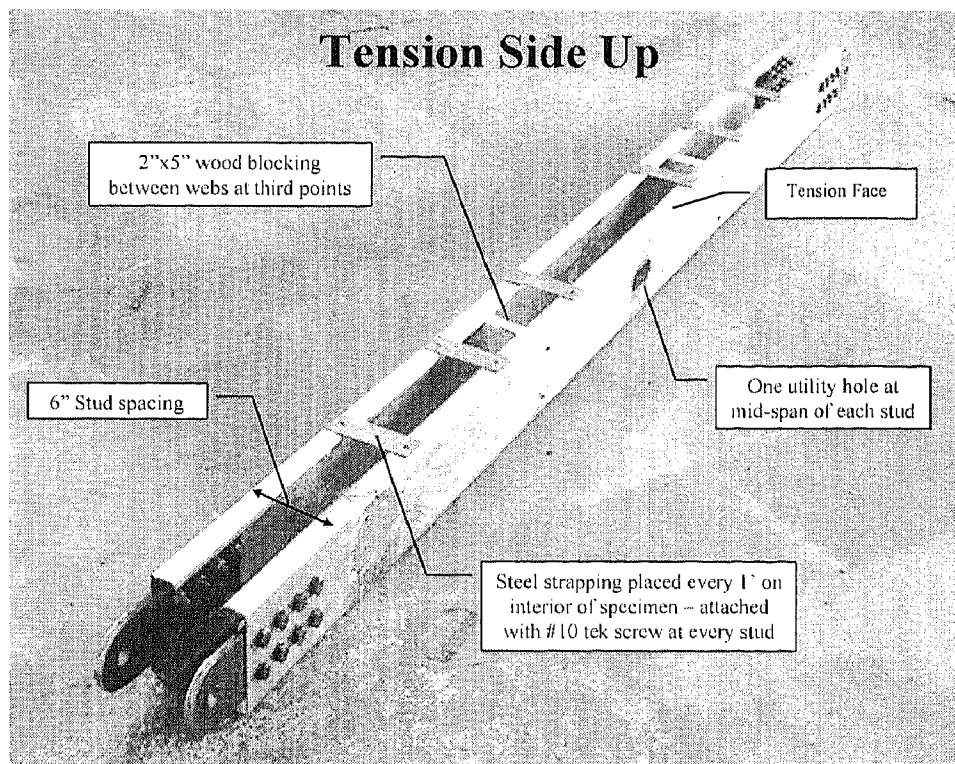


Figure 4.11: Fully Constructed Steel Hinge Test Specimen (Tension Face)

Shown above, Figure 4.11, is a fully constructed steel hinge test specimen before testing. The steel studs are spaced 6-in apart. Three steel straps are placed at every foot above and below the utility hole and 2-in x 5-in wood blocks are placed at third points for stability. The steel straps are connected to the stud using one #10 tek screw and the wood blocks are secured in place by screwing two #6 x 1¼-in drywall screws on both sides of the block.

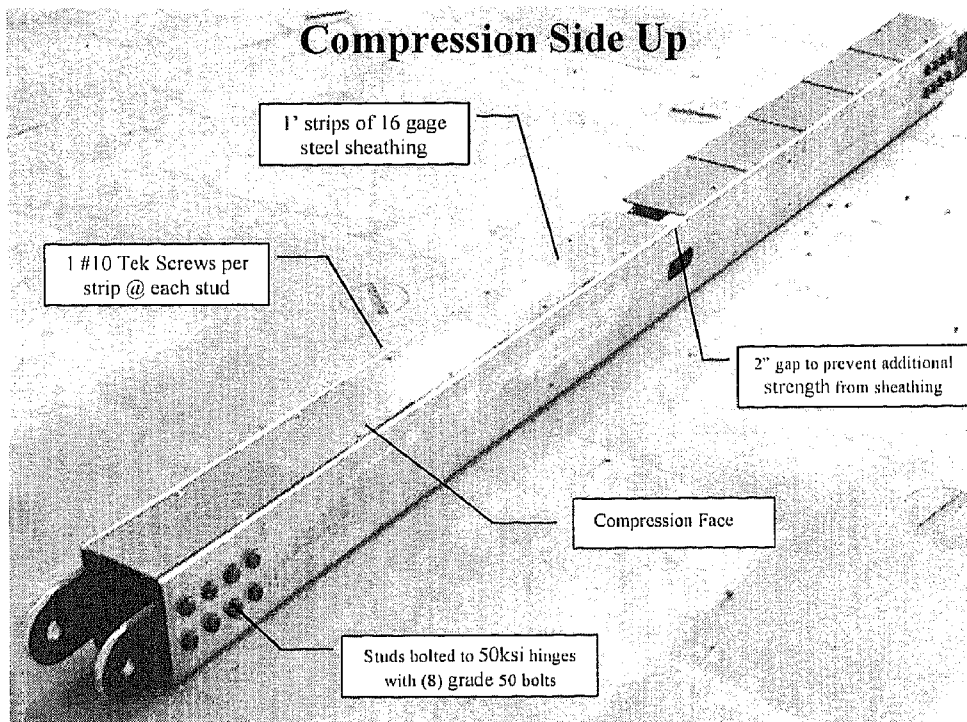


Figure 4.12: Fully Constructed Steel Hinge Test Specimen (Compression Face)

One foot strips of steel sheathing are placed on the compression face of the specimen using one #10 tek screw for each strip at each stud. A 2-in gap is placed in the steel sheathing at mid-span to prevent any composite action that the sheathing may add to the specimen, and are overlapped to allow slipping. The steel hinges are connected to the studs using eight Grade 50 bolts.

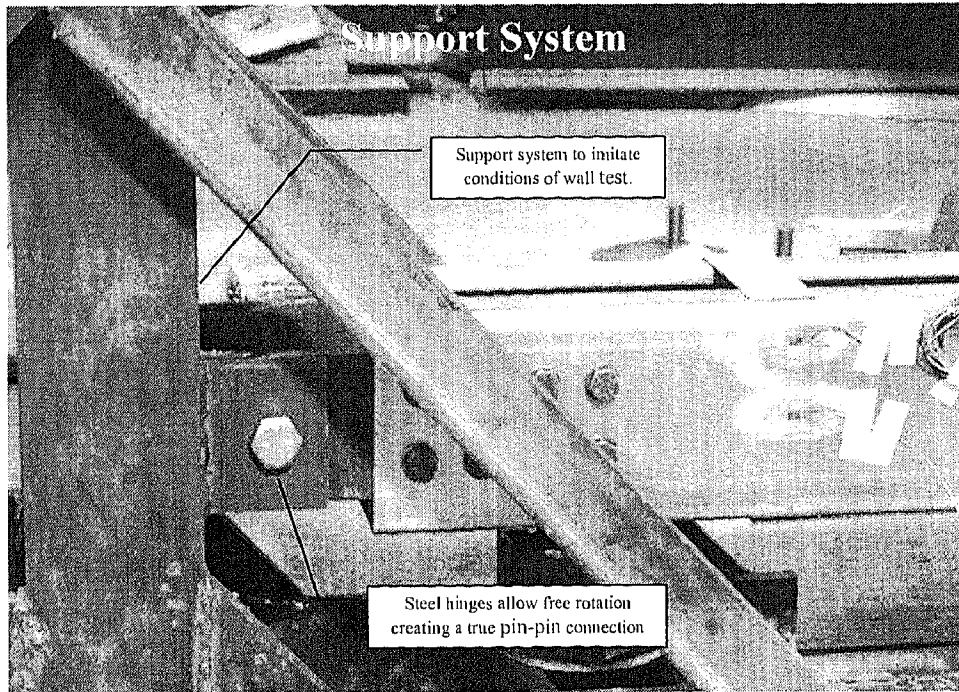


Figure 4.13: Steel Hinge Specimen in Testing Apparatus

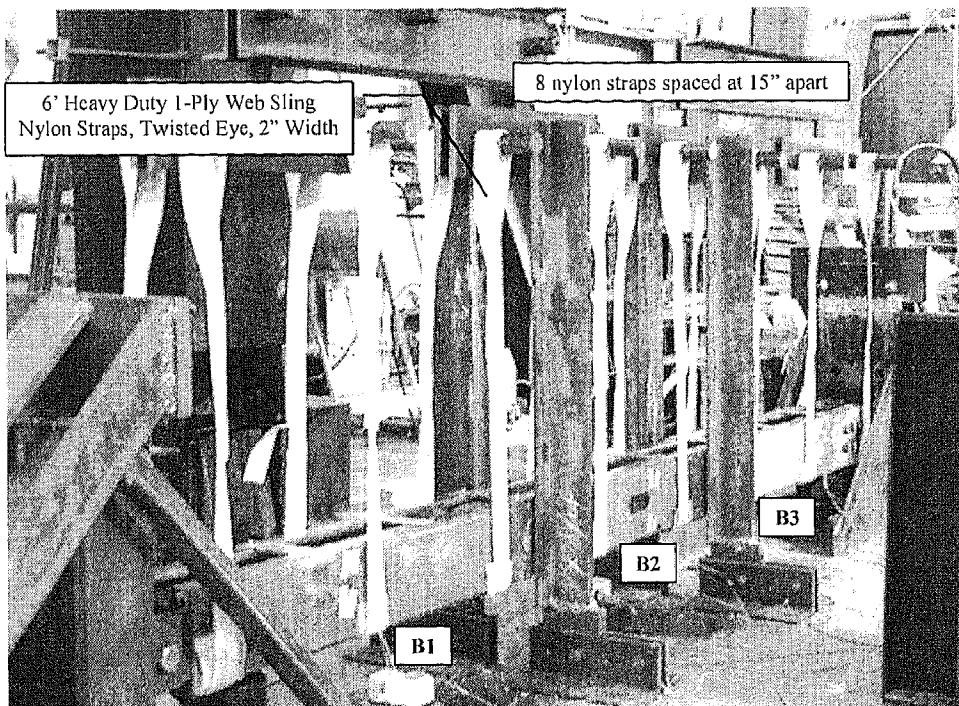


Figure 4.14: Steel Hinge Specimen with Nylon Straps Attached to Tree

When the steel hinge specimen is fully constructed and ready for testing, the steel hinges are connected to the support system using one $\frac{7}{8}$ -in grade 50 bolt at each hinge to allow free rotation of the stud, Figure 4.13. Eight nylon straps are used along the length of the stud and spaced at 15-in apart to simulate uniform pressure created in the vacuum chamber, Figure 4.14. The nylon material is a soft material that allows high loads to be applied to the stud without causing stress concentration points resulting in local buckling. The heavy duty nylon straps used are 6-ft long and 2-in wide, one ply web sling with a twisted eye and are rated to carry a load of 6400-lbs each.

Three string potentiometers (B1, B2 and B3) are used at quarter points along the length of the beam to record deflection measurements, Figure 4.14. A spot weld is used to attach a piece of wire to the specimen to avoid drilling holes in the beam or sheathing, which could affect the behavior. The small weld is attached to the outside of the steel to keep from changing the material properties. B2 is attached to the specimen at mid-span and is connected with a piece of wire to the stud. B1 and B3 are attached at quarter points and are connected with a piece of wire to the steel sheathing.

4.3.2 Steel Angle Connection

The plate design for the steel angle connection is discussed in Section 4.1.4. In this type of test, a 65-ksi 6-in x 8-in x $\frac{1}{2}$ -in structural angle is used to connect the steel studs to the support system. Six (2 rows with 3 bolts in each row) $\frac{5}{8}$ -in Grade B7 bolts spaced 2-in apart with the rows being spaced at 2 $\frac{1}{2}$ -in apart. A 24-mm Grade B7 ($f_{u \text{ min}} = 150,000$ -ksi) is used to anchor the steel hinges to the support system and are placed at the center of the angle base. The angles are placed back to back with two steel studs in between them.

The studs are punched to match the bolt pattern on each angle and standard structural washers were used on each connection.

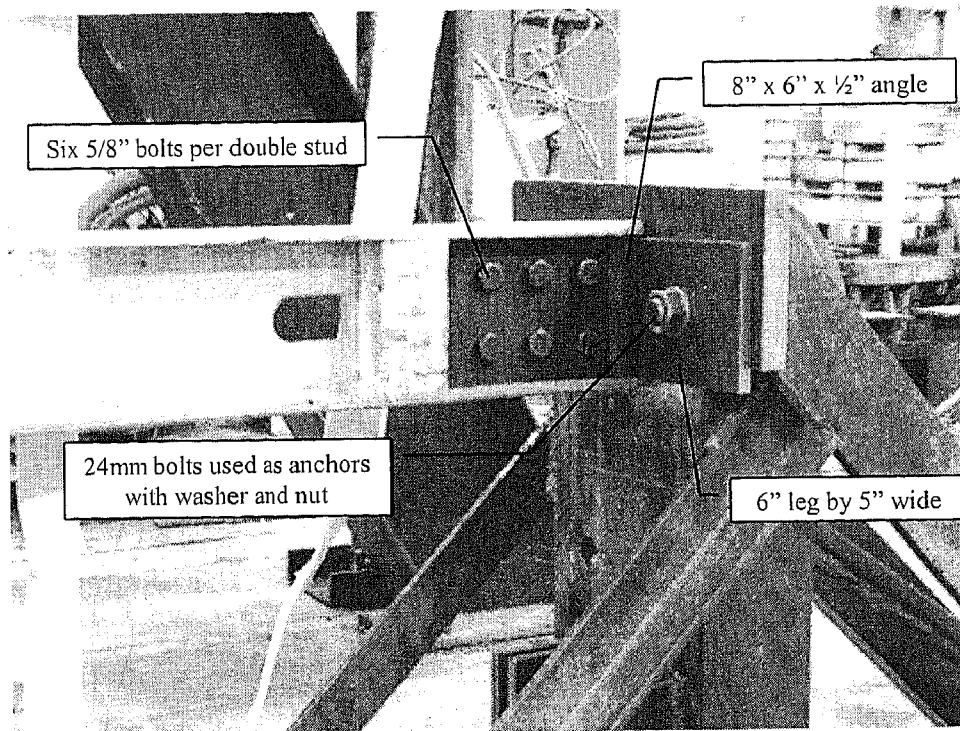


Figure 4.15: Steel Angle Connecting Studs to Support System

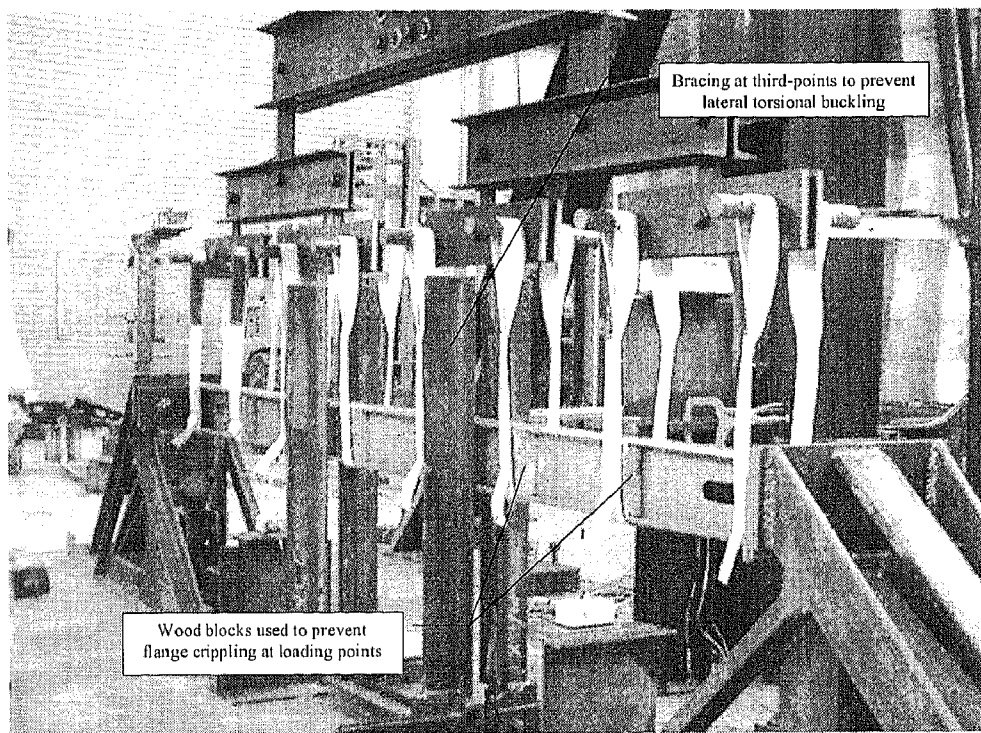


Figure 4.16: Steel Angle Specimen with Nylon Straps Attached to Tree

A bracing system is used at third points to prevent torsional buckling after the studs yield. 2-in x 5½-in wood blocks are placed in the C-section of the cold-formed steel studs at the loading points to avoid crippling of the flange, Figure 4.16. Steel sheathing, steel straps, and wood blocking are all used for the steel angle connection during wall tests in the vacuum chamber. When testing using the bending tree, since the studs are placed back to back, no sheathing or steel straps are used.

Wood blocking is used in between the flanges, but not in between the studs like they are used for the steel hinge connection test. #10 tek screws are used to secure the studs to each other and are screwed through the webs of both studs. The screws are staggered 12 inches apart along both the top and bottom portions of the web. The screws are used in testing to keep the steel studs from separating from each other high stress.

Three string pots are used and setup in the same manner as with the steel hinge connection test. The same procedure is followed as with the steel hinge connection to attach the three string pots to the steel stud. For the steel angle connection setup, all three spot welds are done directly on the steel stud, since there is not any sheathing on the studs. The same type of nylon straps and strap spacing are used for both steel hinge and steel angle tests. The only difference is the length of the straps. For the angle connection setup, 4-ft straps are used because the angles attach higher on the support system and are closer to the bending tree. Now that each type of tests setup has been discussed in detail, the experimental results will be presented.

4.3.3 Experimental Results

A summary of results from a number of different tests will be given in this section using both the steel angle and steel hinge connection. Results from wall systems tested in the vacuum chamber will be compared to stud pairs tested in the bending tree. The static resistance function obtained from testing will be compared with the static resistance function predicted in Chapter 3.

Cold-formed steel studs are used in all of the tests performed. Stud section properties necessary for the purposes of this thesis are included in Table 1 (for more detailed stud property information specified by the manufacturer, refer to Clark Manual (2000)). All the experimental results included in this thesis are for a unit width of the wall (psi/in).

Table 1: Cold-Formed Steel Stud Section Properties

Stud Section Properties											
Designation	Gage	Depth (in)	Thickness (ln)	A (in ²)	Weight (lb/ft)	I _{effec} (in ⁴)	S _{effec} (in ³)	EI (lb-in ²)	EA (lb)	M _{yield} (lb-in)	F _{yield} (ksi)
600S162-43-33	18	6	0.0451	0.447	1.52	2.316	0.767	6.95E+07	1.34E+08	25311	33
600S162-43-50	18	6	0.0451	0.447	1.52	2.316	0.767	6.95E+07	1.34E+08	38350	50
600S162-43-75	18	6	0.0451	0.447	1.52	2.316	0.767	6.95E+07	1.34E+08	57525	75
600S162-54-33	16	6	0.0566	0.556	1.89	2.860	0.953	8.58E+07	1.67E+07	31449	33
600S162-54-50	16	6	0.0566	0.556	1.89	2.860	0.927	8.58E+07	1.67E+07	46350	50
600S162-54-75	16	6	0.0566	0.556	1.89	2.860	0.927	8.58E+07	1.67E+07	69525	75

Not only are the stud section properties important for design calculations, but material properties of steel studs need to be known as well. When cold-formed steel studs are ordered through the manufacturer, studs can have a wide range of properties including strength and ductility. For example, a 33-ksi steel stud has to at least have a yield strength of 33-ksi, but can be higher. Also, there are no specifications for ductility when purchased through a manufacturer, but this property is crucial in the behavior of a stud. It is important to know both the strength and ductility of steel studs before testing. A list of all the beams tested and their material properties are included in Table 2.

Table 2: Summary of Beams Tested with Material Properties

Description			Stamped Properties		Measured Properties		Utility Holes	
Beam Number	Connection Type	Identification	Gage	σ_y (ksi)	Ductility	σ_y (ksi)	Shape	Location
Beam 0	Steel Hinge	600S162-54-50	16	50	25% **	50 *	Oval	Center
Beam 2	Steel Angle	600S162-43-33	18	33	49%	26	Oval	2' Spacing
Beam 18	Steel Angle	600S162-43-33	18	33	49%	26	Oval	2' Spacing
Beam 20	Steel Hinge	600S162-54-50	16	50	4%	74	Oval	Center
Beam 21	Steel Hinge	600S162-54-50	16	50	23%	64	Oval	Center
Beam 24	Steel Angle	600S162-43-33	18	33	37%	43	Diamond	2' Spacing
Beam 25	Steel Hinge	600S162-54-50	16	50	23%	64	None	N/A
Beam 33	Steel Angle	600S162-43-33	18	33	50% **	43	Oval	2' Spacing

* No measurements available, stamped properties assumed

** No measurements available, based on SSWAC (SSWAC - Steel Stud Wall Analysis Code)

Data received from Beverly P. DiPaolo, Engineer Research and Development Center - U.S. Army Corp of Engineers, April 2003. Specimen preparation conducted by John Gullet and testing conducted by Joe Torn.

The ASTM E8 standard sheet tension test specimens were waterjet machined on an Omax 55100 JetMachining Center using 40-ksi water pressure and garnet grit. The specimens were from the center of the stud web in the longitudinal stud length direction.

4.3.3.1 Steel Hinge - Beam 0

Beam 0 is the first test performed using the bending tree. The primary focus of this test was for “proof of concept”. The bending tree used in this test was a hand-me-down from a separate research project, and therefore the spacing of the loading points was not uniform. However, the testing setup was proven effective by this test, and improvements were made to the mechanical loading tree to achieve uniform spacing.

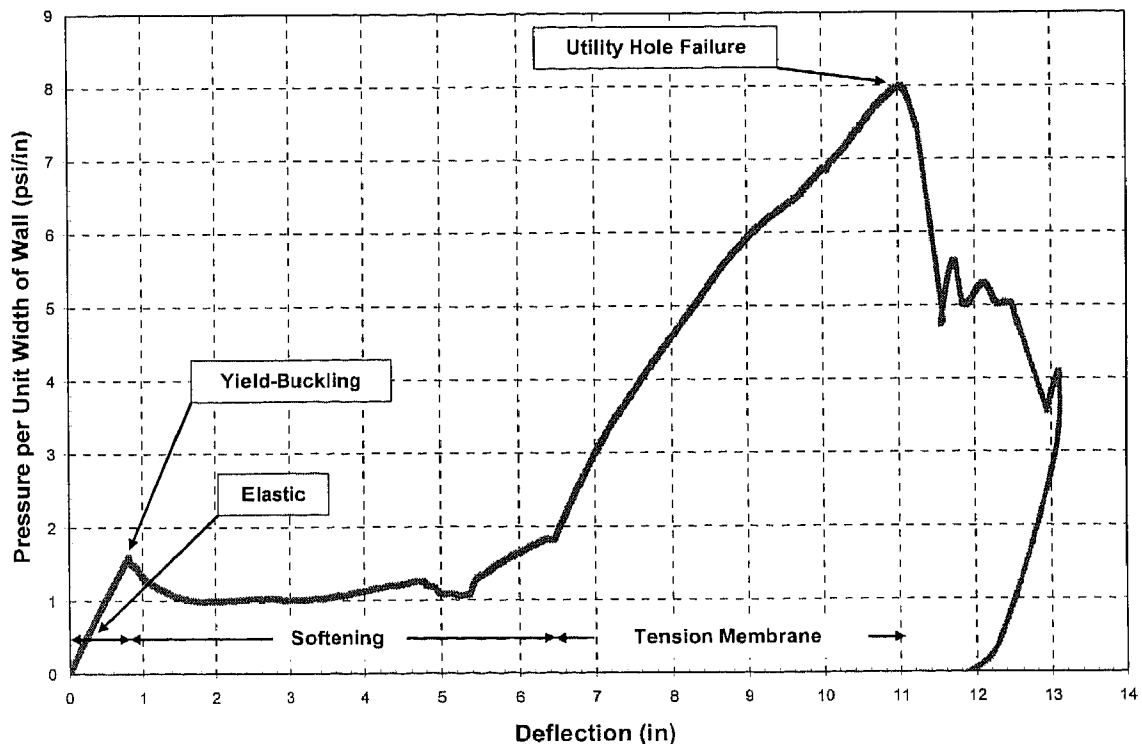


Figure 4.17: Beam 0 (Steel Hinge Connection) – Proof of Concept

Beam 0 is a steel hinge connection and the pressure-deflection graph is shown above in Figure 4.17. The spacing of the loading points for this test were concentrated more toward the center of the beam. It is believed that because of this type of load application, a well-defined softening region occurred. Once the loading points on the bending tree were properly spaced along the length of the beam, not as much softening took place in any of the beams thereafter.

To conclude that the setup of the bending tests using the bending tree is effective, comparisons are made to the wall systems tested in the vacuum chamber. One of the comparisons very encouraging to note is the mode of failure of both the bending tree test and the vacuum chamber wall test. In both tests, failure occurred in the center utility hole. The cracks in the utility hole in both cases follow similar paths. The tension membrane region of behavior of the pressure-deflection curves is also very similar in both cases. The slopes of the curves are very similar when tension membrane becomes dominant (shown in Appendix II, Figure A2.1), but the point at which it becomes dominant differs by about 2.5-in of deflection. The tension membrane region becomes the dominant behavior in the wall system test at about 4-in of deflection, while the same is true for the bending tree test at about 6.5-in of deflection (refer to Appendix II, Figure A2.2). With these two comparisons as well as other comparisons made, the bending tree was determined to be an effective way for testing stud pairs of a wall system to obtain accurate experimental data. After this conclusion was made from the proof of concept test, improvements were made to the bending tree testing setup and more tests were conducted.

4.3.3.2 Steel Hinge – Beam 20

The experimental data for Beam 20 will be presented in this section along with the pressure-deflection graph and pictures of the cross-sectional stud failure. The material properties for Beam 20 are very inconsistent with typical cold-formed steel stud properties. As mentioned above, when a manufacturer produces steel studs, the only material property of concern is the minimum yield strength of the stud. If a steel stud is rated at a yield strength of 50-ksi, that implies the stud has at least a yield strength of 50-ksi, but could be higher and in some cases much higher.

It is believed for Beam 20, because of the combination of strength and ductility, a thicker high strength steel was used to make the studs. The yield strength of the stud is 74-ksi and the ductility is only 4%, Table 2. This can occur when a thick high strength sheet of steel is cold-rolled into a thinner sheet, and in this case used for a steel stud. Cold-rolling a very high strength sheet of steel can result in a high strength stud with a very low ductility, which is not desirable for blast resistance.

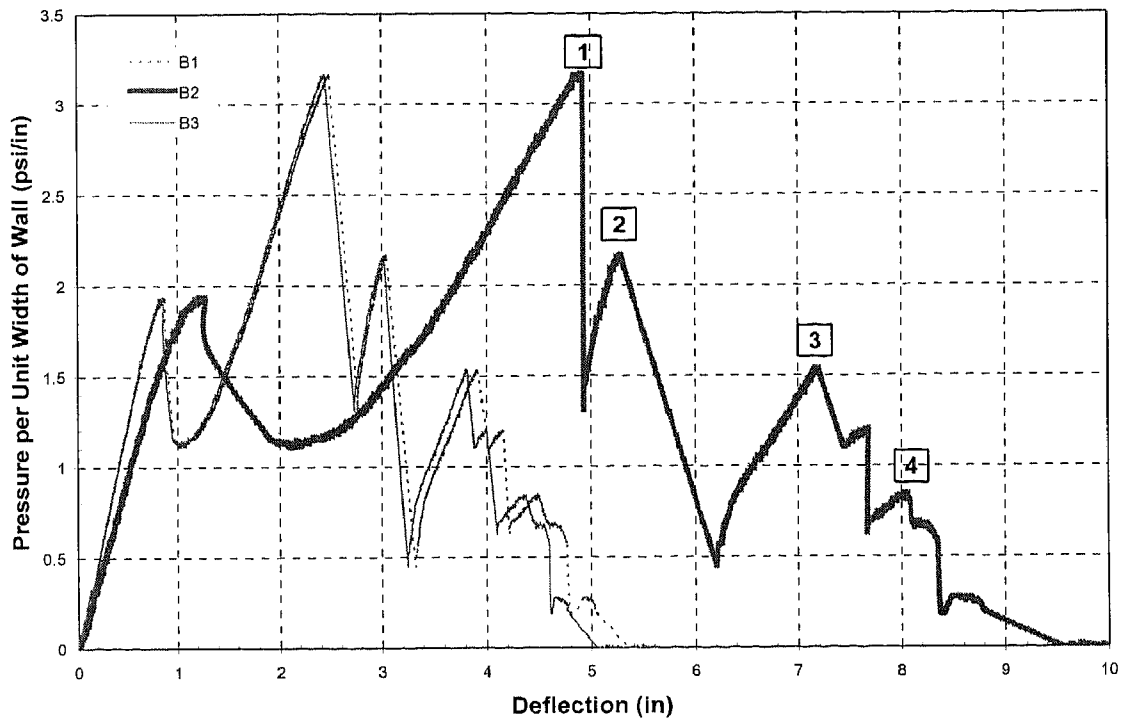


Figure 4.18: Beam 20 (Steel Hinge Connection) – Shiny Studs

These high strength and low ductility studs are referred to as “shiny studs” because of the shiny appearance of the steel. Because of the low ductility of the shiny studs, adequate tension membrane behavior can not be achieved, therefore limiting the amount of energy the system can absorb. The yield pressure is expected at about 2-psi, but the ultimate pressure is only a fraction of what it normally should be, Figure 4.18.

The mode of failure for the shiny studs is similar to that observed in the wall system test as well as other bending tree tests. The failure occurred in the utility hole in the mid-span of the stud in a similar manner as Beam 0. The failure crack initiates in the tension side of the utility hole at the point of highest stress concentration (Roth 2002) and propagates through the web and into the flange. The crack then initiates in the

compression side of the web at the utility hole and propagates through the web and into the other flange. The result is a crack through the entire cross-section of the steel stud, Figure 4.19.

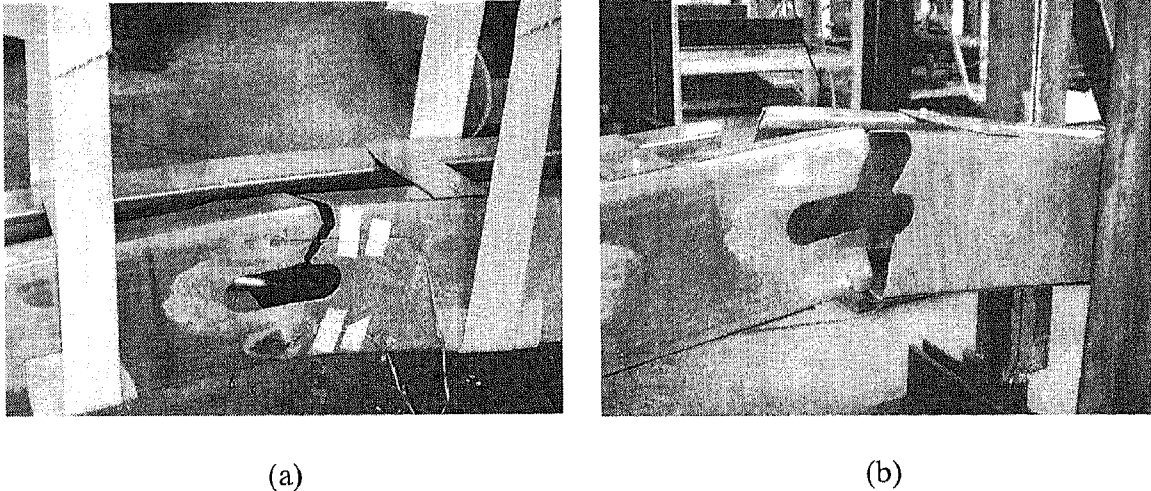


Figure 4.19: Shiny Stud Failure (a) Initial Crack (b) Cross-sectional Failure

Each time a crack occurred at different locations in the utility hole, the pressure-deflection curve would drastically drop. This type of utility hole failure resulted in a pressure-deflection curve with sharp peaks, resulting in complete failure. Four major peaks occurred in the response from four cracks initiating in the utility hole, Figure 4.18. Two cracks occurred in each utility hole, one on the tension side of the web and one on the compression side of the web. Since a complete pressure-deflection curve is not obtained from Beam 20, more tests with adequate data are needed.

4.3.3.3 Steel Hinge – Beam 21

Another steel hinge connection test was performed similar to Beam 20, except steel studs with typical material properties are used. Experimental data from this test will be

presented here. The pressure-deflection response is significantly different than seen in Beam 0. A very brief softening region occurred with this beam and tension membrane behavior dominates quickly after yield-buckling of the steel, Figure 4.20. Failure of the beam occurred at the mid-span utility hole at a pressure of 10.9-psi. The mid-span deflection of the beam at rupture is 10.5-in.

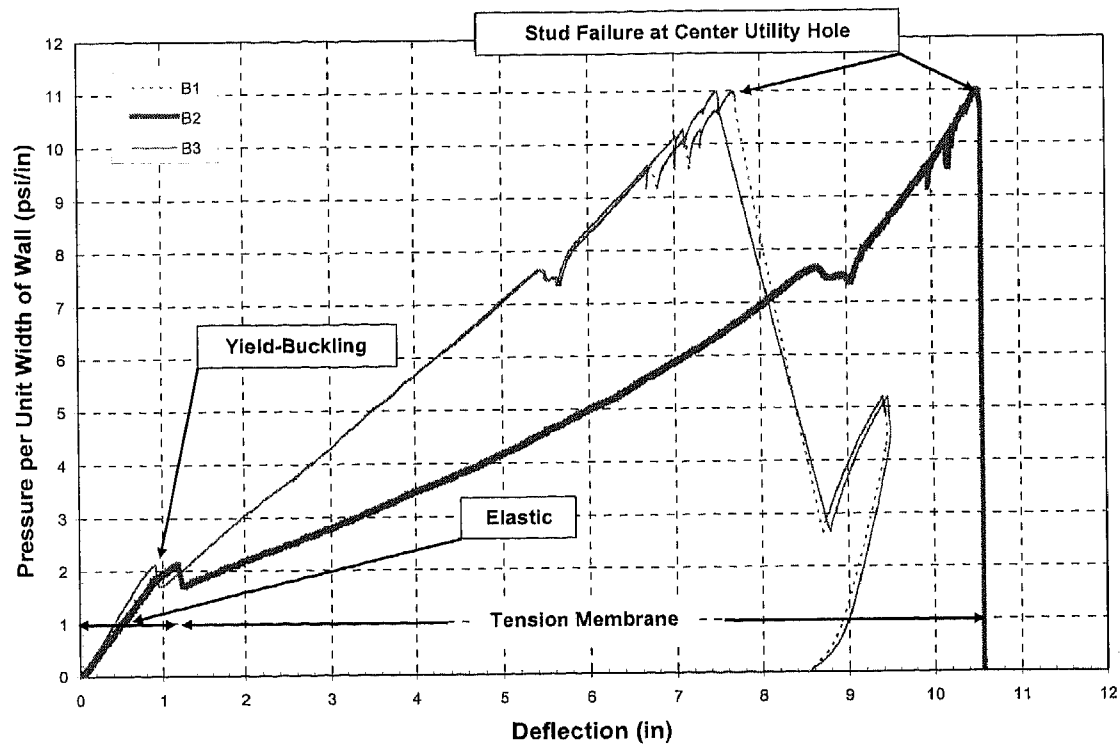


Figure 4.20: Beam 21 (Steel Hinge Connection)

Two different types of behavior are discussed in Section 3.2, therefore needing an upper limit response and a lower limit response in the analytical static resistance function. The behavior seen in Figure 4.20 with Beam 21 is characterized by the upper limit response, and is referred to as catenary action. In this type of action, tension membrane

dominates the behavior soon after yield-buckling of the steel. A comparison of both types of behavior is given in Appendix II, Figure A2.3.

It is believed that the mode shape of the beam determines the type of behavior the beam will experience. With catenary action, the mode shape of the beam is more of an arch shape, as compared to a triangular shape (refer to Appendix II, Figure A2.4). When a beam experiences catenary action during the tension membrane region, a combination of bending stress as well as tensile stress are both present. On the other hand, when a beam takes on a triangular mode shape and forms a well-defined 3 hinge-mechanism, the beam primarily experiences tensile stress, even though a small amount of bending stress is still present. It is believed that the behavior of a beam, either upper limit response or lower limit response, is determined by the mode shape. The mode shape may be determined by the type of load applied (spacing of the load). Further investigation is currently under way at the University of Missouri-Columbia to better understand the difference in beam behavior.

4.3.3.4 Steel Hinge – Beam 25

Another steel hinge connection tests conducted to consider the effects of a beam not having a utility hole at mid-span will be given in this section. One of the primary interests of this test is to focus on the post buckling region and the point at which tension membrane dominates behavior. Beam 25 is a typical steel hinge connection except without a center utility hole.

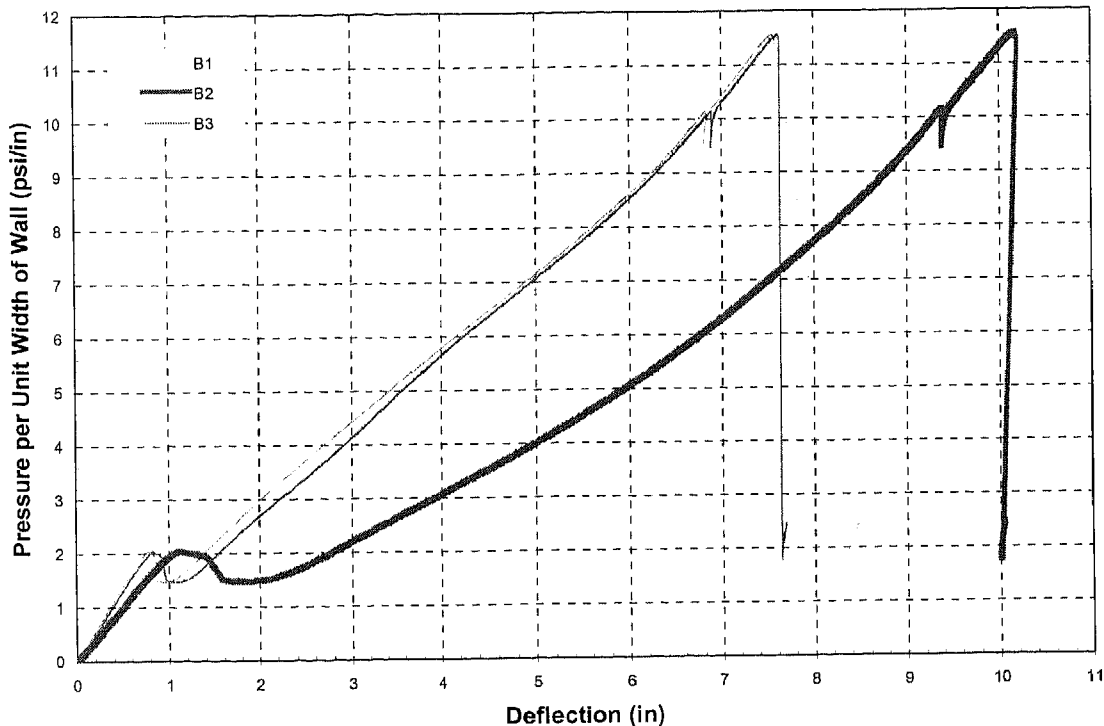


Figure 4.21: Beam 25 (Steel Hinge Connection) – No Utility Hole

The pressure-deflection curve is shown for Beam 25 in Figure 4.20. The behavior of this beam is very similar to the behavior of Beam 21. Pressure at yield, ultimate pressure achieved and deflection at rupture are comparable to the steel hinge test with the utility hole. The main difference in the behavior of this beam occurs in the softening region. Beam 25 experiences more softening than Beam 21 even though the deflected shapes of the beams are similar.

The more defined softening region for Beam 25 without the utility hole happened because of the post yield-buckling behavior. It is believed that for a beam without a utility hole, the buckling that takes place will be transferred throughout a greater middle portion region of the beam. For a beam with a utility hole, the hole is a concentrated

region where the buckling can take place. The buckling of material around and at the utility hole is very noticeable in beams with a utility hole and has been observed during testing, Figure 4.22. For a beam without a utility hole at mid-span, the softening region occurs throughout more of the behavior of the beam because of the nature of the buckling. It does not happen as suddenly as it does when hole is present, and therefore the beam experience more deflection during this time of softening.

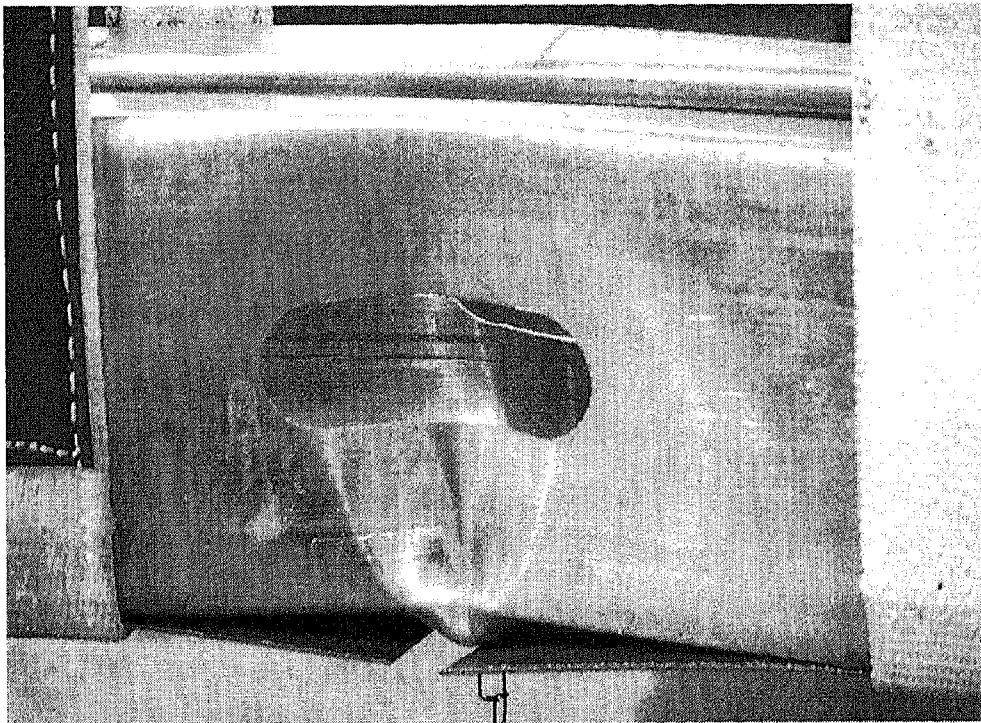


Figure 4.22: Post Yield-Buckling Behavior at Utility Hole

Beams having utility holes are more common than beams without and are popular for construction purposes. The amount of softening that takes place in any steel stud depends not only on the mid-span geometry, but also on the type of behavior the stud experiences. Since the softening is not as sudden with Beam 25 because of the mid-span

geometry, it is characterized by the lower limit behavior response. Therefore, not only is the mode shape believed to determine the type of response experienced by a beam, but the mid-span geometry also effects whether a beam will take the upper limit response or lower limit response.

Four different steel hinge connection tests have been presented and discussed in this section. The effects of the material properties of the steel stud as well as stud geometry have been seen in the pressure-deflection curves and comparisons have been made. In the next sections, steel angle connection tests will be presented and discussed in detail.

4.3.3.5 Steel Angle – Beam 2

The steel angle connection tests are the other type of tests that are included in this thesis and will be discussed in this section. Beam 2 was the first steel angle connection test performed using the bending tree and results from this test are presented in this section. The steel angle connection details are shown in Figure 4.4 and the experimental setup is discussed in Section 4.3.2. The studs used for the steel angle connection tests discussed in this thesis are 600S162-43-33 (AISI 1996). These studs are gage 18 with a yield strength of 33-ksi and the section properties are given in Table 1.

All of the steel angle connection tests with oval utility holes presented here are characterized by the upper limit behavioral response. Beam 24 is a beam with a utility hole that has a different geometry, and results from that test differ from the beams with oval holes.

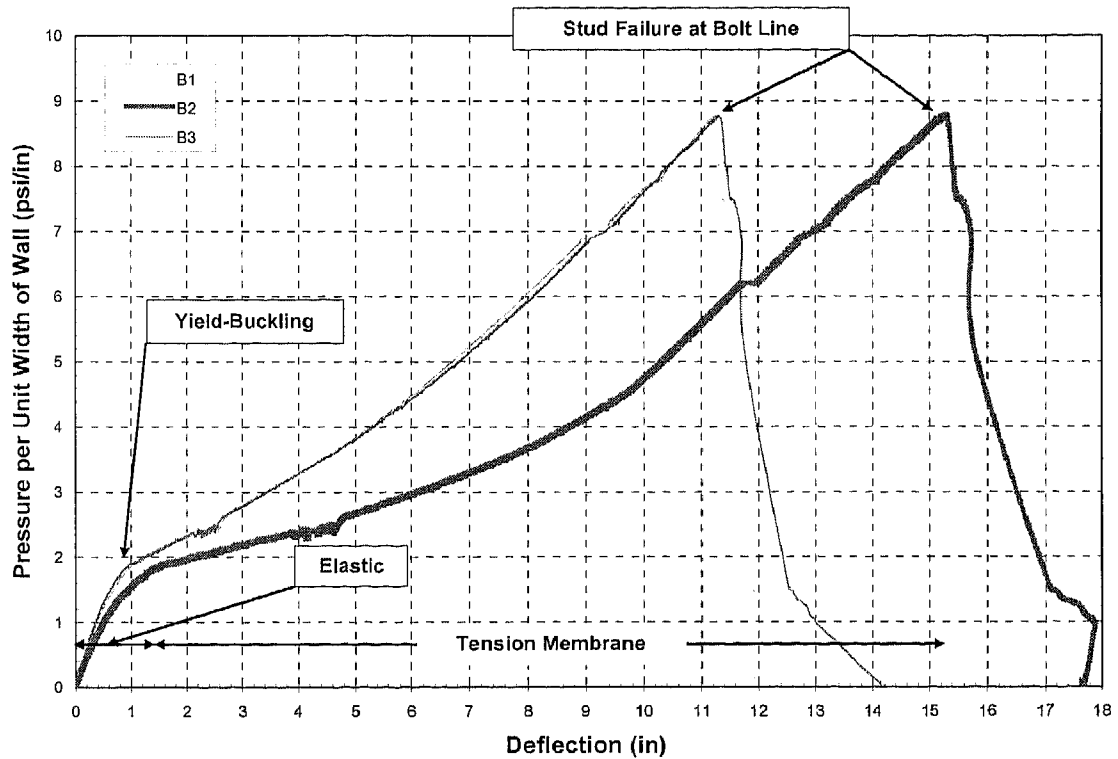


Figure 4.23: Beam 2 (Steel Angle Connection)

As can be seen from Table 2, from the coupon results obtained from Beam 2 and Beam 18, the measured yield strength does not meet the manufacturer's specifications. The measured yield strength is only 26-ksi and the manufacturer's requirements are 33-ksi. The reason for this low yield strength is not known, but the use of steel studs with this type of deficiency should be avoided.

The behavior that occurs in Beam 2 seems to be characterized by the upper limit response, shown in the pressure-deflection curve in Figure 4.23. However, the pressure-deflection response in the tension membrane region is much softer than predicted because of the lack in material properties. Yield-buckling happens much higher than predicted and is not very clear-cut. Yielding of the stud seems to happen at about 2-psi, when

based on the Equation 3.5 for predicting the pressure at yield it should only be 0.7psi. Ultimate deflection at rupture is around 15-in and ultimate pressure achieved is almost 9-psi. Because of the discrepancy in the material properties of Beam 2 and Beam 18, it is not used for comparison with the analytical model.

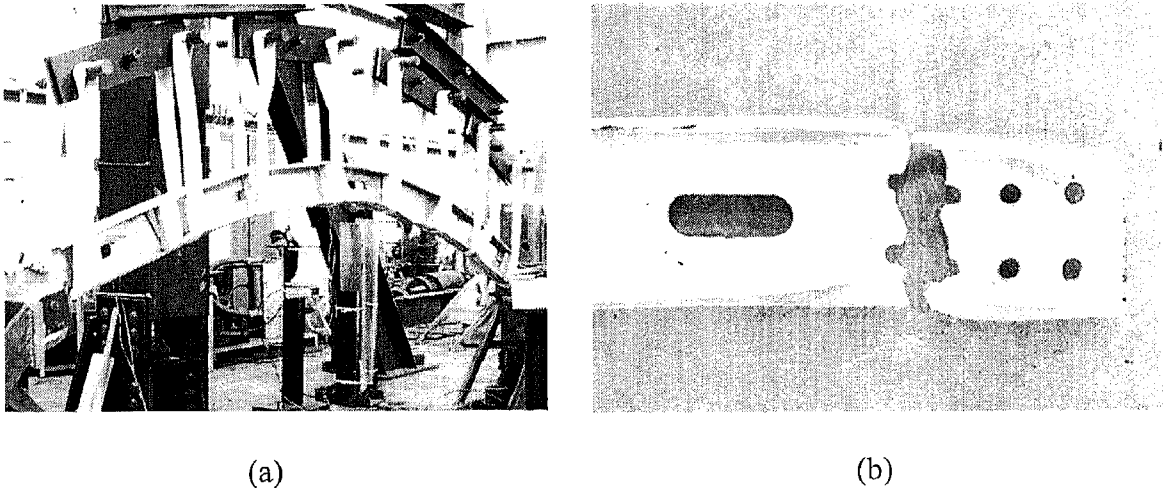


Figure 4.24: Beam 2 – Steel Angle Test (a) Deformed Shape (b) Connection Failure

The deformed shape of the beam after testing and failure mode are shown in Figure 4.24. It can be seen that the deflected shape with eight loading points is an arch shape. The arch shape observed in testing is compared to a parabolic shape function as discussed previously in Section 3.2.2. Comparisons that are made about the shape of the post-test beam are important in determining the ultimate pressure and deflection at failure.

The failure of the beam occurred in the connection of the steel angle in the stud at the bolt line. This is a common failure mode for this type of connection and is more desirable than other types of connection failure that have been designed against. Failure

in the bolt line of the stud allows for adequate tension membrane action in utilizing stud capacity. Failure of any type besides cross-sectional failure of the steel stud results in a loss of capacity. If the bolts shear or the steel angle fails, full stud capacity is not being utilized. Two desirable types of stud cross-sectional failure that have been observed in testing are failure in the bolt line and failure at the utility hole, both of which are caused from a reduction in cross-sectional area of the member.

4.3.3.6 Steel Angle – Beam 18

In this section, test results from Beam 18, a steel angle connection test, will be presented. In testing, similar results for numerous tests of the same design are desirable and can be advantageous in analytical predictions. Beam 2 and Beam 18 have very similar load paths and a comparison of the pressure-deflection curves can be seen in Appendix II in Figure A2.5. Not only is the behavior almost identical, but the failure modes happened in the same manner as well. The failure that occurred in the stud cross-section happened at the bolt line as discussed in Section 4.3.3.5.

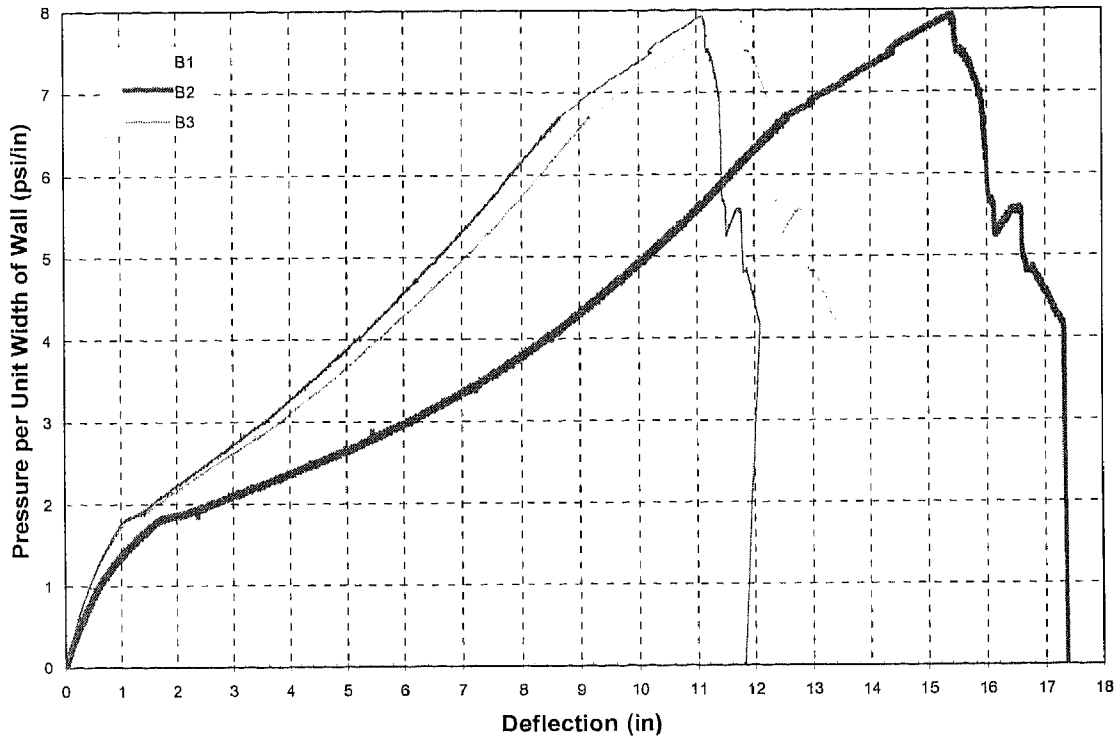


Figure 4.25: Beam 18 (Steel Angle Connection)

The behavior of Beam 18 was not expected because of the low yield strength of the steel, as with Beam 2. Yielding occurred at 1.8-psi and tension membrane dominated soon after yield-buckling of the stud. The path of the function does not have as much resistance as a beam that meets its manufacturing requirements should. Therefore, the slope of the tension membrane region is much lower than expected and comparison to the analytical model will not be made. The ultimate deflection at mid-span reached more than 15-in and the ultimate pressure achieved is almost 8-psi. The deflected shape of the beam is an arch shape and is very similar to the deflected shape of Beam 2.

4.3.3.7 Steel Angle – Beam 24

Experimental data for Beam 24 will be discussed in this section. Beam 24 is similar to other steel angle tests except for the stud geometry. The utility holes for this beam are diamond shape holes verses oval shape holes which are more common in steel studs. The pressure at yield for this test is higher than that for others, being about 2.5-psi. A distinct softening region occurs in the beam and a mid-span deflection of about 2.5-in occurs as the plastic hinge is forming, Figure 4.26.

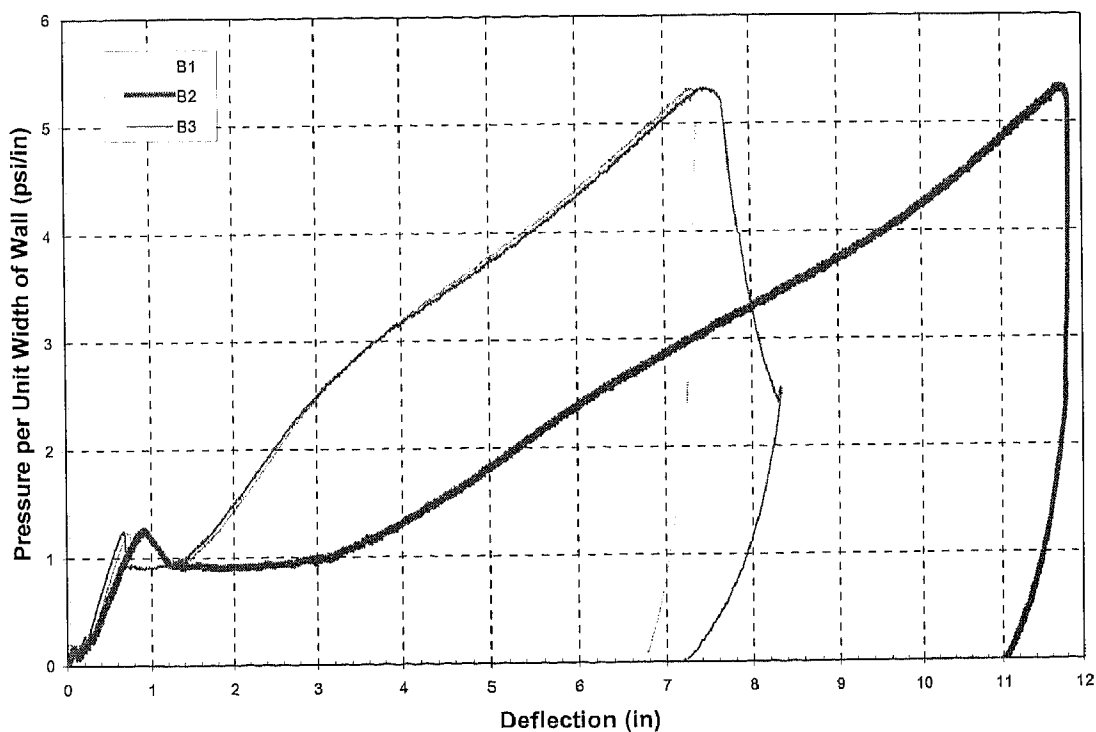


Figure 4.26: Beam 24 (Steel Angle) – Diamond Shape Utility Holes

For this test, a different type of failure occurred due to a restraint on the MTS. The hydraulic actuator ran out of travel just before the stud reached failure. The test was

stopped and the load held constant. During the hold period at the high load, a crack initiated at one of the utility holes and propagated through the tension side of the web and into the top flange, shown in Figure 4.27.

The test was put on hold at a pressure of 10.6-psi with a mid-span deflection of 11.8-in, shown in the pressure-deflection graph, Figure 4.26. It is believed that if more travel would have been possible in the hydraulic actuator, stud failure would have taken place soon thereafter. The failure path of the crack travels through a screw hole for a #10 tek screw, Figure 4.27. Screws are placed in the webs of the studs to allow the two studs to behave together as one beam. The screws are placed every six inches apart and are staggered from the top to the bottom of the web. It should be noted from the failure seen in Beam 24 that any screws placed in the studs should not be placed near the utility holes.

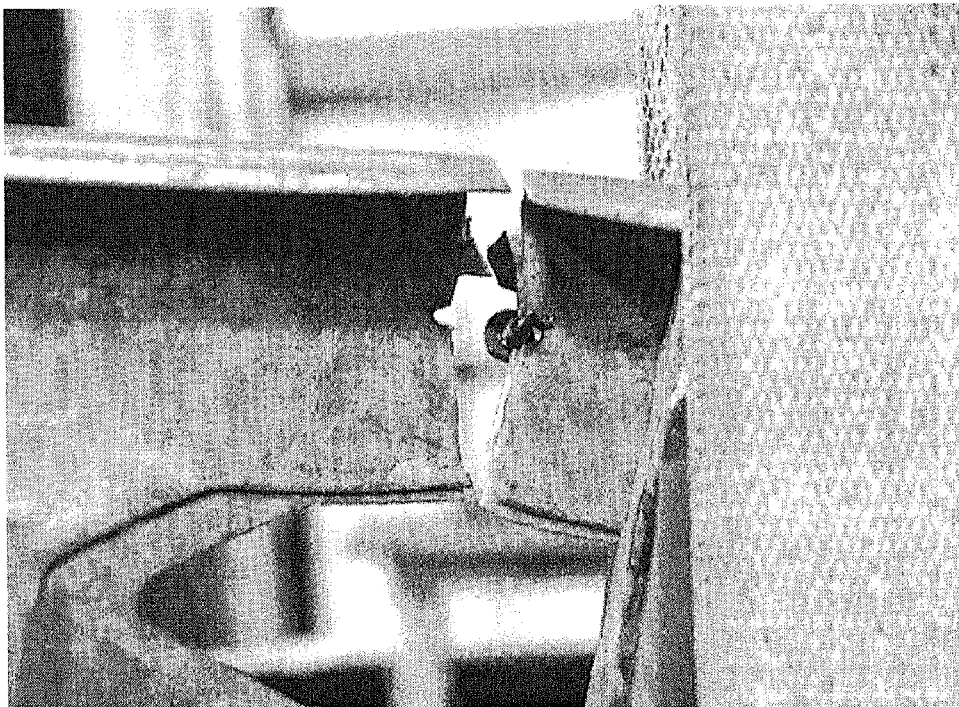


Figure 4.27: Beam 24 Failure Crack at Utility Hole

The pressure-deflection curve for Beam 24 has a more distinct softening region than Beam 2 or Beam 18 and therefore, the response is referred to as a lower limit response. This could be a result of a different type of load application or from the geometry of the utility hole. Beam 2 and Beam 18 were both tested using the bending tree with eight point loads, while Beam 24 was tested using the sixteen point bending tree. Also, the diamond shape geometry of the utility holes can cause the beam to deflect differently than beams with oval holes. Different mode shapes for beams will follow different pressure-deflection curves, this either being the upper limit or the lower limit. Some beams can even be characterized by both the upper and lower limit type response, which can be seen in the next beam.

4.3.3.8 Steel Angle – Beam 33

The experimental data for Beam 33 will be presented in this section along with the pressure-deflection graph. Beam 33 behaves differently than any of the other three steel angle connection tests. Yield-buckling of the stud happens in this test about 2-psi, which is expected. A very brief softening region takes place and then tension membrane dominates behavior. The pressure-deflection response after buckling initially is stiff. After about an inch of deflection with this “stiff” slope, the response begins to soften and move from an upper limit response to a lower limit response. The stud behavior undergoes a transition phase for 2 inches and is then characterized by a lower limit type response, Figure 4.28.

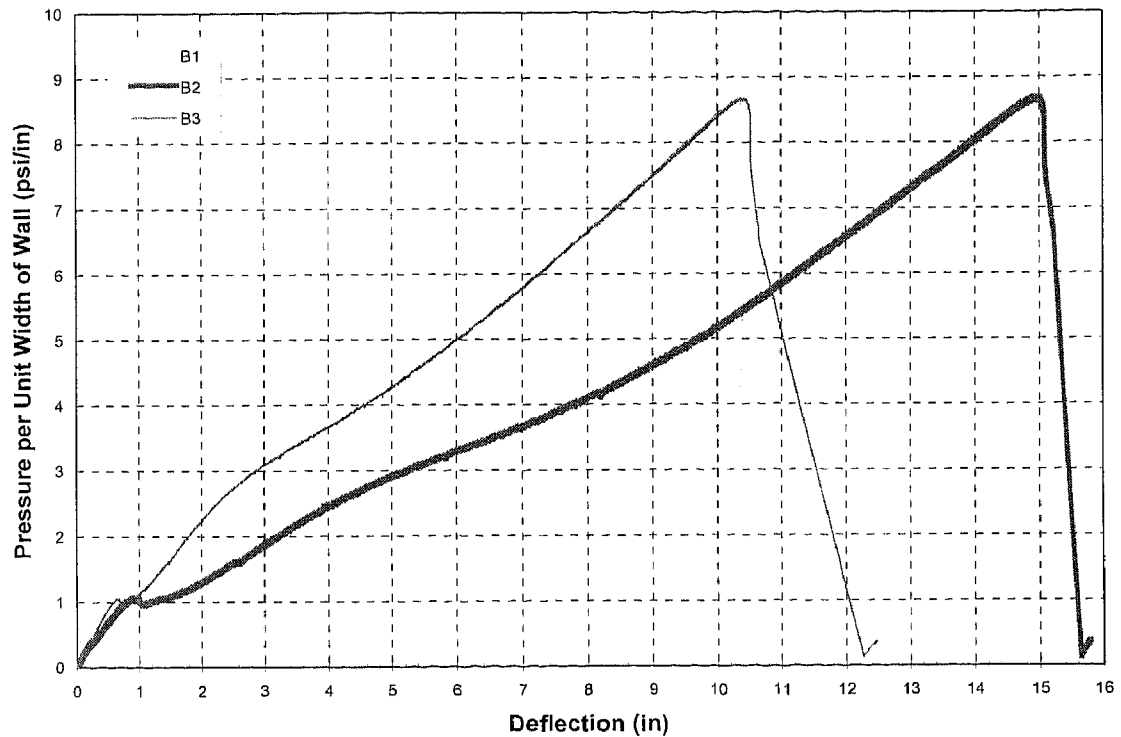


Figure 4.28: Beam 33 (Steel Angle)

The maximum pressure achieved in this test was 17.3-psi and the maximum deflection at mid-span was 15-in. The pressure and deflection for this test is substantially higher than that of the other three steel angle connection tests. This test is believed to behave this way because of the amount of ductility in the stud. A stud with a high ductility will deflect a significant amount more than other studs. The type of failure that occurred is similar to Beam 2 and Beam 18. Failure occurred in the stud cross-section in the bolt line where the stud connects to the steel angle. A picture of this type of behavior is shown in Figure 4.24 (b).

Now that the experimental results have been presented and discussed in detail, more comparisons will be made between different tests and will be specifically graphed

along with the analytical static resistance function. The comparison of the pressure-deflection curve and the analytical model will give insight into the validity of the model. With a valid analytical model, proper blast resistant design can then be performed for steel stud wall systems.

4.3.4 Analytical Model Comparison

To conduct dynamic modeling for steel stud wall systems to obtain engineering design tools for blast loads, not only is it important to develop an analytical static resistant function, but it is necessary to verify the model. In this section, the analytical model developed in Chapter 3 will be compared to steel hinge connection tests as well as steel angle connection tests. Once the analytical model is proven adequate, it can be used along with experimental data to design steel stud wall systems for explosive field tests.

One issue that must be considered when predicting the resistance of a steel stud is the ultimate deflection at rupture. As discussed in Chapter 3, failure is assumed to be localized over a reduced cross-sectional area of the steel stud. During elongation in a beam, the majority of the plastic strain will invariably occur at a reduced cross-section like a utility hole or at the bolt line, as seen in previous sections. ξ is the percent of the total length L that is assumed to be the localized cross-sectional area of the stud.

By doing a parametric study of the tests included in this thesis, as well as other tests that have recently been conducted, a value of ξ has been determined for use in predictions. The percent of the beam that is assumed to take on most of the plastic strain for modeling purposes is 4%. Also, for the comparisons between the analytical model and experimental data, only the center deflection of the beam is considered.

4.3.4.1 Modeling of the Steel Hinge Tests

The first steel hinge test that will be modeled is Beam 0 which was the first test conducted using the bending tree. Recall that the spacing for this test was not uniform and the load is focused toward the center of the beam. However, comparisons for this test are still useful and can be helpful in validating the model developed.

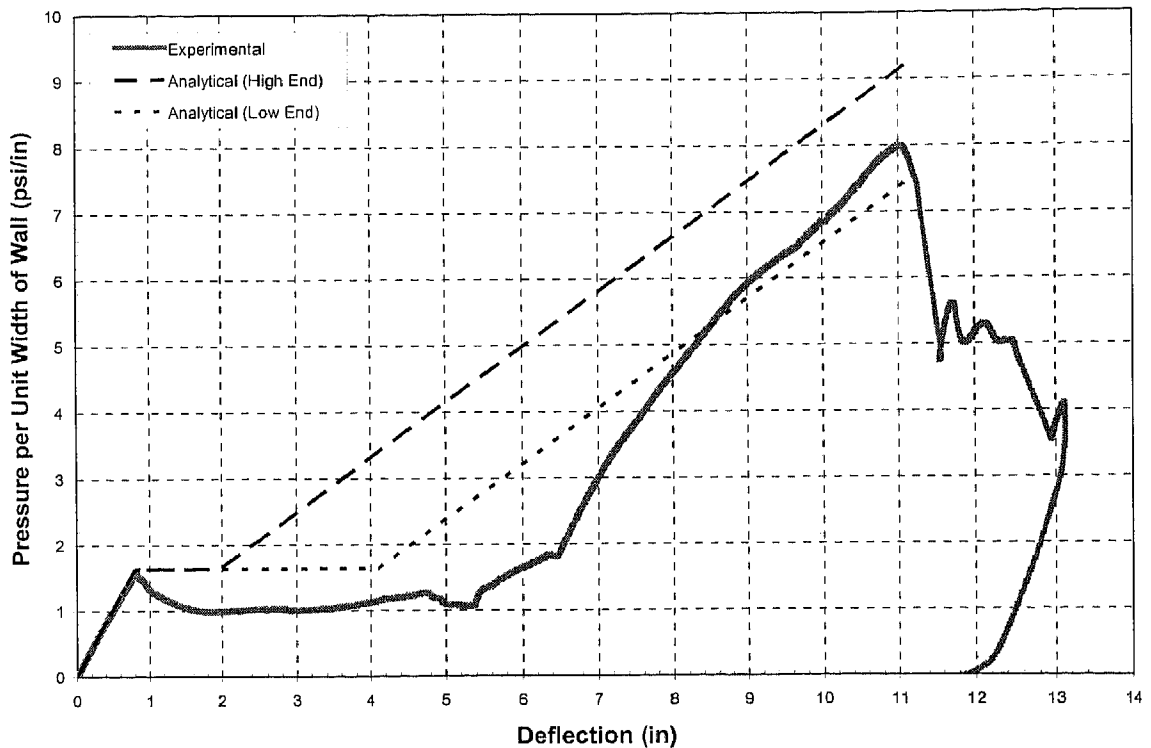


Figure 4.29: Analytical Model for Beam 0

The experimental data along with the analytical predictions for Beam 0 are given in Figure 4.29. As can be seen from the graph above, the elastic portion is predicted very nicely, while the post-buckling region is not as accurate for this beam. The model would more closely represent the experimental behavior if the proper load spacing would have

been used in testing. The softening region for this test is much greater than any other test and is believed to be a result of the non-uniform loading. The model predicts that the beam will absorb more energy than it actually does. This is true because the amount of deflection during softening is not well understood. As mentioned earlier, sometimes 3 to 4 inches of softening takes place during a test, while other times only a brief softening region occurs. The reasons for the type of behavior are currently under investigation at the University of Missouri.

If the amount of deflection during softening, the flat portion of the model, could be accurately predicted and incorporated into the analytical static resistance model, the energy absorbed in each test could more accurately be predicted. For example, it can be seen in Figure 4.30 that increasing the amount of deflection during softening can allow for better analytical predictions. In the figure below, the energy absorbed for the system is more accurately predicted than in Figure 4.29. In the analytical model, the amount of deflection is a function of the depth of the stud section and provides good results. However, this region of prediction is still not well understood and with more testing of wall components, improvements upon the model can be made with a better understanding of post-buckling behavior.

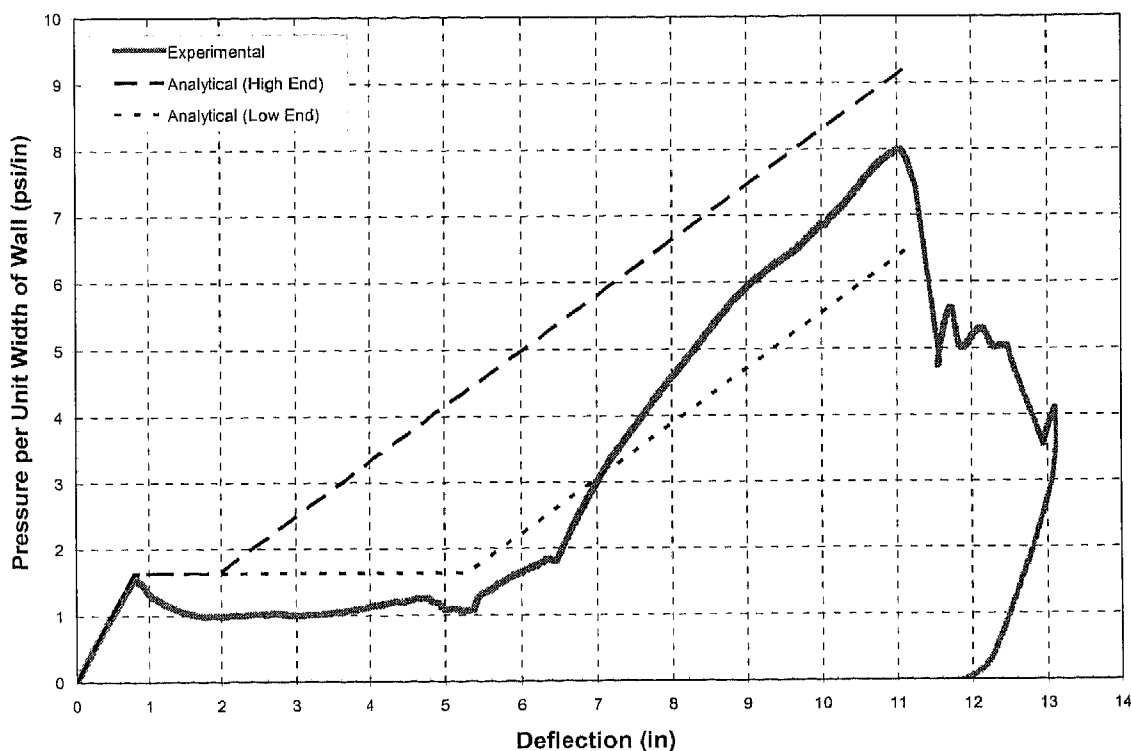


Figure 4.30: Analytical Model for Beam 0 with an Increased Flat Portion

The next test that will be used for comparison is Beam 20. Beam 20 is the beam with the high strength and low ductility, a combination that is not well suited for design purposes. It was previously shown that the behavior achieved in the pressure-deflection curve is not typical of steel studs and premature failure occurred due to ruptured utility holes. However, comparisons up to this point of rupture are made and can be beneficial for future predictions.

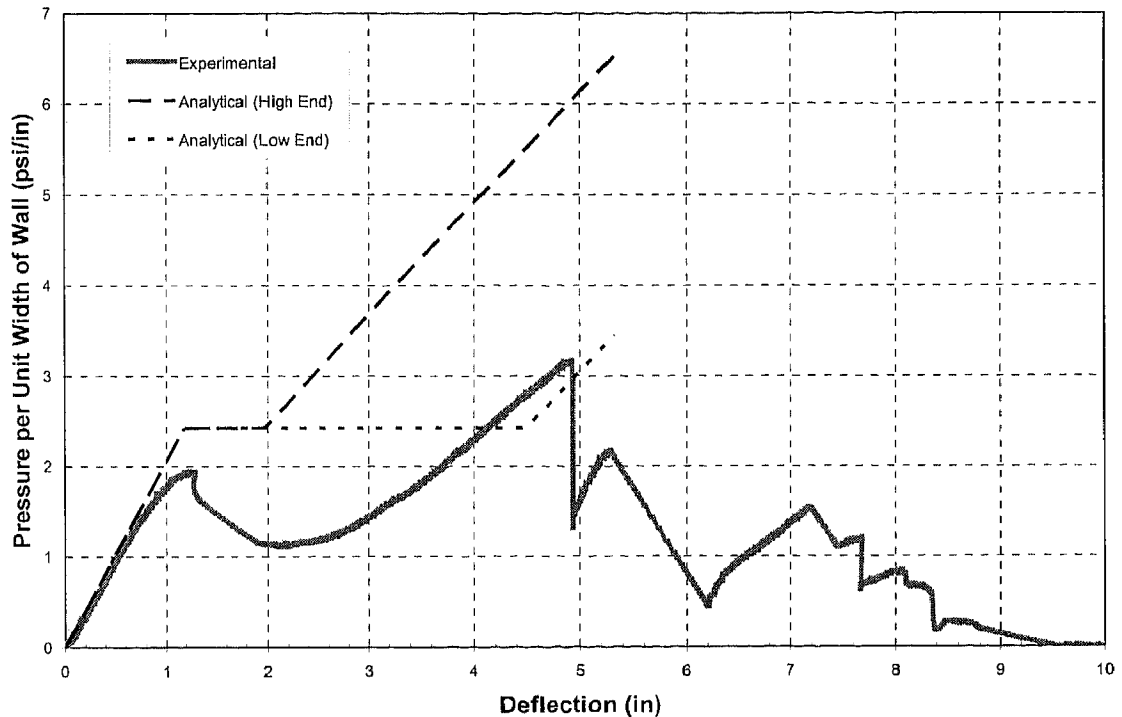


Figure 4.31: Analytical Model for Beam 20

The analytical model predicted for Beam 20 is shown in Figure 4.31. The pressure at yield is predicted higher than actual yielding, however, the deflection at rupture is modeled very closely assuming ξ to be 4%. The discrepancy in the pressure at yield with this prediction could be due to unusual stud behavior because of the high strength and low ductility. A stud with this type of combination will not behave as normally expected and therefore another test of this type was performed. The slope of the tension membrane region appears to be the same of that which is predicted. However, results from a typical steel stud are needed for comparison and are presented next.

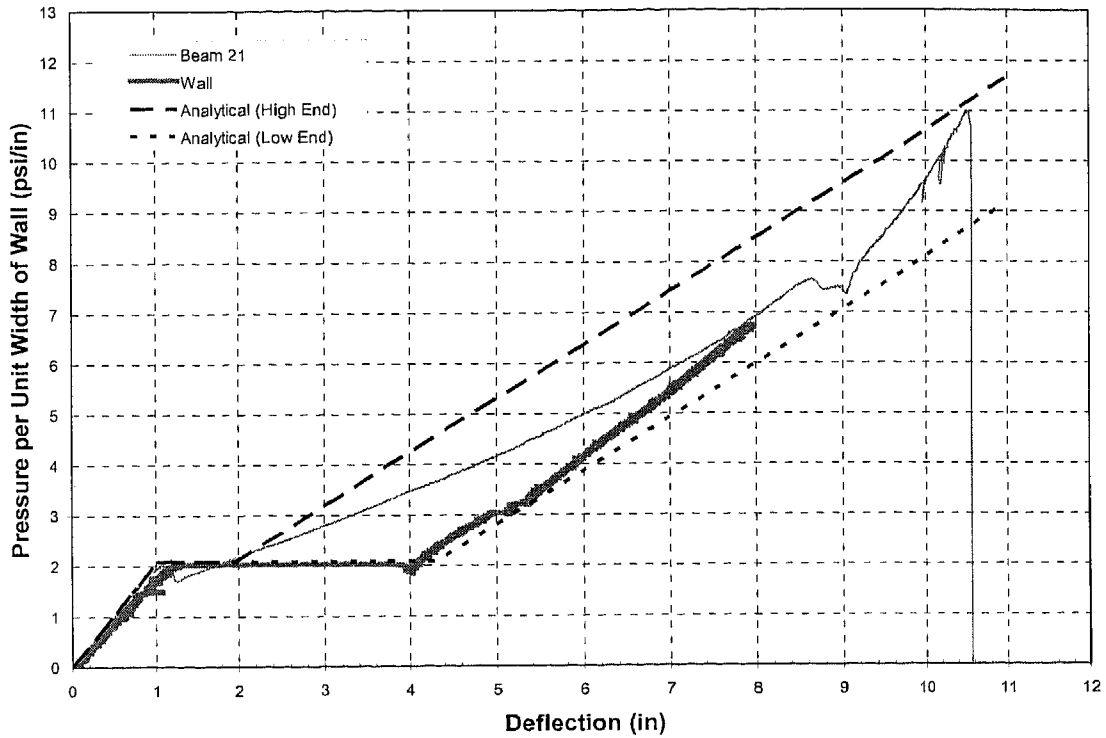


Figure 4.32: Analytical Model for Beam 21 and Wall

The analytical model for Beam 21 and the steel hinge connected wall, Test M1c (discussed in Section 3.1) are given in Figure 4.32. The wall test follows the analytical model very closely, from the point of yield-buckling to the point where tension membrane becomes dominant. The slope of the tension membrane behavior in the wall is a little stiffer before rupture than in the model. The wall test was stopped after cross-sectional failure occurred in the weakest steel stud, and it is believed this is why the test does not reach the amount deflection predicted or the amount of deflection that Beam 21 experienced.

Beam 21 is modeled very closely up to the point of buckling. After yield-buckling, the beam experiences a brief softening region before the tension membrane

region. The behavior starts out near the upper limit response and then transitions toward the lower limit response. For a conservative prediction in this case, the lower limit response would be used to model the design for blast resistance. Beam 21 gives a good representation of when failure will occur. The analytical model takes into account the 4% localized region of the stud where most of the plastic strain occurs and is really close in predicting the energy absorbed by the system. Since the analytical model does not take into account any damping in the system, and in live blast field testing, some damping has been observed, the model is somewhat conservative in the predictions. Therefore, if more deflection is predicted than the actual beam experiences in experimentation, it is not considered to be an over-prediction and is believed to be sufficient for design purposes.

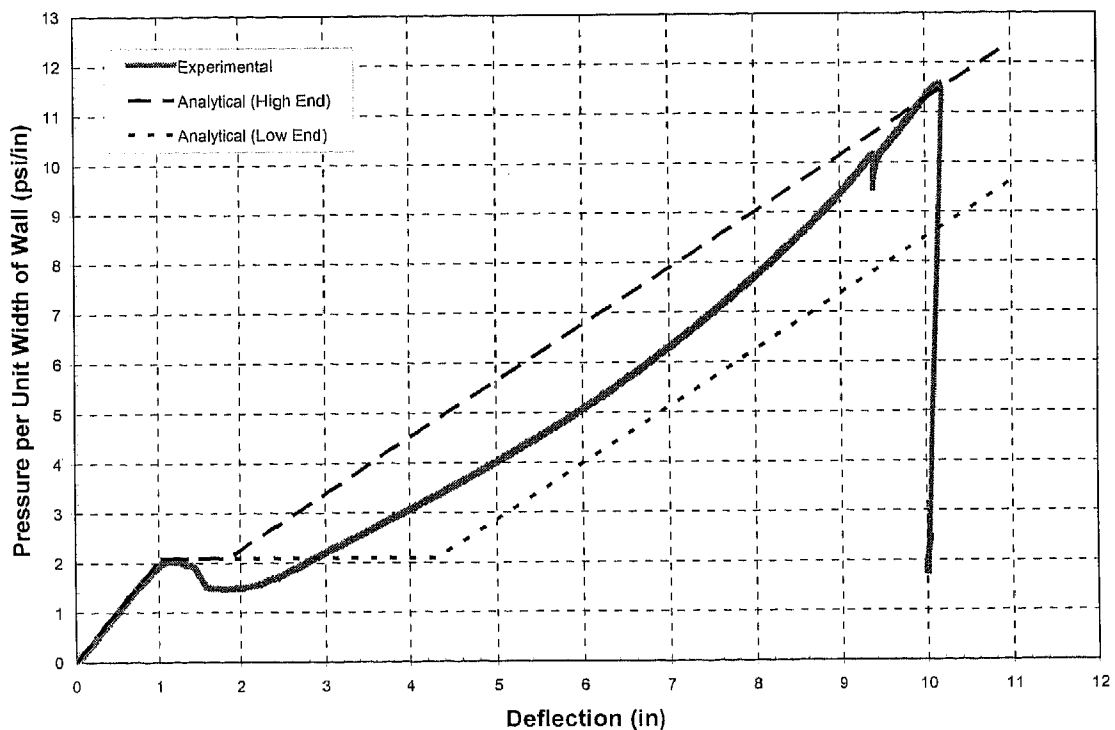


Figure 4.33: Analytical Model for Beam 25 – No Utility Hole

In Figure 4.33, the analytical prediction for Beam 25 is given, which is a steel hinge connection beam similar to Beam 21. The only difference is that Beam 25 does not have a utility hole. The model follows the behavior very closely to the point of yield-buckling. After buckling, a softening region occurs before tension membrane behavior dominates the behavior. For this test, the lower limit prediction would be used for blast modeling since it gives a conservative value of energy absorbed by the system. The point at which stud failure occurs is predicted very closely using a 4% value for the total stud length where the majority of the failure occurs. In the next section, more modeling will be done with the steel angle connection tests.

4.3.4.2 Modeling of the Steel Angle Tests

Modeling of the steel angle connection tests is very important since this type of connection is the retrofit connection that is currently popular in the design field. Accurately modeling this type of retrofit concept will be important in the next chapter when it is used in the design of a live field explosion test.

Since Beam 2 and Beam 18 do not have sufficient material properties to conduct useful comparisons, Beam 24 and the wall tests with this same beam will be the first tests that are modeled. However, Beam 18 has been modeled and given in Appendix II in Figure A2.6, to see how predictions compare. Beam 24 is the beam with diamond shape utility holes. This test along with a wall test conducted which has the same type of stud characteristics, will be compared to the analytical resistance model and is shown below.

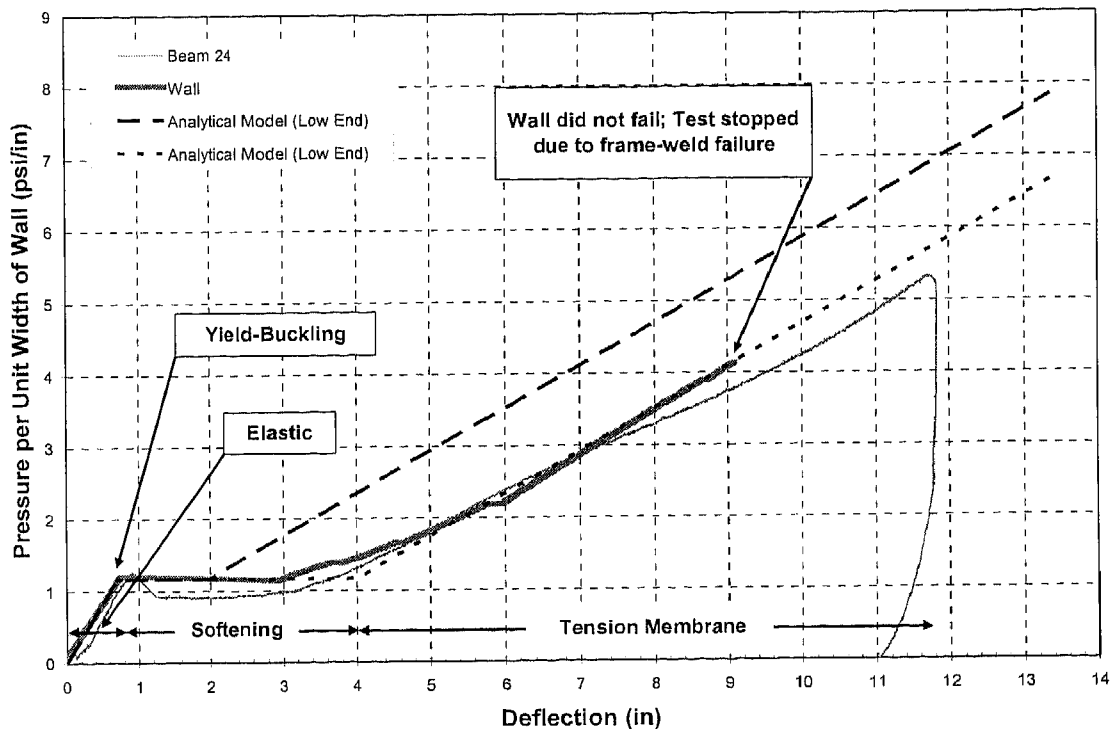


Figure 4.34: Analytical Model for Beam 24 and Wall

The analytical model for Beam 24 and the wall test conducted is shown in Figure 4.34. The setup for the wall test given in Figure 4.34 is similar to the Test M1c previously discussed in Chapter 3. The test is conducted in a similar manner, the differences are the studs used have different properties, 600S162-43-33 is used rather than 600S162-54-50. Also, the connection is a steel angle rather than hinged, and the utility holes are diamond shaped like in Beam 24. The response for both the component beam and the complete wall system take the lower limit approach after a well-defined softening region occurs. Both responses compare closely through yield-buckling, softening and the tension membrane region. The wall test was stopped prematurely due to a structural frame issue with vacuum chamber. Even though the beam results are a

little softer than predicted in the tension membrane region, the bending tree test behaved as expected through failure at 11.8-in and an ultimate pressure of 5.3-psi, which is accurate with the analytical model.

It must be noted that the analytical model predicted for these tests were done before testing. Once a prediction for a test has been performed, then the experimental data can be used to verify what has been predicted. The predictions made for these two tests are very encouraging and it is believed that a sufficient design of a live explosion field test can now be achieved.

Beam 33 is similar to Beam 2 and Beam 18, except the material properties measured for this beam meet the manufacturer's requirements. However, the response is a little different than normally observed because of the change in the tension membrane slope. The response is initially characterized by the upper limit, and then softens and dips down toward the lower limit, but then approaches the upper limit near failure.

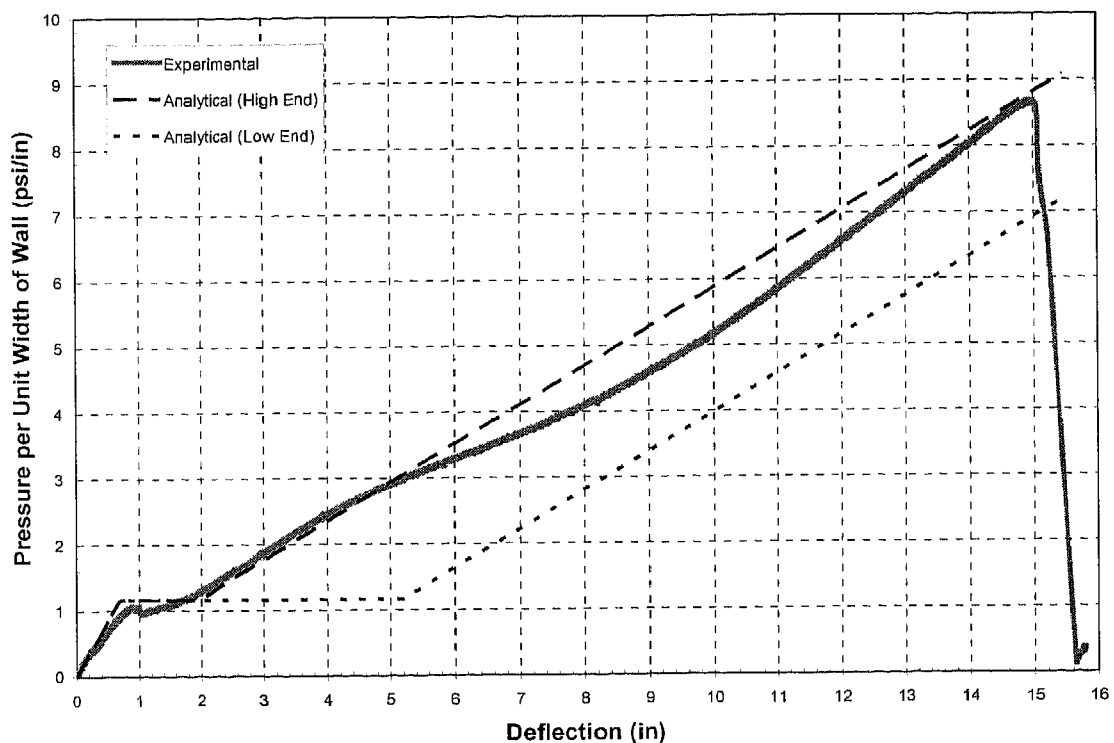


Figure 4.35: Analytical Model for Beam 33

Beam 33 has been modeled and the results are shown in Figure 4.35. The point of yield-buckling is very close to the predicted pressure, which is 1.2-psi. The stud experiences a brief softening region before tension membrane dominates. The early tension membrane response is characterized by the upper limit, which is considered to be catenary action. The response then softens and transitions toward the lower limit, and then regains stiffness before rupture. The rupture occurs at a deflection of 15-in and a pressure of 8.6-psi, which is very closely modeled analytically. Because of the conservative nature of the analytical model as previously discussed, the upper limit response can be considered a good representation of the resistance the beam has and the amount of energy the system will absorb.

4.4 SUMMARY AND CONCLUSIONS

In this chapter, an overview of previous testing conducted and the contributions to design have been reviewed. This overview included different experimental setups that have been used and the pros and cons of these setups. Previous design concepts were introduced and the improvements made to these concepts have been presented and discussed in detail. The value and importance of component testing beams from wall systems using the bending tree has been stated, and a good working experimental setup has been established.

Experimental data for beams with hinge and angle connections has also been presented from the bending tree tests that have been conducted. The static resistance functions for these tests have been discussed and comparisons have been made with each other and with results from the wall data available. The analytical predictions for each test were given and comparisons were made with the actual behavioral data achieved in testing. With these comparisons, the analytical model has been verified and can now be utilized as a design tool in the field. In Chapter 5, the analytical model will be used to design a live explosive field test.

For wall system analysis, an SDOF model is needed as a computational tool. There is also a need for a static resistance function to determine how a wall will respond under a static load. If the resistance of a steel stud wall is not well understood, then the wall can not properly be modeled. An analytical static resistance function has been defined and verified using experimental data. The analytical predictions based on the model are believed to be adequate, but improvements in certain areas of the model are desirable. The softening region and the point in which tension membrane action

dominates steel stud behavior are not well understood. Further investigation on the difference between the upper limit response and the lower limit response and the controlling factor of the type of behavior the steel stud experiences is encouraged. Also, the value of ξ and its use in predicting ultimate deflection of a stud is not well understood. Additional testing using the bending tree can provide useful experimental data in further verifying a 4% value for ξ .

5 Design Procedures

Now that the experimental data and results have been summarized, the focus of this chapter will be on design. Design is to conceive or fashion an idea and then carry out the idea by executing plans with a specific goal or purpose in mind. When designing steel stud wall systems, one must first have an idea in mind and be able to implement the design into the construction field. Some ideas that are tested in the laboratory are not suitable for construction purposes because of high cost or intensive labor demands. Thus far, the need for modeling steel stud wall systems has been introduced and the need has been stated. In this chapter, general design procedures will be listed. A design example will be discussed and compared against a component test in the bending tree, a wall system test in the vacuum chamber, and a live field explosion test. The analytical static resistance function will be used in an SDOF model to predict the dynamic behavior of a steel stud wall system during a blast. Finally, the program used to design the wall system will be discussed in detail and summarized with conclusions and recommendations. (Refer to Appendix IV for complete details of a Steel Stud Wall with Steel Angle Connections and Muntin Window Frames).

5.1 GENERAL DESIGN STEPS

When designing steel stud wall systems against blasts, there are certain design steps that must be followed to efficiently develop a sufficient design that meets the appropriate standards. There are many details in the design of a wall system against blasts and range anywhere from the size of the blast to how the wall interacts with the structure. Below is a list of general design steps and a brief discussion of each.

1. Define the threat
2. Define the wall system
3. Determine stud connections
4. Consider wall structure interaction
5. Analyze the wall system

When defining a threat, the first step is to determine what needs to be protected and then how much protection is necessary for these assets (Conrath et al. 1999). After one determines what is of value and how much damage can be allowed, then the level of protection can be provided with the appropriate design constraints. In blast design, the most important design constraints are that harmful projectiles do not enter the building and that collapse of the structure does not occur.

As mentioned in Chapter 2, the two parameters that characterize a blast are peak pressure and impulse. A structure can be designed against a certain blast if these two parameters are known. Programs such as ConWep can be used to determine the threat based on peak pressure and impulse (Hyde 1992). These two values can then be entered into an SDOF program for design.

The next step in the design process is to design the wall system that will resist the threat defined. When there is a known threat, if a wall system is not designed adequately, it will not serve its intended purpose. There are many factors to consider when defining a wall system. What type of material to use for a wall system is one of the first decisions that is made. Cold-formed steel studs provide both strength and ductility to resist high loads as well as absorb much energy. Below is a list of design parameters for defining a wall system.

1. Veneer – Brick, CMU, granite, pre-cast panels, none
2. External Sheathing – Gypsum board, oriented strand board (OSB), plywood, steel sheets, etc.
3. Stud selection
 - Section properties – shape, strength, thickness, etc.
 - Configuration – single versus double
 - Utility hole variability and geometry
4. Internal Sheathing – Gypsum board, OSB, plywood, steel sheets, etc.
5. Connections
 - Stud to stud
 - Stud to sheathing
 - Stud to window
6. Windows framing (Appendix IV)

Another consideration when designing a wall system is the stud to structure interaction. The main concern for this consideration is the connections. If a steel stud

wall system is designed with adequate strength to resist a load and has an adequate amount of ductility, but is not sufficiently connected to the structural system, all is lost. When designing a structure, one must have a good understanding of the load path to ensure safety. If a load is applied to a structure, the load will initially be resisted in the wall system, then travel through the wall and connections and into the floor and ceiling slabs of the structure. Once the structure is loaded, it must transfer the load to the structural system and finally into the foundation. The crucial area for blast resistance is the load path from the wall system to the structure through the appropriate connections. The appropriate connections should transfer loads to the appropriate places without creating large line or point loads.

After a sufficient wall system is designed suitable for a defined threat, the wall system must be analyzed to verify its performance. To suitably analyze a wall, the static resistance function must be known and used in an SDOF model to compute the dynamic response. A program for determining the dynamic behavior of steel studs has been developed and will be presented next.

5.2 SSWAC

A program has been developed at the University of Missouri-Columbia in conjunction with the ERDC at Vicksburg, Mississippi to determine the dynamic response for a steel stud wall system under a blast. The program is called Steel Stud Wall Analysis Code (SSWAC) and uses the static resistance function presented earlier along with numerical integration of an SDOF system to determine dynamic response of a wall system.

The way in which the program is used is as follows:

1. Wall properties can be entered in the “Data Entry” sheet, Figure 5.1. The first entry is for veneer, which is basically a decorative facing of a structure which adds mass to the system. With the use of a drop down window, shown in Appendix III in Figure A3.1, the appropriate material and size can be selected. The density of each of the materials is incorporated into the mass calculations for the wall, and if the user needs to define a different material and density, this can be done so in a separate cell.

2. The next wall property that can be selected is the external sheathing, which is the layer in between the veneer and the steel studs. This is the component of the wall system where fire ratings and vapor barriers should be considered and possibly incorporated into the design. “Corrugated” steel or any other type of siding can be used as external sheathing if there is no veneer.

3. Steel studs can then be specified based on section properties and strength. The ductility of the stud can also be entered if it is known, or a standard value can be used. The number of studs, either single or double, can be specified, along with the spacing of the studs and the height of the wall, all of which are taken into account for the static resistance function and the numerical calculations. Utility holes can also be accounted for if present in the stud geometry.

4. The last wall property that is entered is the internal sheathing. This is the inner most layer of the wall, such as gypsum board. After the internal sheathing has been entered, the total weight of the wall is computed and shown in the data entry sheet, Figure 5.1. A figure of a general wall system is also shown in the data entry sheet.

5. Once the wall properties are defined and have been entered, the blast parameters can be entered. The two parameters are the peak pressure (psi) and the impulse (psi-msec). The time interval for numerical integration also needs to be known and should not be greater than one-tenth of the natural period of the system (Biggs 1964). If the time step entered in the data sheet is too coarse to get an accurate response or too fine and the maximum response is not reached, a warning will appear in the response sheet and will give the user suggestions.

	Name	Weight (lb/in ²)
1. Veneer		0.27778
Select From List:		
4-in Brick	4-In Brick	0.27778
OR User-Defined		0.00000
2. External Sheathing		0.01696
Select from List:		
G16 Steel Sheets	G16 Steel Sheets	0.01696
OR User-Defined		0.00000
3. Steel Studs		0.0079167
Select Stud:		
600S162-43-33	600S162-43-33	
Single/Double Studs (1 or 2)	1	
Stud Spacing (in)	16.00	
Wall Height (in)	120.00	
Studs Have Utility Holes? (Y/N)	Yes	
Ductility	20%	
Fy (ksi)	33.00	
4. Internal Sheathing		0.01713
Select from List:		
CoreGuard	CoreGuard	0.01713
OR User-Defined		0.00000
Total Weight		0.31978
Blast Results		
Enter Peak Pressure (psi)		32.5
Enter Impulse (psi-msec)		200
Enter Num Integration Time Step		0.0001

Do NOT Edit Cells in RED

INCERD
MIZZOU

NATIONAL CENTER FOR EXPLOSION RESISTANT DESIGN

10100 Research Building, Department 3010
Waterways Experiment Station, Vicksburg, MS

Figure 5.1: Data Entry Sheet for SSWAC

Once the wall properties have been entered as well as the blast parameters, the static resistance function for the wall and the dynamic response of the wall can be seen in the "Response" sheet. Shown below in Figure 5.2 is the response for a general wall

analysis showing the static resistance function of the wall, the dynamic response of the wall, and the loading function.

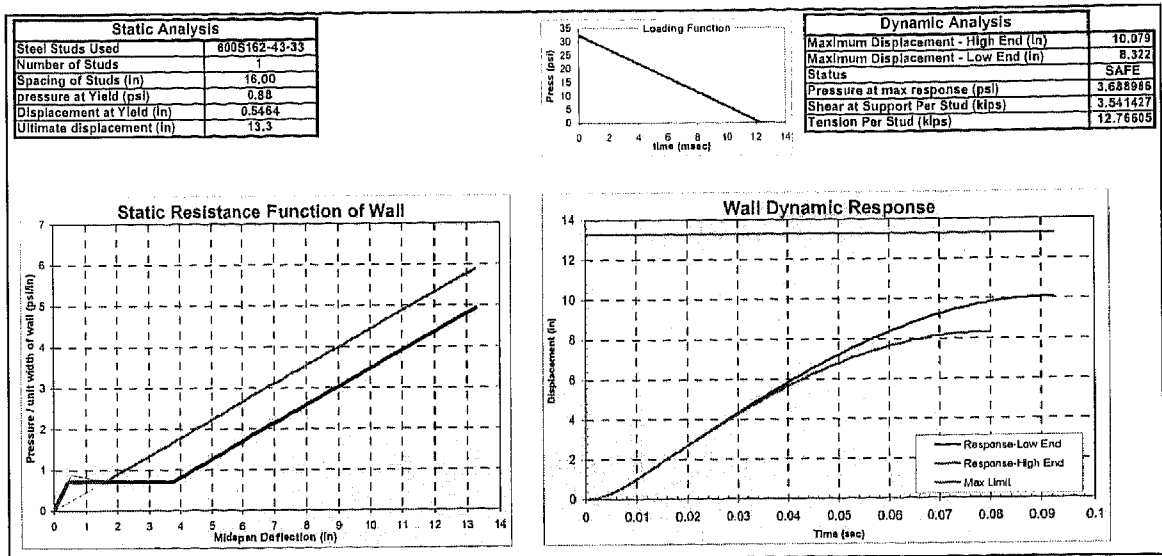


Figure 5.2: Response Sheet in SSWAC

In the dynamic response, the upper limit and lower limit response is considered as it is with the static resistance function. The horizontal line seen in the figure is the amount of deflection the wall can experience before rupture. The curved lines are the actual amounts the wall deflects at mid-span with time, depending on which type of behavior occurs, either upper limit response or lower limit response. The curved lines, which are determined from numerical integration, stop when they reach the point of maximum response. This point of maximum response is the main consideration in blast design and not what happens after that point. The time after maximum displacement occurs is the region where the system rebounds, which is not important when determining

if a system can survive a blast load. The system either survives or it fails, and if it survives as in Figure 5.2, rebound is insignificant.

The numerical integration performed in SSWAC is for one-degree elasto-plastic systems and is discussed in detail by Biggs (1964) in Section 1.5. The mass of the wall system calculated in the data entry sheet is taken into consideration in the numerical integration as well the resistance of the wall. These parameters are incorporated into the equation of motion for the system and the response at each time step can be computed and seen in Figure 5.2. Now that the static resistance function developed in Chapter 3 can be incorporated into an SDOF model for steel studs, and dynamic response can be determined for a wall system with the use of SSWAC, a design example will be performed in the next section.

5.3 DYNAMIC FIELD TEST

Testing using live explosives in the field are even more expensive and labor intensive than static testing in the laboratory. In addition, dynamic field testing is more dangerous since live explosives are used. Many hours of planning and a great collaborative effort are involved for a successful test, in which timing is everything. Therefore, the purpose of field testing is to verify design concepts developed through the static vacuum chamber results and the bending tree results as well as analytical predictions. Researchers should have a good idea in mind of what to expect and predictions should be made prior to testing.

A dynamic field experiment using live explosives has been performed to test two different complete steel stud wall systems. The purpose of the test was to compare the

results of the experimental data to the predictions performed using SSWAC, and also to demonstrate the contribution that mass adds to a wall system in dynamic response (Dinan et al. 2003). The testing setup and details will be described in this section along with the analytical predictions and experimental results.

5.3.1 Experimental Setup

A full-scale blast test experiment was conducted at the Air Force Research Laboratory (AFRL) range at Tyndall Air Force Base in Florida. The purpose of the experiment was to validate the performance of the steel stud anchor systems in developing the full tensile capacity of the studs. This is done by proper connection design so that if failure of the system occurs, it will not occur in the connections, but in cross-sectional failure of the studs, thereby utilizing the stud capacity. Also, the experiment was performed to demonstrate the contribution that mass alone adds to the dynamic response of a wall system and to compare the results of the experimental data to the predictions performed in SSWAC, as described by Dinan et al. (2003). For complete testing setup, predictions, and results of experimental data, refer to Dinan et al. (2003).

Two steel stud wall systems with blast-resistant connections were tested in this experiment. Both steel stud walls consisted of 600162-43-33 studs (refer to Table 1 for section properties), with a specified yield strength of 33-ksi. The walls were 144-in tall with single steel studs spaced at 16-in apart. The wall systems were attached to a reinforced concrete floor slab using concrete anchors with a steel angle connection, and to a steel plate in the ceiling structure using a steel angle welded to the plate (which represents a steel beam or an embedded steel plate in the concrete). The vertical leg of the angle is connected to a steel plate attached to the web of the steel stud through an

anchor hole and a bolted connection to allow for a hinged connection, shown in Figure 5.3.

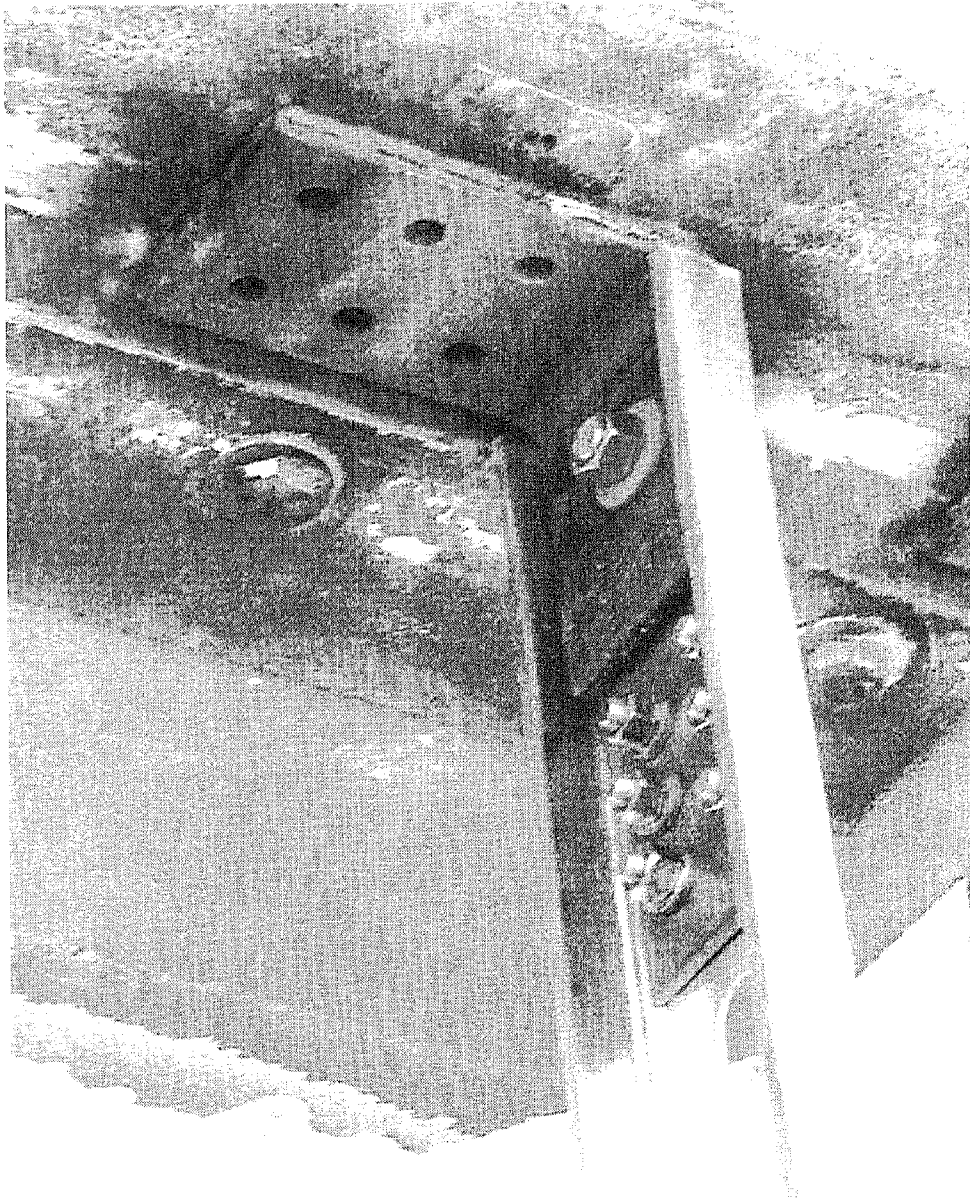


Figure 5.3: Connection Detail at the Top of the Stud (Dinan et al. 2003)

One of the walls contained a brick façade consisting of $7 \frac{9}{16}$ " wide x $2 \frac{3}{16}$ " tall x 4" deep clay bricks with an area density of 30.5 lb/ft^2 . The façade of the other wall was constructed using a typical External Insulation and Finish System (EIFS) exterior, which has an area density of 1.5 lb/ft^2 . The exterior sheathing for both walls consisted of 16-gage sheet steel, and the interior sheathing consisted of CoreGuard. CoreGuard is a product consisting of $\frac{1}{4}$ " gypsum board glued to 20-gage steel sheets to provide a finished interior surface, while preventing fragmentation of the gypsum board. A picture of wall construction and a picture of both walls after construction are shown below in Figure 5.4.

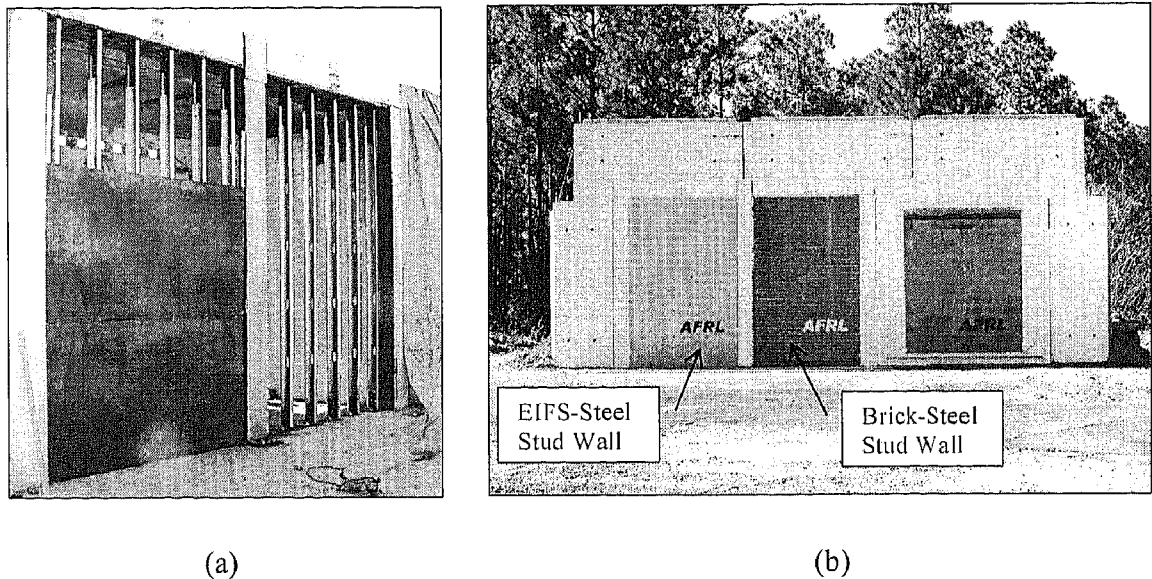


Figure 5.4: Dynamic Field Test (a) Walls During Construction (b) Pretest Exterior Photo

(Dinan et al. 2003)

5.3.2 SSWAC Data Entry

The walls were subjected to a blast load with a peak reflected pressure of 33-psi and a peak reflected impulse of 200-psi-msec, shown in Figure 5.5. SSWAC was used to predict the behavior of the steel stud wall systems under this blast load.

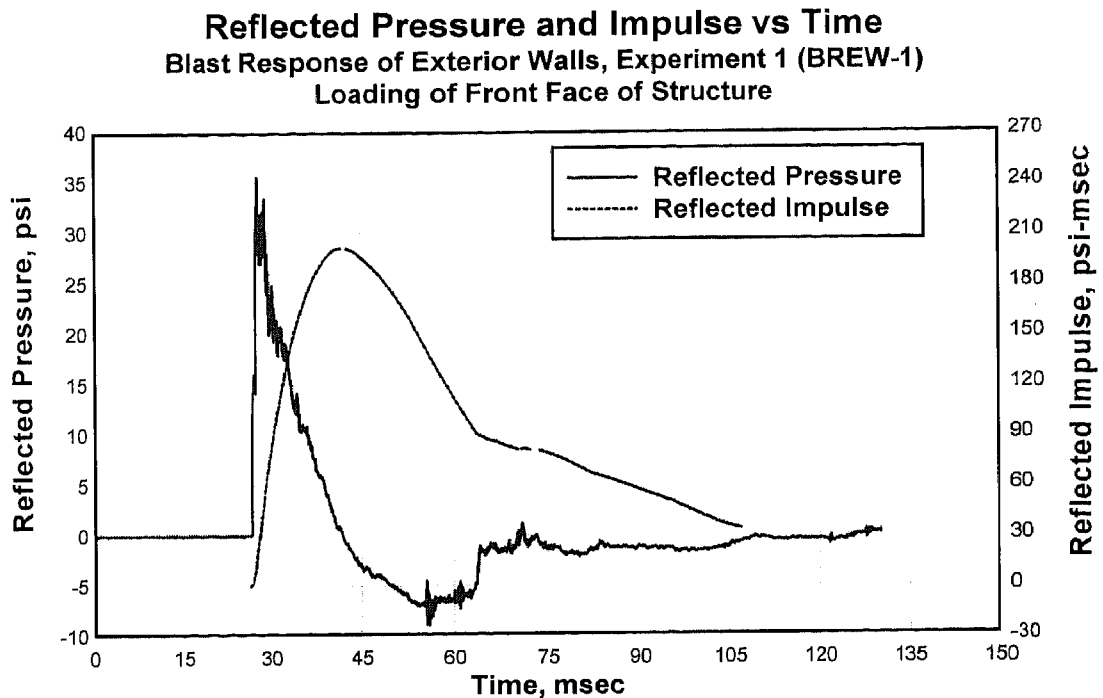


Figure 5.5: Parameters of the Blast Load for Dynamic Field Test (Dinan et al. 2003)

For the wall with the brick façade, the following parameters were input into the Data Entry sheet in SSWAC.

Veneer: 4-in Brick

External Sheathing: G16 Steel Sheets

Steel Studs: 600S162-43-33

Single/Double Studs (1 or 2): 1

Stud Spacing (in): 16

Wall Height (in): 144

Studs Have Utility Holes? (Y/N): Yes

Ductility: 25%

F_y (ksi): 43 (Measured)

Internal Sheathing: CoreGuard

Peak Pressure (psi): 33

Impulse (psi-msec): 200

Numerical Integration Time Step: 0.0001

The properties for the wall with the EIFS façade were entered in the same way, except for the veneer. The veneer was entered as follows:

Veneer: None, since EIFS is not listed in the drop-down menu

User-Defined: EIFS; (Weight = 0.01042 lb/in²)

5.3.3 Analytical Predictions

The wall with the brick façade was predicted to survive the blast load, while failure was predicted for the wall with the EIFS façade. For the brick wall, the analytical model for the steel stud behavior predicts yield-buckling at 0.80-psi and rupture at an ultimate deflection of 18.3-in. This is the amount of deflection the steel studs can undergo without failure. From the SDOF dynamic analysis, the wall is predicted to respond with a maximum displacement of 14.4-in and a minimum displacement of 11.9-in, and therefore predicting the wall will survive even under maximum displacement, shown in Figure 5.6.

The wall with the EIFS façade was predicted to fail during the blast. The analytical model predictions of the static resistance are the same as the brick wall for the steel studs since the same studs are used. The only difference to consider for modeling is how the dynamic response for the wall and how the loss of mass will affect behavior. As can be seen in Figure 5.7, from the SDOF dynamic analysis, the wall is predicted to respond with a maximum displacement of 34-in of deflection and a minimum displacement of 31-in. However, the EIFS façade wall will not experience that kind of deflection since failure is predicted to occur from a ductility limit failure of the steel studs at a displacement of 18-in.

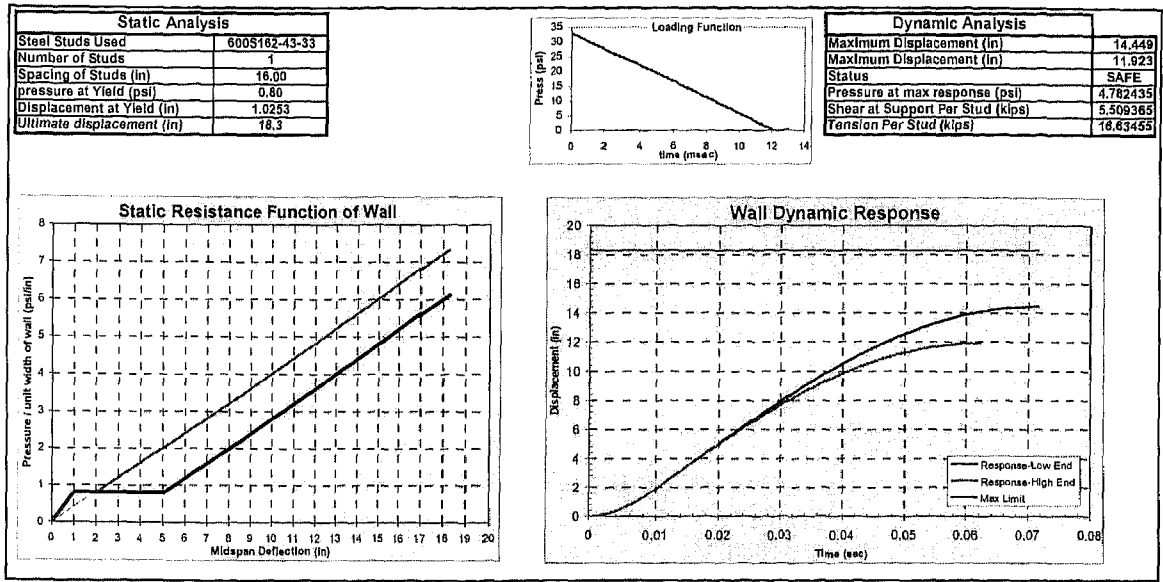


Figure 5.6: Dynamic Response for Brick Façade Wall from SSWAC

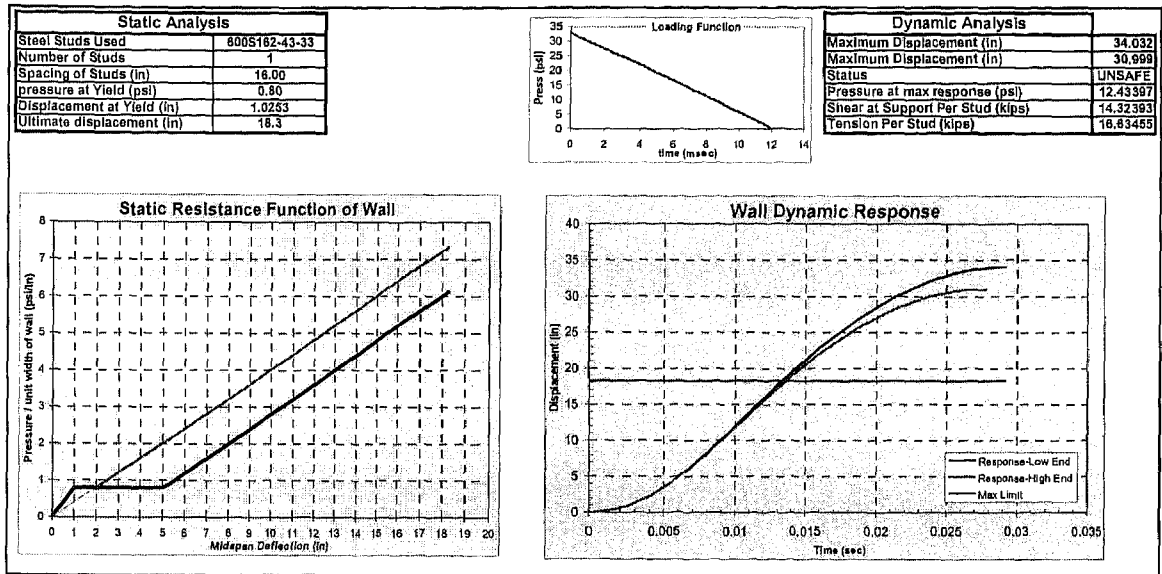


Figure 5.7: Dynamic Response for EIFS Façade Wall from SSWAC

5.3.4 Experimental Results

Now that the predictions have been made for both walls, the experimental results will be presented. The 4-in brick-steel stud wall system was predicted to survive the blast while the EIFS-steel stud wall system was predicted to fail during the blast. This is consistent with what was observed during the dynamic field test. The mass of the brick wall had dramatic effects on the wall behavior resulting from the inertial effects of the mass wall (Dinan et al. 2003). This dramatic difference can be seen in Figure 5.8 with the post-test pictures and in Figure 5.9 with the deflection measurements.

The measured response for the steel stud wall with the brick façade indicated a maximum center wall deflection of 6.8-in and a residual center wall deflection of 5.8-in, due to a 1.4-in rebound in the steel stud wall system. It can be seen in Figure 5.9 that the theoretical prediction for the brick façade wall compares well with the measured response. The paths of the deflection-time curves are consistent with each other up to about 55-msec. It is believed that the difference in the response is due to the type of loading placed on the wall system. In SSWAC, an equivalent uniform pressure is assumed on the SDOF model for the wall system. However, in a dynamic field test, a very non-uniform blast pressure is applied to the wall system, which might result in a softer experimental deflection-time curve. The difference in response can be seen for both the brick façade wall and the EIFS façade wall.

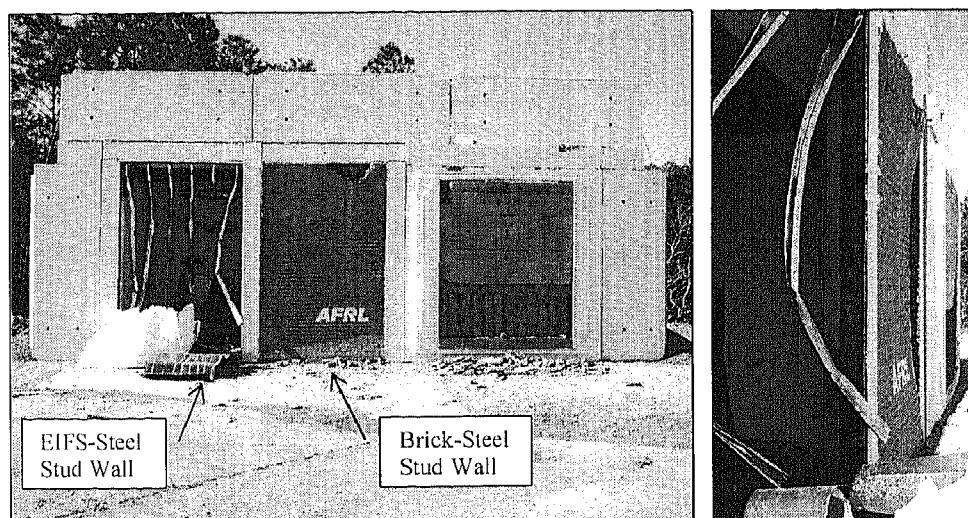


Figure 5.8: Post-Test Exterior View of EIFS Façade and Brick Façade Walls

Measured Center Deflection of Steel Stud Walls Blast Response of Exterior Walls, Experiment 1 (BREW-1) Steel Stud: 600S162-43, 16" Spacing, $F_y = 33$ ksi

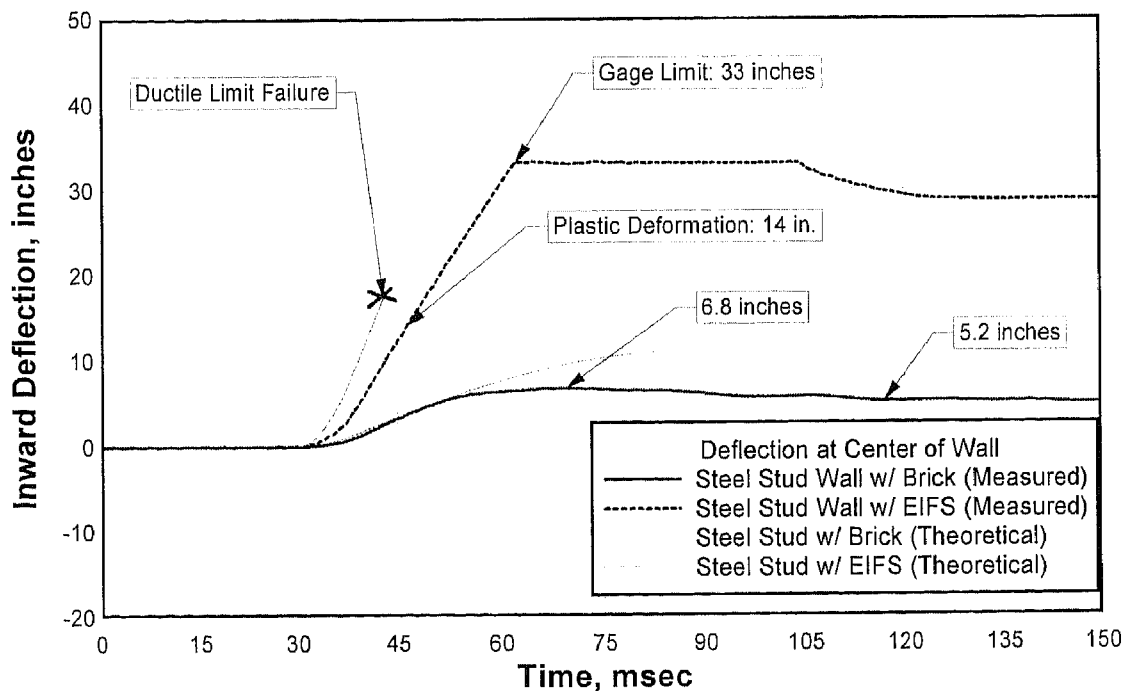


Figure 5.9: Measured and Predicted Center-Deflections (Dinan et al. 2003)

The measured response for the steel stud wall with the EIFS façade indicated a maximum center wall deflection of 32-in, which is the gage maximum, and gave no indication at what point the steel stud wall failed. However, the steel studs that failed on the EIFS wall during the test were eased back into place during post-test forensics to get an estimate of the plastic deflected shape when failure actually occurred (Dinan et al. 2003). The average peak center plastic deflection for the wall that occurred at stud failure was measured to be approximately 14-in. Because of the uncertainty of measuring total deflection, only the plastic deflection was measured in this process. The elastic deflection, from Figure 5.7, is estimated to be anywhere from 1-in to 5-in at the center of the steel studs, resulting in an estimated total deflection of 15-in to 19-in. This compares well to the EIFS steel stud model from SSWAC, which predicts stud failure to be 18-in, which is the elastic plus plastic deformation. The path for the deflection-time curve for steel stud wall with EIFS was measured a little softer than it was predicted. As previously stated with the brick steel stud wall, the difference in response could be a result of the type of loading placed on the system. But even though the model is somewhat conservative, predictions from SSWAC compare well with experimental results.

5.3.5 Conclusions and Recommendations

The experimental setup, analytical predictions and experimental results have been presented from a dynamic field test. The dramatic inertial effects that mass alone adds to a steel stud wall system have been observed in the wall response. The effectiveness of mass by minimizing wall deflection under blast loadings is demonstrated in this experiment as well as in the analytical model. The reason for this effectiveness can be

understood by considering the amount of energy imparted to a system is substantially reduced by adding mass. Adding mass to a system reduces the amount of energy by a factor of $\frac{1}{M}$ (Equation 5.1). According to SSWAC, the brick façade wall system has a mass that is six times the mass of the EIFS façade wall system. The added mass of the brick façade wall system greatly affects the kinetic energy imparted to the wall system, reducing it by a factor of 6 for a purely impulsive loading with a very short duration. This difference can be seen in Equation 5.1:

$$K_E = \frac{i^2}{2M} \quad (5.1)$$

where:

K_E = kinetic energy imparted to the system

i = peak reflected impulse

M = mass of the steel stud wall system

It is recommended to resist a given explosive threat, that adding mass to the system be considered in design. It is also recommended that appropriate connections be used with steel studs to get the needed strength and ductility to resist a blast load. The connection design for this dynamic field test has proven to be very effective in developing the yield capacity a steel stud provides and also achieving a ductile failure in the stud. Properly anchoring a steel stud wall system with the use of appropriate steel connections has been demonstrated to be an effective solution for construction of blast resistant walls, both for new and retrofit construction.

The analytical static resistance function has been used in an SDOF model to predict the dynamic behavior of a steel stud wall system during a blast. SSWAC was

used to design a wall system and has been verified through a dynamic field test using live explosives. It is recommended that improvements be made to the program in areas that are lacking. A better understanding of the softening region of response for a wall system as well as incorporating the mass-structure interaction into the resistance of a wall is recommended and would be beneficial for improved dynamic modeling.

6 Conclusions and Recommendations

Modeling and design of explosion-resistant steel stud wall systems has been presented in this thesis. The way in which an SDOF model and a static resistance function are used to predict dynamic behavior has been shown and discussed in detail. A valid analytical static resistance function has been defined and each region of behavior has been presented. The analytical model has been verified using experimental data from component testing in the bending tree, wall system testing in the vacuum chamber, and also from a field test using live explosives. Conclusions and recommendations will be made in the following sections.

6.1 CONCLUSIONS

The investigation conducted in this research has shed light on modeling and designing explosion-resistant steel stud wall systems. The testing described in this thesis has proven useful on many levels and experimental data described here can be useful for further investigation. The most significant progress made is the improvements that have been made to the existing empirical static resistance function developed by Muller (2002) and Roth (2002). This has been accomplished largely due to a good working experimental setup of the mechanical loading tree. Component testing via the bending

tree is valuable in obtaining behavioral data for components of steel stud wall systems and can provide crucial insight into areas that need improvement.

The linear elastic region of the analytical static resistance function can be modeled using simple theoretical equations and is well understood. More uncertainty and variability in the behavior of steel studs are present in the softening region of response. Better understanding of this region can add significant improvements to the analytical static resistance model and can increase the accuracy of predicting the tension membrane region of response. The point at which rupture occurs in a steel stud is believed to be accurate, but further verification would be useful. For the tests that have been conducted, it is believed that a 4% value for ξ is accurate and provides a good estimate for the pressure and deflection at rupture. However, it is believed that testing a wider range of steel studs can improve the accuracy of this value.

The key to utilizing steel studs in blast resistant systems comes from properly connecting the steel stud wall system to the floor and ceiling slab of the structure. This is accomplished by designing the steel stud connection so that the connection does not fail, but the stud itself fails from the yielding of the steel material and thereby achieving cross-sectional failure of the steel stud from excessive strain elongation. This ideal failure occurs in the tension membrane region of behavior at the section of the stud that has yielded and usually happens at a reduced cross-sectional area such as a utility hole or bolt line in the connection. Utilizing both strength and ductility of a steel stud allows the structural system to absorb a significant amount of energy in the plastic region while limiting the line loads that are applied to the steel stud connections at the floor and ceiling.

After an analytical static resistance model was developed and verified using experimental results from component testing with the bending tree and the testing of complete wall systems in the vacuum chamber, a program incorporating the analytical model and an SDOF model was developed. Further verification was accomplished through a live explosive dynamic field test. Following a general design procedure is beneficial to develop a sufficient steel stud wall design. The program developed for predicting dynamic behavior along with using the appropriate design steps provide improvements to existing predictions and design tools. Improvements that have been made to existing design tools as well as the development of SSWAC are valuable for the design of blast resistant walls for either new or retrofit construction.

6.2 RECOMMENDATIONS AND FUTURE STUDIES

In addition to developing and verifying an analytical static resistance model and incorporating this model into an SDOF program for dynamic predictions, testing and experimental results this thesis has provided might be even more valuable to the investigation. Testing components of the wall systems using the bending tree has provided much insight for future testing. Testing steel stud pairs via the bending tree is fast and efficient compared to testing in the static vacuum chamber or field testing with explosives. Deflection controlled bending tests allow stable tests to be performed, which provides insight to the softening region of the resistance function. Also, the vacuum chamber is limited by atmospheric pressure, but high loads can be applied to a beam using the bending tree and correlated as a uniform pressure. This allows for the entire

beam response to be recorded, therefore obtaining the static resistance of any steel stud wall system.

As previously stated, a better understanding of the softening region of steel stud behavior is desirable. Improvements in this region can increase the accuracy of predicting the tension membrane region of response, which is crucial to understand to determine the amount of energy absorbed by the system. It is recommended that a complete matrix of stud sizes and strengths be tested to have a more complete base of results to verify predictions. Testing different depth, thickness, strength, and length studs can provide much insight into the post-buckling behavior of a stud, primarily the deformed mode shape, the shape of buckling at stud mid-span, and the ultimate strain at failure. A better understanding of this type of stud behavior can help predict which type of response will occur, either upper or lower limit, as well as the amount of energy that will be absorbed.

SSWAC has proven to be very useful in predicting the dynamic response of steel stud wall systems. Analytical predictions are somewhat conservative, but comparisons that have been made are valuable in design. It is crucial that the material properties of a stud are known before predictions or testing is performed. SSWAC allows for the measured material properties by allowing the user to input the appropriate yield strength and ductility of the stud. Both of these parameters have a major role in the calculations performed in the modeling.

It is even more important that the material properties of steels studs are known when used in field construction. The studs used for experimental testing that did not meet proper requirements (ductility in Beam 20 and yield strength in Beam 2 and 18)

were procured from a major manufacturer. It is recommended that the use of studs that do not have the required strength and adequate ductility be avoided for construction purposes in which any blast threat is involved, since this type of stud characteristics results in a loss of blast resistant capabilities.

A design typical of the one seen in Chapter 5 for the dynamic field test is recommended to achieve blast resistance in a wall system. Suggested connection detail for new construction as well as retrofit construction are given in Appendix IV and are recommended to increase energy-absorption by utilizing stud capacity. Also, considering some type of façade that adds mass to a system can be essential in resisting a threat without having to use high-strength steel studs. As seen in Chapter 5, mass alone can significantly reduce the amount of energy imparted to a wall system. Typical 600S162-43-33 studs have a good combination of strength and ductility to allow a system to absorb energy while minimizing line loads present. Higher strength studs can sometimes create large shear loads in the floor and ceiling slab of a structure which can be problematic in structural design.

The experimental testing and results thus far have shown that a union must be found between component testing, testing wall systems in the vacuum chamber, and dynamic field testing with explosives. By utilizing these types of testing methods, valuable improvements have been made to existing design tools and new tools have been developed. A better understanding of complicated stud behavior will lead to more confidence in the modeling and design of explosion-resistant steel stud wall systems and the development of a comprehensive SSWAC design tool.

APPENDIX I – TYPICAL WALL TEST

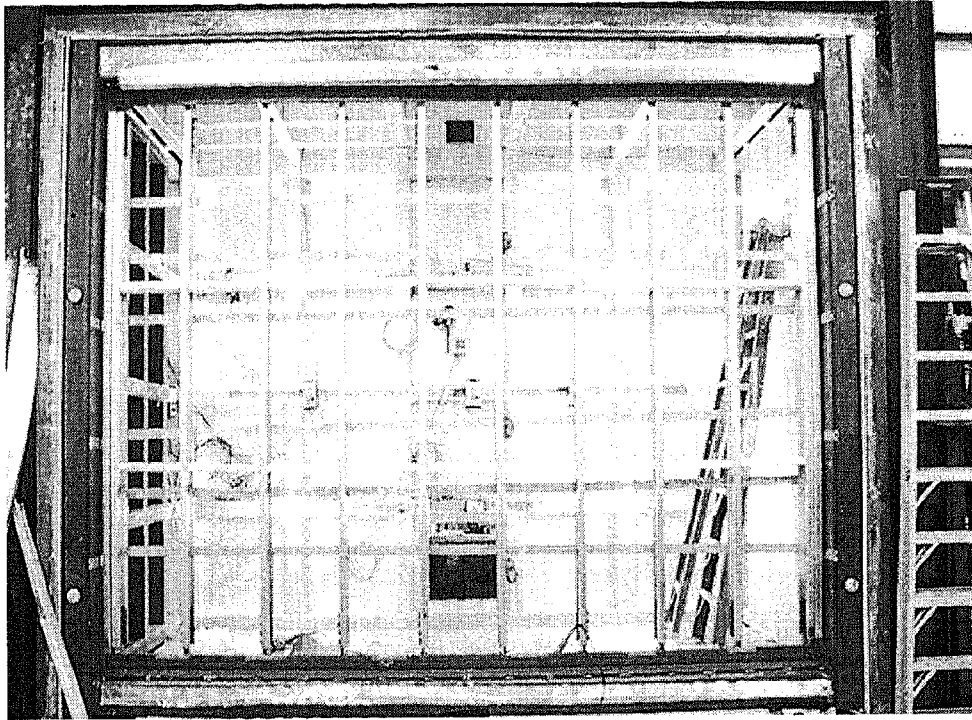


Figure A1.1: Typical Steel Stud Wall in the Vacuum Chamber

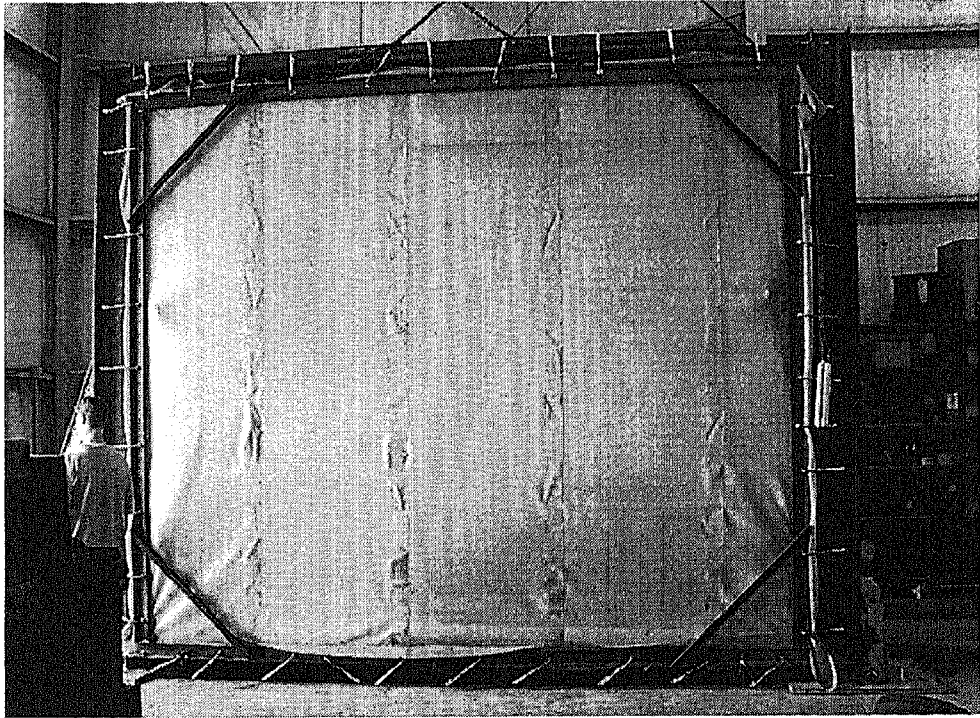


Figure A1.2: Typical Steel Stud Wall Test with Latex Membrane in Place

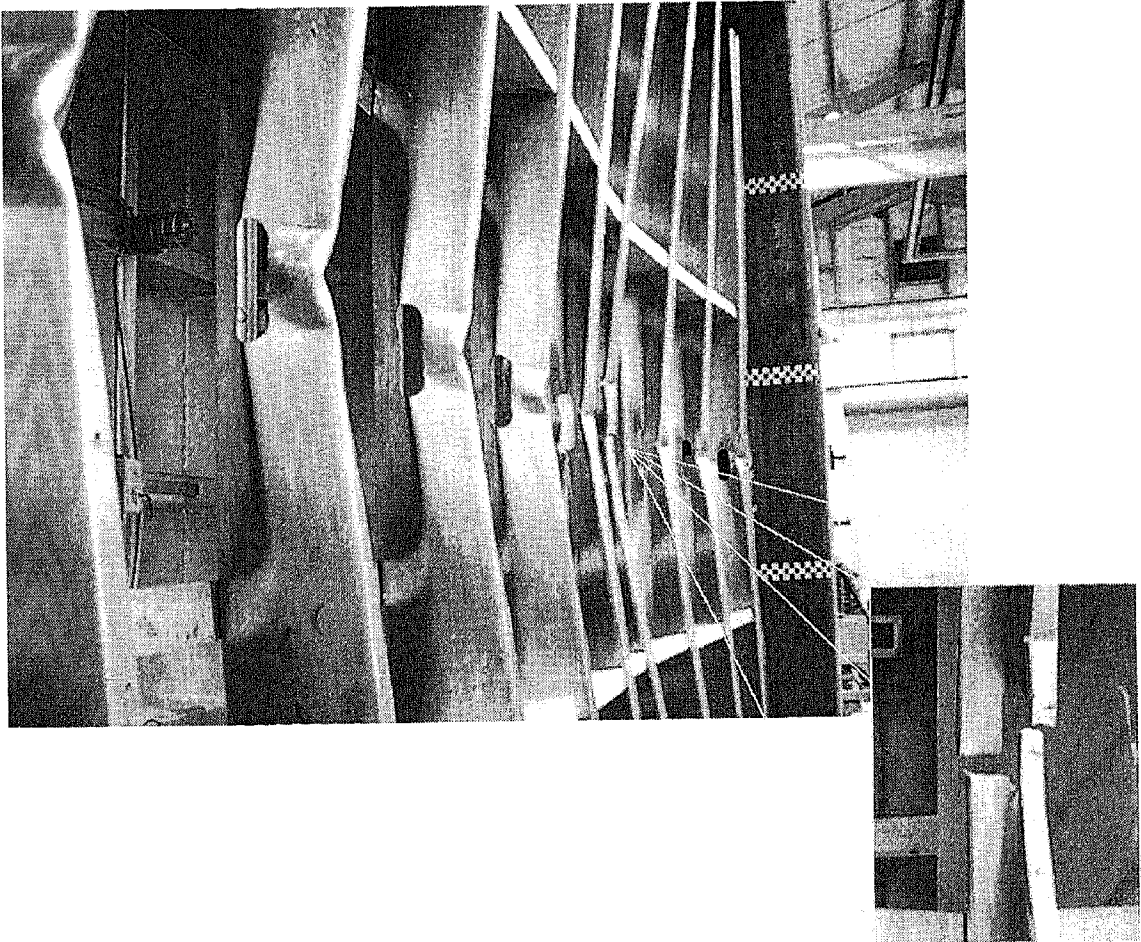


Figure A1.3: Failed Wall with Ruptured Steel Stud at Center Utility Hole

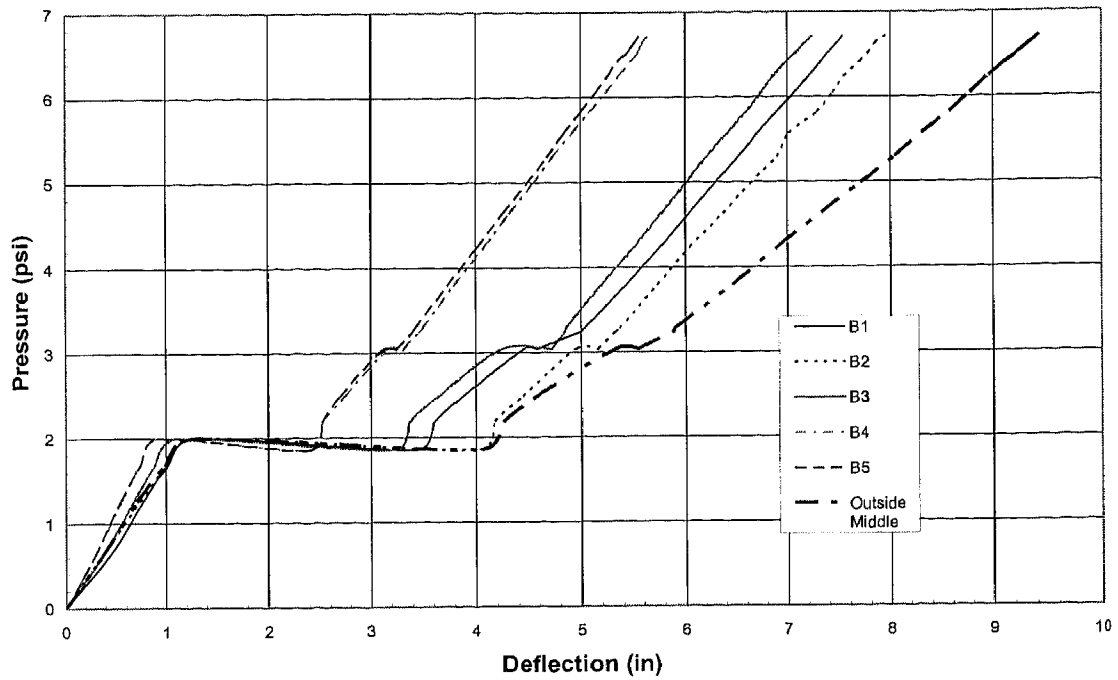


Figure A1.4: Typical Steel Stud Wall Static Resistance Function

APPENDIX II – EXPERIMENTAL TEST DATA

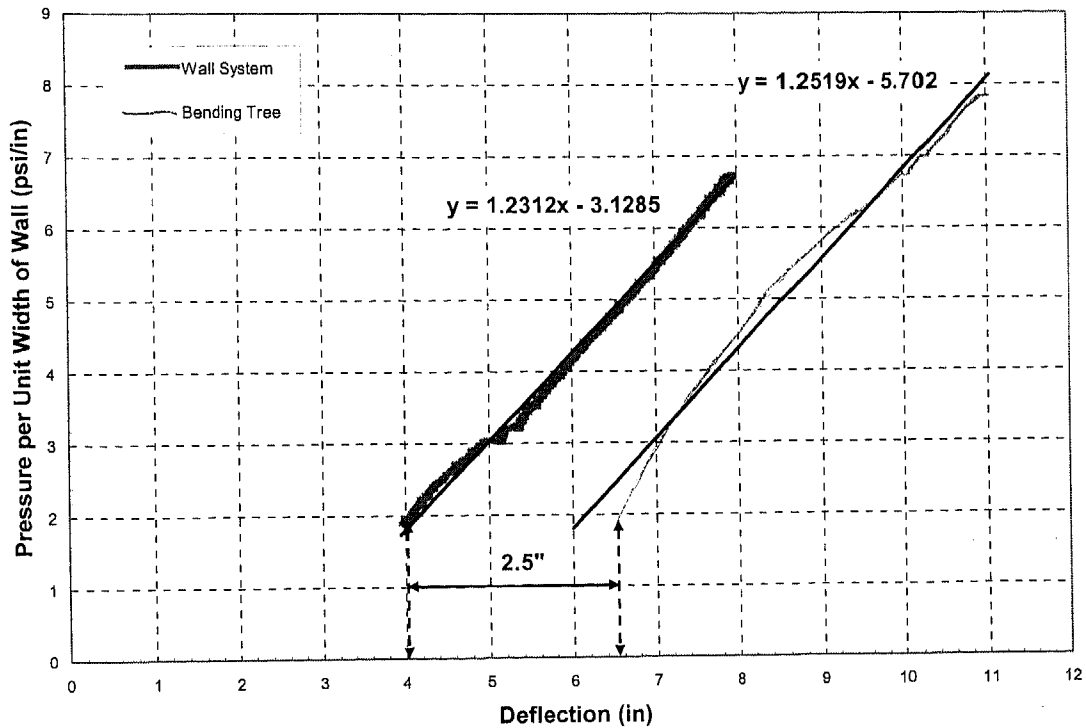


Figure A2.1: Slope Comparison of Tension Membrane Region for Beam 0

The pressure-deflection curves are shown above for a wall system test in the vacuum chamber and a beam test using the bending tree. Both connections are steel hinge with the same beam properties and geometry.

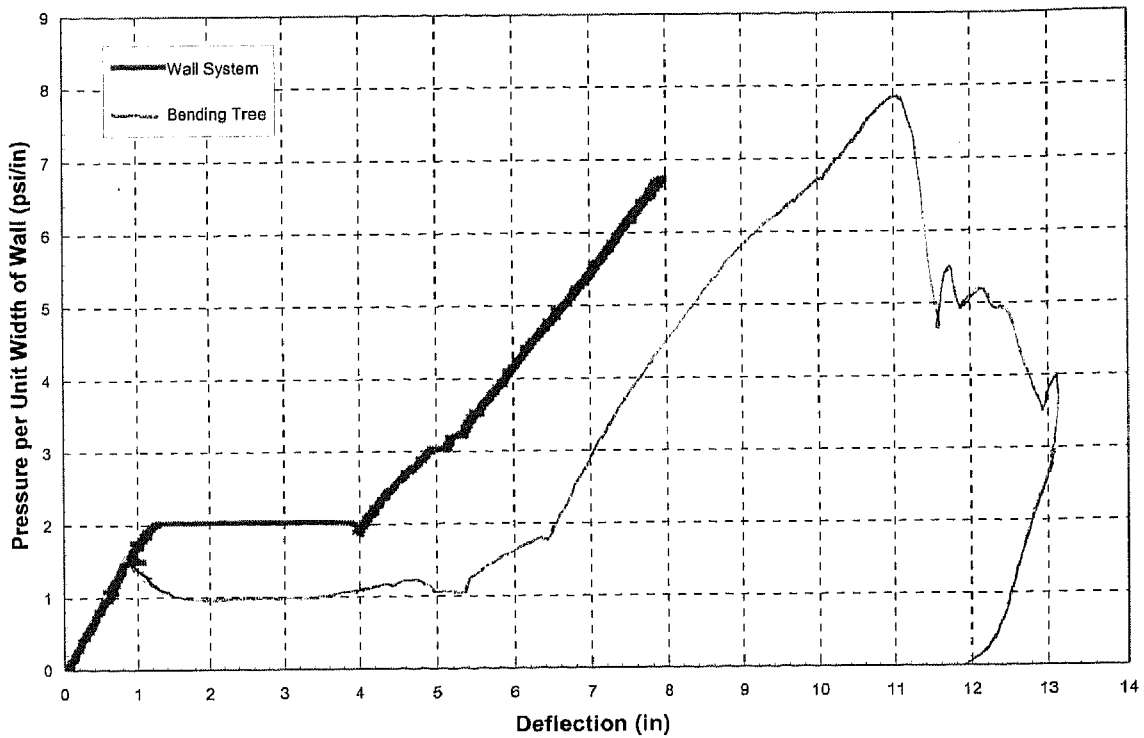


Figure A2.2: Steel Hinge Pressure-Deflection Curve

The pressure-deflection curve shown above is a comparison of a wall system test and the bending tree test (Beam 0) using a steel hinge connection. The steel studs used for both test have the same material properties and geometry, and the deflection recorded was measured at the mid-point of the studs.



Figure A2.3: Pure Tension Action verses Catenary Action

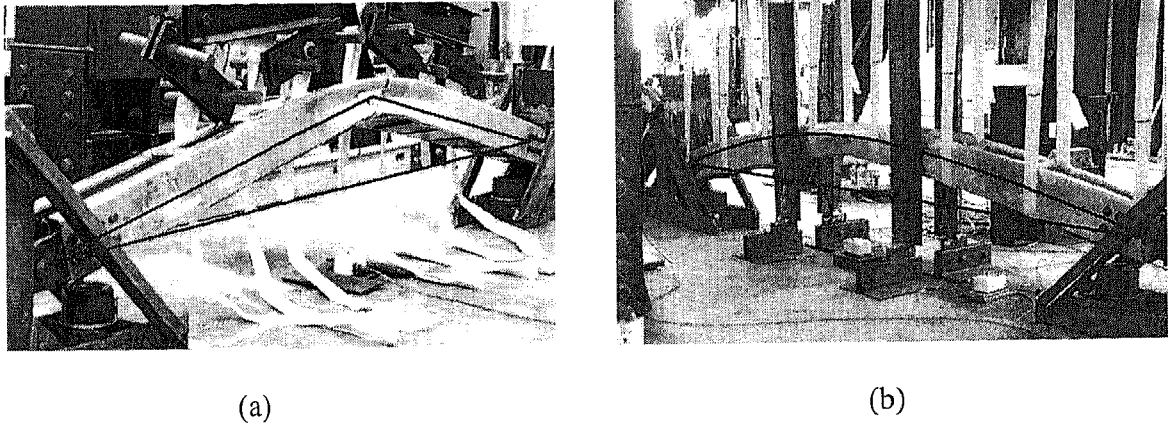


Figure A2.4: Mode shape of beams (a) triangular shape (b) arch shape

Figure A2.3 is the deflected shape of two steel hinge connection tests using 600S162-54-50 studs. A best fit line is drawn through the beams to highlight the difference in mode shapes. In Figure (a), a triangular shape occurred resulting from the formation of a distinct three-hinge mechanism, where in Figure (b), an arch shape occurred.

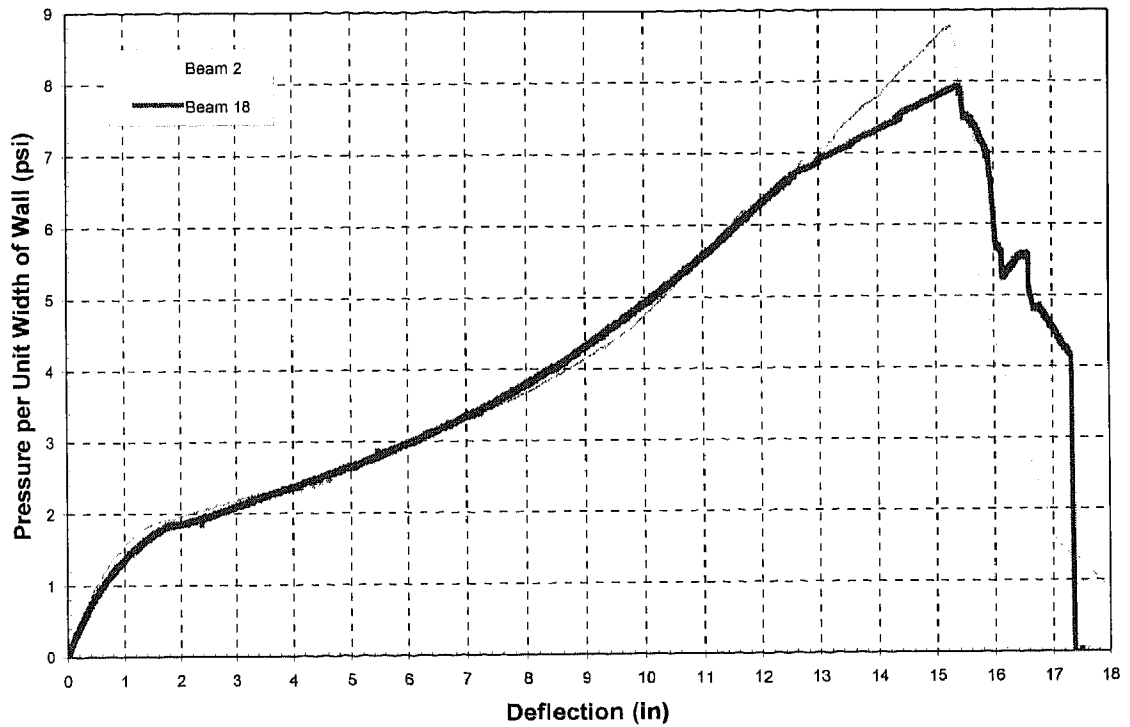


Figure A2.5: Beam 2 and Beam 18 Comparison (Steel Angle Connection)

Above in Figure A2.4 is a behavioral comparison of two steel angle connection tests. The pressure-deflection curves for beam 2 and beam 18 are almost identical. The only significant difference being that beam 2 was stiffer right before failure and ruptured at a higher pressure.

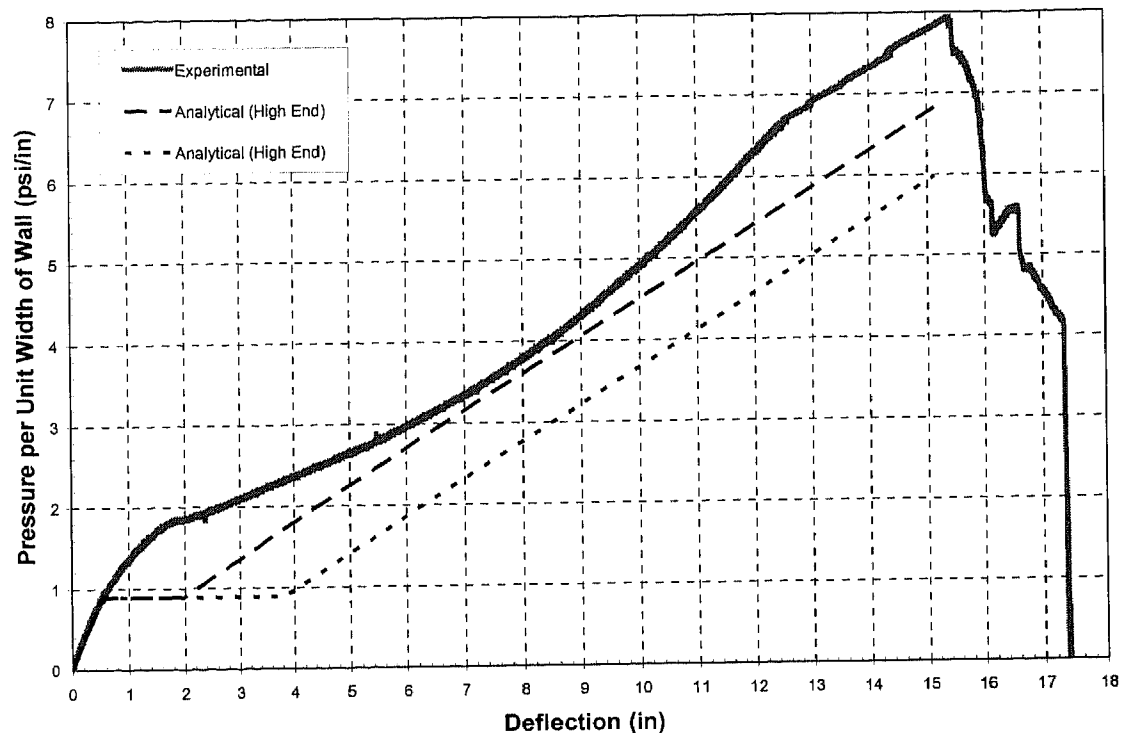


Figure A2.6: Analytical Model for Beam 18

A comparison for the pressure-deflection response and the analytical model are given in Figure A2.5. Modeling is not very accurate because the material properties of for this beam, as well as for Beam 2, do not meet the manufacturer's requirements. The specified minimum yield strength by the manufacturer is 33-ksi, while the actual measured yield strength is only 26-ksi for these studs. Therefore, the behavior does not compare well with that which is predicted. The use of steel studs that do not meet minimum requirements should be avoided in blast design.

APPENDIX III – SSWAC

	Name	Weight (lb/in ²)
1. Veneer		0.27778
Select From List:		
4-in Brick	4-in Brick	0.27778
None		0.00000
2. External Sheathing		0.01696
8 in. Brick		
12 in. Brick		
4 in. CMU - Heavy	G16 Steel Sheets	0.01696
6 in. CMU - Heavy		0.00000
8 in. CMU - Heavy		0.007917
12 1/2 in. CMU - Heavy		
4 in. CMU - Light	600S162-43-33	
6 in. CMU - Light		
8 in. CMU - Light		
12 in. CMU - Light		
1 in. Granite		7
2 in. Granite		16.00
3 in. Granite		120.00
4 in. Granite		Yes
6 in. Granite		20%
		33.00
3. Internal Sheathing		0.01713
1 in. Precast Concrete		
2 in. Precast Concrete		
3 in. Precast Concrete		
Core Guard	CoreGuard	0.01713
OR User Defined		0.00000
Total Weight		0.31978
Blast Results		
Enter Peak Pressure (psi)		33
Enter Impulse (psi-msec)		200
Enter Num Integration Time Step		0.0001

Do NOT Edit Cells in RED

INCERD
MIZZOU.
NATIONAL CENTER FOR EXPLOSION RESISTANT DESIGN
Waterways Experiment Station, Vicksburg, MS

Figure A3.1: SSWAC Showing Veneer Drop Down Menu

Figure A3.1 is the Data Entry sheet for SSWAC showing the veneer drop down menu and some of the choices available. The material used for wall construction can be chosen from the list in the drop down menu. If a material is used in wall construction that is not listed in the menu or if a material with a non-standard density is used, then a different density for calculations can be defined by the user. A drop down menu for external sheathing, steel studs, and internal sheathing is used in a similar fashion as the drop down menu for veneer.

APPENDIX IV – WALL SYSTEM DETAIL SUMMARY

The information on this page is restricted

Removed by request of the sponsoring agency

The information on this page is restricted

Removed by request of the sponsoring agency

The information on this page is restricted

Removed by request of the sponsoring agency

The information on this page is restricted

Removed by request of the sponsoring agency

The information on this page is restricted

Removed by request of the sponsoring agency

The information on this page is restricted

Removed by request of the sponsoring agency

REFERENCES

- Biggs, J. M. *Introduction to Structural Dynamics*, New York: McGraw-Hill, Inc., 1964.
- Brown, J. A. "Experimental Evaluation of Infill CMU and Steel Stud Wall Systems Under Uniform Lateral Pressure." M.S. Thesis, University of Missouri-Columbia, 2003, in press.
- "Clark Product Technical Data and Tables." Clark Steel Framing Systems, January 2000.
- "Cold Formed Steel Design Manual." Amer Iron and Steel Inst, 1996 Edition, p.25, 1997.
- Conrath, E.J., Krauthammer, T., Marchand, K.A., and Mlakar, P.F. *Structural Design for Physical Security*, Reston, Virginia: American Society of Civil Engineers, 1-7, 1999.
- Dinan, R.J., Salim, H., Ashbury, W., Lane, J., and Phillip, P.T. "Recent Experience using Steel Studs to Construct Blast Resistant Walls in Reinforced Concrete Buildings." 11th International Symposium on "Interaction of the Effects of Munitions with Structures." Germany, May 2003.
- DiPaolo, Beverly, Written Communications: Data: 23A&B, 24A&B, 25A, 28ab, 29ab, 30b1, 31c1, 32d1, April 4, 2003 and Data:18g18,19,28,29,38,39, April 9, 2003, (Engineer Research and Development Center-US Army Corp of Engineers).
- Hyde, D.W. "ConWep-Application of TM 5-855-1." U.S. Army Corps of Engineers Waterways Experiment Station, Vicksburg, MS, August 1992.
- Kiger, S. and Salim, H. "Use and Misuse of Structural Damping in Blast Response Calculations", *Concrete and Blast Effects*, ACI Special Pub. SP-175, 121-130, 1998.
- Muller, P. "Static Response Evaluation of Cold-Formed Steel Stud Walls." M.S. Thesis, University of Missouri-Columbia, 2002.

- National Research Council (NRC). *Protecting Buildings from Bomb Damage*, Washington, D.C.: National Academy Press, 1995.
- Park, R. and Gamble, W.L. *Reinforced Concrete Slabs*, Canada: Rainbow-Bridge Book Co., 1980.
- Roth, J. "Response Evaluation of Channel Section Cold-Formed Steel Wall Stud Members Under Uniform Lateral Pressure." M.S. Thesis, University of Missouri-Columbia, 2002.
- Shull, J. "Steel Stud Retrofit Connection Development and Design." M.S. Thesis, University of Missouri-Columbia, 2002.
- Smith, J. and Sidebottom, O. *Inelastic Behavior of Load-Carrying Members*, New York: John Wiley & Sons, Inc., 1965.
- TI 809-07. U.S. Army Corps of Engineers Technical Instructions. November 1998.
- TM5-1300. "Structures to Resist the Effects of Accidental Explosions." Departments of the Army, Navy, and Air Force, Washington, D.C., November 1990.
- U.S. State Department "The Steel Stud Wall/Window Retrofit a Blast Mitigating Construction System." DS/PSD/SDI – TIB # 01.01, Washington, D.C. 20521, 2001.
- Wesevich, J.W. "Analytical Review of Tested DOS/DS Steel Stud Walls." Prepared for the U.S. Agency for International Development, WBE project No. A184-001, January 2001.
- Whitton, B. "New UW Research Group Studies Cold Formed Steel." Internet: <http://www.adm.uwaterloo.ca/infonews/release/1999/132%20Research%20into%20cold%20formed%20steel%20underway%20at%20UW,%20June%2030,%201999.html>, 2003.
- Young, C.Y. and Budynas, G.B. *Roark's Formulas for Stress and Strain*, 7th Edition. New York: McGraw-Hill, Inc., 2002.
- Yu, W. W. *Cold-Formed Steel Design*, 3rd Edition. New York: John Wiley & Sons, Inc., 2000.